THE ELECTRONIC AND GEOMETRIC STRUCTURES OF SOME XENON OXYFLUORIDES AND RELATED COMPOUNDS

by

HSU Show-chee (徐守淇)

A thesis submitted in partial fulfilment of
the requirements for the degree of
Master of Science in
The Chinese University of Hong Kong
1972

Thesis Committee :

Dr. W. K. Li, Chairman

Dr. K. Y. Hui

Dr. Thomas C. W. Mak

Dr. Y. W. Chan

Prof. C. A. Coulson, External Examiner

A C K N O W L E D G M E N T S

The author wishes to express her gratitude to Dr. W. K. Li for his guidance and advice throughout the course of the research and the prepartaion of this thesis.

Thanks are due to members of the Computing Center of the Chinese University of Hong Kong for their kind assistance during the computation of the present work.

Special thanks are due to Miss Margaret Fung for her skillful typing of this thesis, and the demonstrators of the Department of Chemistry for their stimulating and encouraging discussions.

S. C. Hsu

CONTENTS

LIST OF TABLES

LIST OF FIGURES

ABSTRACT

The modified Wolfsberg-Helmholz (WH) approximation has been applied to calculate the MO eigenvectors and eigenvalues for several molecules. Structural modifications for $XeOF_2$, XeO_2F_2 and $XeOF_4$ have been rationalized and predicted basing on the nodal characters of the highest filled MO('s). Results show that $XeOF_2$ may have the C_{2v} symmetry with angle OXeF less than 90^o. For XeO_2F_2 however, the OXeO angle is predicted to be greater than 120^o while the FXeF angle on the side of the oxygen is less than 180^o. According to this model, $XeOF_4$ has the C_{4v} symmetry with angle OXeF greater than 90^o. In addition, the relative bond lengths in these systems have been commented on. Except for $XeOF_4$, the exact structures of the other two remain unknown. These results seem to imply that double bond and lone pair are of similar bulkiness in the coordination sphere and that the Pauli force in the valence-shell-electron-pair-repulsion model and nodal repulsion are intimately related.

The second-order Jahn-Teller (SOJT) effect has been applied on the systems PH_5 and SF_4. For PH_5, the D_{3h} symmetry is expected to be the more stable structure from the viewpoints of SOJT effect and total orbital energy. The instability of PH_5 may be rationalized by the additivity of bond energies, i.e., it isunstable towards the decomposition to H_2 and PH_3. With SF_4, the result is not as

satisfactory as those for PH_5 and xenon oxyfluorides. Using the Clementi's set of valence state ionization potential (VSIP) data, a sensible picture leading to the most stable structure C_{2v} is obtained. With the set of VSIP data from Ballhausen and Gray, the situation is not so simple and straightforward. The tetrahedral structure is found to be more stable which itself undergoes first-order Jahn-Teller distortion. This may be viewed as the shortcoming of the WH method : its high sensitivity towards input parameters.

Chapter I

HISTORICAL REVIEW

Up in the thirties, long before the synthesis of any 'real' inert gas compounds, Pauling [1] predicted the formulas KrF_6 and XeF_6 with analogy to complexes like $(NH_4)_3AlF_6$, KBF_4. Later, Pimentel [2] also mentioned the expectation of rare gas halides. Xenon, inert as it was believed to be, formed its first compound $XePtF_6$ [3] in 1962 under laboratory environment. Shortly afterwards the first binary fluoride of xenon, XeF_4, was reported [4], with other fluorides following in rapid succession.

The formation of chemical compounds with this inert element roused a new field of interest as to how this was made possible. Chemists used different ideas [6-9] to discuss the actual situation in these molecules. Among these approaches, it is of value to note that there is close analogy between interhalogen compounds and the xenon fluorides [10]. The bonds in inert gas compounds are essentially the same as those present in many other well known chemical species, like the interhalogens and halogen oxides [6,9-12]. Comparisions have been made between isoelectronic species such as ICl_2 and XeF_2 [5] where results are quite satisfactory.

In relation to molecular structure and stability, the following points are worth mentioning [8].

(i) These are stable compounds, not transient species detected in mass-spectrography, with an even number of fluorine atoms.

(ii) The structural phenomena are: XeF_2(linear), XeF_4 (square planar), $XeOF_4$ (square pyramidal), XeO_2F_2 (distorted tetrahedral), $XeOF_2$ (T-shaped), etc.

(iii) The compounds are mainly formed between electronegative ligands like oxygen, fluorine and chlorine, and a heavy central atom like Xe or Kr. Superficially this may be regarded to be a simple requirement for bond formation: sufficiently large differences in electronegativity.

Models [5,8,13,14] have been proposed for the bonding schemes of XeF_2 and XeF_4 and quite pleasing results have been obtained. However difficulties have come into the way when XeF_6 is considered [15,16]. Even at present this remains a riddle to be solved. As expected, the principles of quantum mechanics find its way into the description of these chemical compounds and calculation of different levels of sophistication have been

performed on these molecules. For XeF_2 and XeF_4, the results have turned out to be quite satisfactory. The following will be a brief discussion on some of the bonding theories.

Both the VB and MO theories have been used to describe the electronic structure of the xenon fluorides. In the VB approach, Bersohn [17] considered the hybridization scheme. However, the promotion energy for both $5s^2 5p^6 \rightarrow 5s^2 5p^5 5d$ and $5s^2 5p^6 \rightarrow 5s^2 5p^5 6s^1$ are about 10 e.V., which, according to Malm et al. [5], cannot be compensated by bond formation. Still within the VB formalism, when resonance approach is adopted, the most important resonance structures for XeF_2 are: $Xe{-}F^+\ F^-$, $F^-\ Xe^+{-}F$, $\overline{\ulcorner F\ Xe\ F \urcorner}$, and $F^-\ Xe^{++}\ F^-$. The $Xe^+{-}F$ bonds here are covalent and xenon carries unit positive charge. The third structure helps to reduce the charge on xenon but, on the other hand, the last one will increase it. Applying Pauling's method, Coulson [8] has calculated that XeF_2 have bonds that are about 50% ionic, i.e., with the apparent structure $F^{-3/4}Xe^{+3/2}F^{-3/4}$. If xenon really possesses so large a charge, its electronegativity for this particular purpose must be greater than if it were neutral. This would have the effect of reducing the extent of charge migration and led to the situation of $F^{-\frac{1}{2}}Xe^{+}F^{-\frac{1}{2}}$. The binding energy comes almost entirely

from the charge transfer structure and very little is derived from the no-bond structure. A simple arithmetical expression for the electrostatic energy for the creation of charge distribution $Xe^{+}F^{-}$ is

$$\text{I.P. (Xe)} - \text{E.A. (F)} - e^2/R$$

$$= 12.1 - 3.6 - 6.8$$

$$= 1.7 \text{ e.V.},$$

where R = seperation between the two concerned atoms. This amount of energy may be recovered by the bond formation of Xe^{+} -F in the other half of the molecule. Therefore for every $Xe^{+}F^{-}$ situation there must be a corresponding bond Xe^{+}-F. Thus an even number of fluorine atoms is observed in every xenon fluoride or oxyfluoride. Owing to the symmetry of the molecule XeF_2, resonance is possible, where energy is lowered and molecule stablized. Here, with this simple argument it is also obvious that the ionization potential of the central atom and electronegativity of the ligand do play an important role in the bond formation. Basing on this argument again, the stabilities of the xenon fluorides will tend to decrease as the number of ligands increases, since an unreasonably large charge will be accumulated on the xenon atom. Other fluorides and oxyfluorides can be treated in a similar way.

Using also the localized bond approach Gillespie has predicted the structure for a series of xenon compounds [15]. In addition, by considering the sum of covalent radii, he has also predicted the bond length(s) in these compounds. A summary is given in Table I.

Table I. Geometry and Bond lengths for Some Xenon Compounds [8]

Compound	Structure	Symmetry	Bond Length (Å) Xe-F	Xe-O
XeO_4	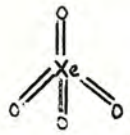	T_d		1.74
XeO_3	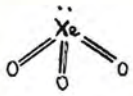	C_{3v}		1.75
XeO_2	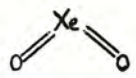	C_{2v}		1.76
XeF_2	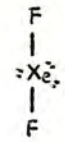	$D_{\infty h}$	1.98	
$XeOF_2$	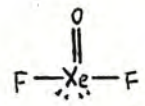	C_{2v}	1.95	1.76
XeO_2F_2	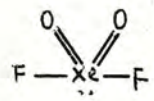	C_{2v}	1.93	1.75
XeO_3F_2	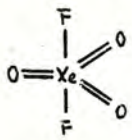	D_{3h}	1.91	1.74
XeF_4	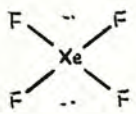	D_{4h}	1.94	
$XeOF_4$		C_{4v}	1.92	1.75
XeO_2F_4		D_{4h}	1.90	1.74
XeF_6		distorted O_h	1.80 1.92	

There is great similarity between these compounds and the interhalogens. The sum of the covalent radii gives good prediction of bond lengths for both families. It can, therefore, be said that bonds in these compounds may simply be electron pair bonds. In the present work, this model is taken to be a challenge and a basis as well. The gross geometry is assumed to follow the structure given here while other minor readjustments are discussed under the pseudo-Jahn-Teller and/or the nodal repulsion effects to be mentioned later.

In the MO approach, it was well recognized that the bondings in interhalogen and xenon compounds were of similar nature. Since the former have been studied extensively [18-23], the xenon compounds have then been treated without too much undue difficulty. The treatments by Rundle [9] and Coulson [8] have been chosen for discussion below.

In Rundle's method [9], only the p_σ orbitals have been considered. The resulting energy levels can be expressed in simple diagrams in a rather elegant and convincing manner. Such an approach has been adopted because:

(i) xenon tetrafluoride and xenon difluoride are isoelectronic analogues of ICl_4^- and ICl_2^- and hence may be expected to be square planar and symmetrically linear respectively;

(ii) as mentioned before, the participations of s and d orbitals involve high promotion energy, the simple basis set including only p orbitals appear to be sufficient.

The p_σ treatment of xenon difluoride leads to a model of 3-centre-4-electron bond (3C-4e). The electronic arrangement shown in Fig. I indicates that there is a withdrawal of electron density from xenon giving rise to a partial ionic bond.

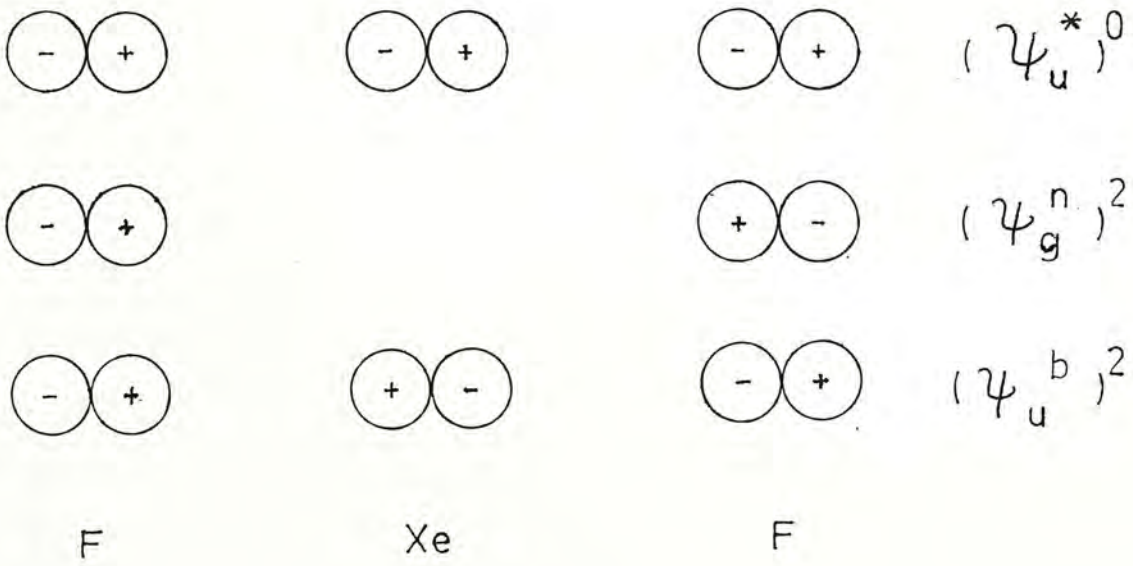

Fig. 1 The M O 's for XeF_2 [9]

It is obvious that in order to form this kind of bond, the terminal atoms must be more electronegative than the central atom; also the bond lengths of these bonds will be longer than ordinary electron pair bond between the same elements. Because the electronegativity of xenon is considerably less than that of fluorine, they are likely to form this kind of bond. Since each bond removes some charge from xenon the high ionization potential of xenon must destabilize the systems with higher co-ordination number. The thermodynamic functions ΔG_f° and ΔH_f° for XeF_4, IF_5, and BrF_5 are given in Table II for comparison.

Table II. ΔG_f° and ΔH_f° for XeF_4 and Isoelectronic Species [9]

	XeF_4	IF_5	BrF_5
ΔG_f°	$\geqslant$ -80.6	-180.6	-127.9
ΔH_f°	$\geqslant$ -102.6	-202.6	-101.9
number of bonding pairs	2	3	3

From these data, Rundle has concluded that XeF_4 is to some extend quite stable as compared with BrF_5. By analogy with 3C-4e I-F distance, Xe-F bond distance of about 1.96 Å is suggested [9].

Similarly, oxyfluorides of xenon contain pairs of linear 3C-4e bonds. Acutally Xe-F bond length for XeF_4 found by neutron diffraction is about 1.951 - 1.954 Å [24] which is very close to the value predicted by this simple bonding theory. Indeed, it has also been shown by Allen [6], Weibenga and Kracht [19], Havinga and Weibenga [20] that p valence orbitals alone account very well for the xenon fluorides as well as interhalogen compounds.

Later, Coulson [5] proposed a more complicated or detailed MO treatment which involves both the σ- and π-type orbitals. The argument is made of the assumption that π-type overlap is less effective than σ-type overlap. As a result, the spread of the π-type molecular orbitals is less than that of the σ-type molecular orbitals. This gives rise to the following energy level diagram:

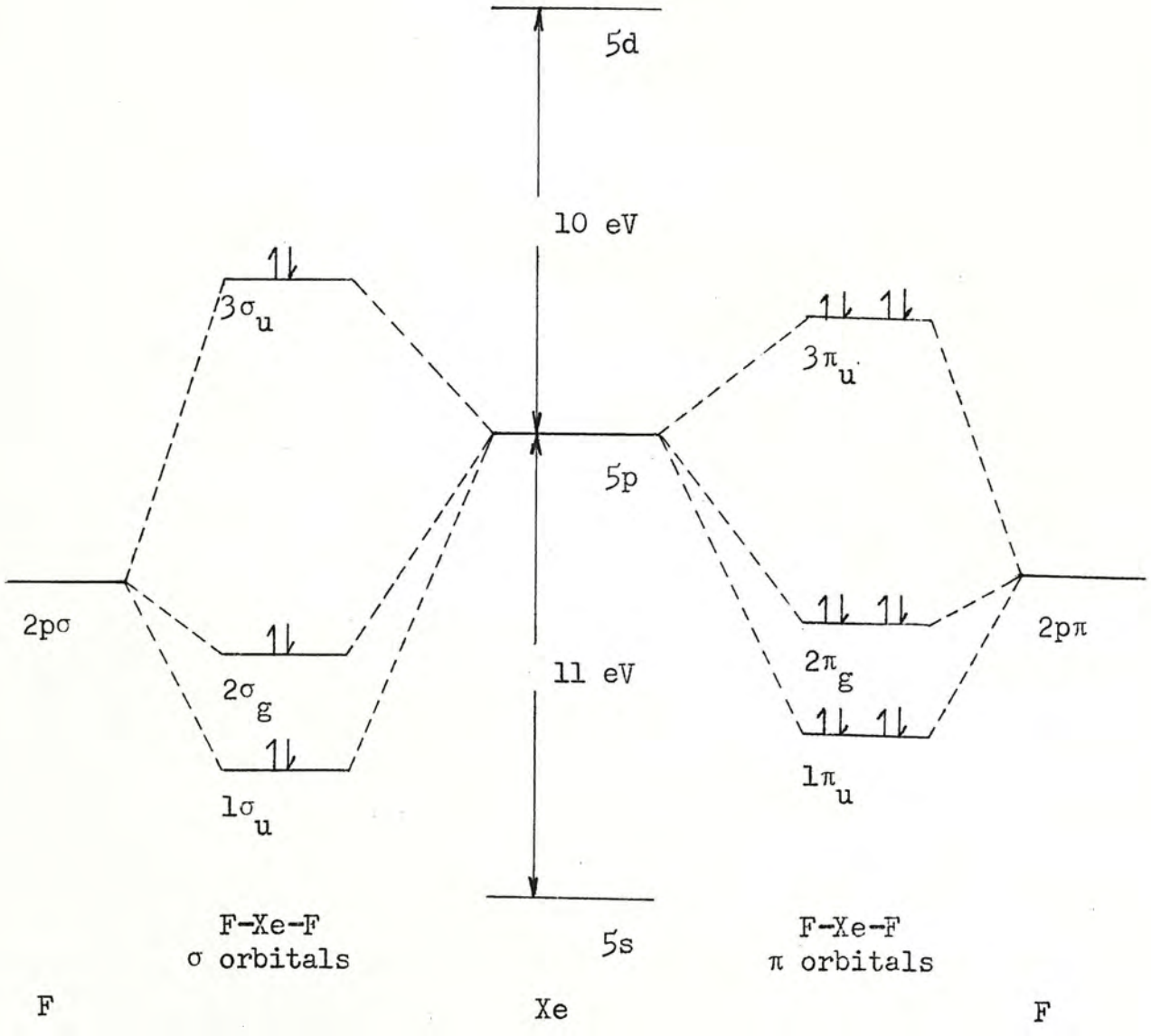

Fig. 2 A Simple MO Energy Level Diagram for XeF_2 Including Both σ and π Orbitals [8]

It is readily seen that the left side (σ orbitals) of Figure 2, is very similar to Rundle's picture. As a result, there is a net migration of charge from xenon to fluorine. This agrees with the fact that these compounds are formed with central atoms having relatively low ionization energies and more electronegative ligands. The π-type orbitals do not lead to a migration of charges and are more or less non-bonding. Also the energy spread is mainly within the extremes of the s and d orbitals for xenon. Therefore, for this and similar systems, it is sufficient to consider only the p orbitals.

Along similar lines, other calculation have been performed on the xenon fluorides in order to obtain more quantitative results. Among these, Lohr and Lipscomb [11], Hinze and Pitzer [25], Catton and Mitchell [13] have treated the difluoride; Yeranos [26] have considered the tetrafluoride. All these calculations adopt the Wolfsberg-Helmholz type [27] approximation, using atomic orbital wave functions of various degree of accuracy. The results for these calculations confirm once again Rundle's picture that the 5s and 5d orbitals of Xe play only very minor role in the bonding. Another fluoride, XeF_6, has been treated by Lohr and Lipscomb [11] Bartell [16], and Willet [28]. Due to the uncertainty in the molecular structure of this compound, the results are not satisfactory.

Finally, it is worth pointing out that, even though the fluorides have been treated extensively, the oxyfluorides of xenon have largely been neglected in quantitative theoretical calculation, with the notable exception of the Valence Shell Electron Pair Repulsion (VSEPR) treatment by Gillespie [15]. In view of this, it is therefore worthwhile to investigate the electronic structure of the oxyfluorides. Particular attention will be paid to the competition between the Xe=O double bond(s) and the lone pair(s) in the same coordination sphere and its structural effect.

Chapter II

SOME THEORIES CONCERNING ELECTRONIC AND MOLECULAR STRUCTURES

The main theme of the present work concerns the investigation of the relationship between the molecular and electronic structures of some xenon oxyfluorides. In doing so, the following theories are considered: nodal repulsion effect suggested by Berry et al. for the case of BrF_5 [29] and the second-order Jahn-Teller (SOJT) effect, which was first suggested by Bartell pictorially [30] and then extended by Pearson by the techniques of group theory [31]. These two models deal chiefly with possible distortion(s) in molecular structure by considering the symmetry properties of certain key wave functions. In many instances, they run parallel to the lone-pair interaction in the Gillespie-Nyholm's VSEPR theory. A description of each will be given in the following parts of this chapter.

A. Nodal Repulsion and its Effect

The presence of nodes or nodal surfaces in a wave function obtained by solving the Schrödinger equation for a system has long been accepted as an indication of certain instability. From bonding theory, the existence of a node in certain part of a wave function tends to lower the electron density there, or, in other words, electrons will avoid these nodes or nodal surfaces. Besides this

avoidance, delocalization may be expected in regions without such nodal property. The composite effect of avoidance and delocalization may be viewed as a force for deformation resulting either in a change of bond angles or a rotation about one center. The forces originating from this effect are assumed to have magnitudes proportional to the population between the concerned atomic orbitals. This assumption is adopted because it can give some insight into the comparable effect of the forces qualitatively. It is however necessary to note that the absolute magnitudes cannot be predicted this way.

As an example, the treatment on BrF_5 by Berry et al. [29] is given below. Adopting the Wolfsberg-Helmholz model, the highest occupied MO ($6a_1$) wave function for BrF_5 has the form:

Table III. The Coefficients and Populations for the $6a_1$ MO of the Square Pyramidal BrF_5

	4s (Br)	4p (Br)	4d (Br)	2s eq (F)	2s ax (F)	2pσ eq (F)	2pσ ax (F)	2pπ eq (F)
AO Coeff.	.45	-.74	.07	-.21	.17	-.67	.26	.42
Population	.09	.40	.01	.02	.00	.33	.04	.11

Or, pictorially, the important AO's, i.e., the AO's with the highest populations, have the arrangements shown in Figure 3.

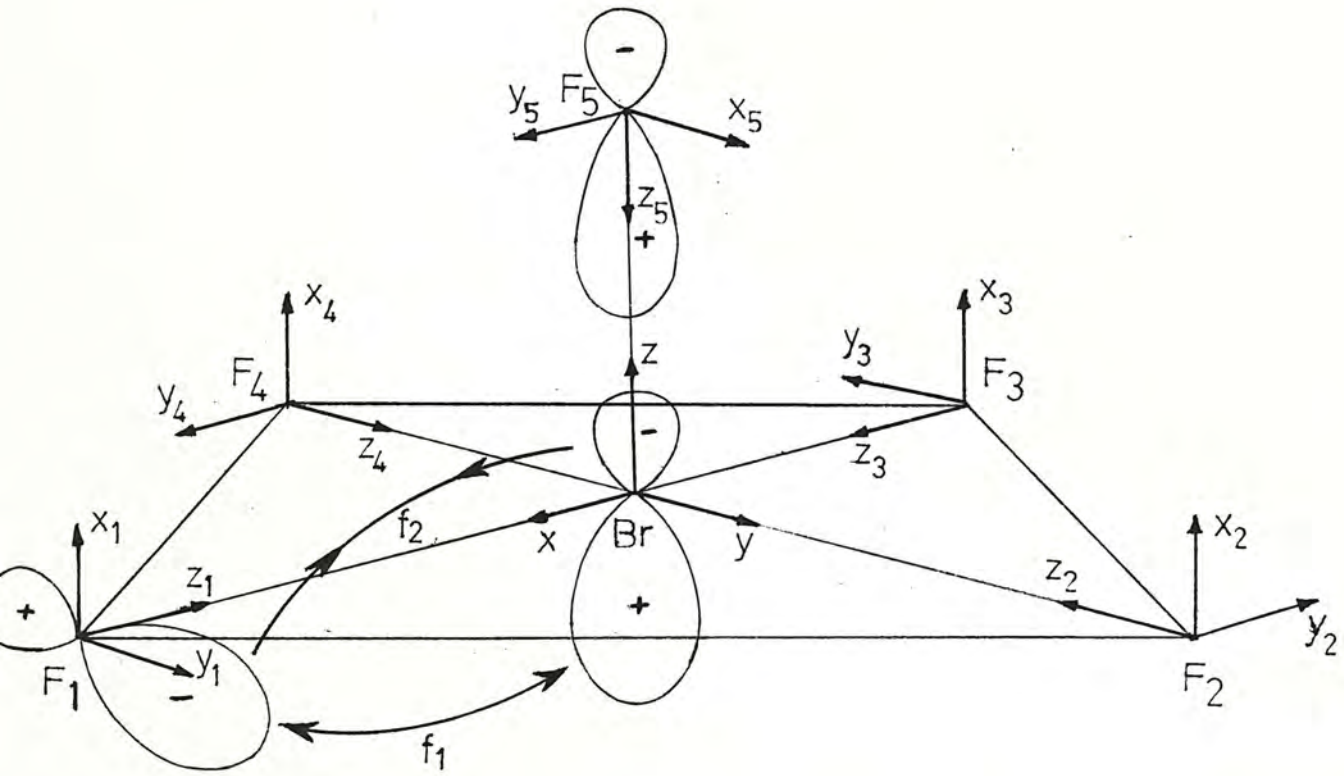

Fig. 3 The $6a_1$ MO of BrF_5 Shown Pictorially After Consideration for Hybridization

By examining Figure 2, due to the nodal characters of the AO's, f_1 will be a repulsive force while f_2 is attractive in nature. The coupling of these two forces will result in the raising of the fluorine plane with respect to the central Br atom. This of course, is in complete agreement with the VSEPR model, which intuitively says that the lone pair will occupy more space in the coordination sphere. Finally, it should be pointed out that the lone pair in the VSEPR theory must, as a rule, correspond to a linear combination of the delocalized MO's. That only the highest occupied (delocalized) MO is considered here to represent the lone pair can be rationalized when the energy values of all the MO's for this system are considered (the following energies are given in kK, $1kK=10^3$ cm^{-1}):
$\ldots[5a_1(-44.15)]^2[5e(-142.65)]^4[3b_1(-142.44)]^2[1a_2(-140.78)]^2$
$[6a_1(-73.45)]^2[7a_1(15.90)]^0[6e(28.22)]^0$. Clearly, the $6a_1$ MO stands alone between the occupied bonding orbitals and the empty antibonding orbitals and is, therefore, sometimes called a non-bonding orbital. Thus any linear combination of all the delocalized orbitals with suitable symmetry to represent the lone pair will have the $6a_1$ MO as the most significant contributor.

Satisfactory results have been obtained for BrF_5 in this manner. Further applicability of this model may be tested on other systems.

A system containing double bond(s) and lone pair(s) should be especially interesting, in view on the fact that the VSEPR theory is very vague when competition between these two kinds of electron pairs in the same coordination sphere is considered. Even with this apparent shortcoming, agreement with the VSEPR theory may be taken as a good evidence of validity for the nodal repulsion effect.

B. Second-Order Jahn-Teller Formalism [30,31]

A molecule may assume a particular nuclear arrangement which will place it in a certain symmetry group. By solving the Schrödinger equation for that system, a series of eigenvalues E_0, E_1, E_2, ...etc. and corresponding eigenstates ψ_0, ψ_1, ψ_2, ...etc. may be obtained. When a distortion of the nuclei is made according to some normal displacements, there may be a resulting raising or lowering in the energy of the system as a whole compared with its original ground state energy. Using perturbation theory, an expression for the change in energy with respect to any one of the normal displacements can be derived. A brief description of this expression is given below.

In order to treat the distortion by perturbation theory, the Hamiltonian $\mathcal{H}$ is expanded as a power series in Q, the displacement coordinate from the original position:

$$\mathcal{H} = \mathcal{H}^{\circ} + (\partial U/\partial Q)Q + (Q^2/2)(\partial^2 U/\partial Q^2) + \ldots \qquad (1)$$

where $\mathcal{H}^{\circ}$ is the unperturbed Hamiltonian and U is the nuclear-nuclear and nuclear-electronic potential energy. The derivatives $(\partial U/\partial Q)$ and $(\partial^2 U/\partial Q^2)$ may be viewed as the shift in potential energy experienced by the electrons when the nuclei are displaced, and rate of change of nuclear repulsion energy respectively. Furthermore, $(\partial U/\partial Q)$ has the symmetry property of the normal coordinate and $(\partial^2 U/\partial Q^2)$ is totally symmetric. Now the ground electronic state energy becomes

$$E = E_0 + Q\langle 0|\partial U/\partial Q|0\rangle + (Q^2/2)\left\{\langle 0|\partial^2 U/\partial Q^2|0\rangle + 2\sum_{p\neq 0}[\langle 0|\partial U/\partial Q|p\rangle]^2/(E_0 - E_p)\right\} + \ldots \quad (2)$$

In this expression for E, the second term is the 1st order Jahn-Teller term which, for non-linear systems, is non-zero only if the original wave function is degenerate. The third term consists of two parts, the former being a positive term owing to the fact that the original wave function is found by optimizing the energy with respect to the assumed coordinate; the latter, however, may be negative because it corresponds to changing the wave function to fit the new environment. This final term, as a whole, will have effect when $\langle 0|\partial U/\partial Q|p\rangle$ is non-vanishing and if the associated energy gap is sufficiently small. Pearson has arbitrarily set this limit of "smallness" to be 4 e.V. [30].

Whether a molecule is stable towards a certain geometrical structure depends on the magnitude and sign of the above-mentioned final term. A large and positive value indicates a stable molecule

with the assumed structure. This value, then, is a measure of the physical force constant for that particular vibration mode having the same symmetry as Q. A small value implies non-rigidity and the molecule, upon activation, is liable to transform into a new structure designated by the symmetry of the product of the concerned states. When the value is negative, the molecule will be unstable with the assumed structure, and spontaneous readjustment of nuclei coordinates will take place.

Even though the last term requires the summation over all the excited states, in actual practice, only the terms corresponding to the lowest one or two excited states need be considered. Though not completely dependent on these two, it is reasonable to assert that they have the largest contribution. Due to the denominator $(E_0 - E_p)$, the energy gap between the ground state and low lying excited states has quite an effect on the second-order Jahn-Teller term [third term in eq. (2)]. It is not because of the smallness of this value that will lead to significant lowering in energy, but because the magnitude of the interaction between the states is highly dependent on their difference in energy.

To show how the SOJT approach may affect the structure of a certain molecule, the following example is taken out of Pearson's paper [30] as an illustration. If SF_4 is assumed to have tetrahedral (T_d) symmetry,

the MO sequence has the order

$$(1a_1)^2(1t_2)^6(2a_1)^2(2t_2)^6(3t_2)^6(1e)^4(1t_1)^6(3a_1)^2(4t_2)^0.$$

The symmetry of the transition density, i.e. $\psi_0 \psi_1$, is T_2 which is the mode of vibration taking SF_4 into the structure of C_{2v} symmetry. When SF_4 is assumed to be square planar (D_{4h}), the corresponding MO sequence would be

$$\ldots (b_{2u})^2(3e_u)^4(a_{2g})^2(3b_{1g})^2(4a_{1g})^2(2a_{2u})^0(4e_u)^0.$$

Now the transition density between the ground and the first excited states has A_{2u} symmetry. However, the energies of the $3b_{1g}$ and $4a_{1g}$ orbitals are approximately the same and the energy gap between them and the $2a_{2u}$ orbital is only about 2.5 e.V. Hence both the A_{2u} and B_{2u} modes of vibration will take effect, and their combination will distort the molecule, leading it again to the C_{2v} structure which is found experimentally.

Chapter III

APPROXIMATE MOLECULAR ORBITAL METHOD EMPLOYED

The molecular orbital theory consists of different degrees of complexity. Among them, the most widely employed method is the LCAO-MO formalism. In this method, the molecular wave function is taken to be a linear combination of the participating atomic wave functions. Each of the molecular wave function (MO) may be represented by an expression $\sum_j C_{ij}\phi_j$, where ϕ_j is the j-th atomic orbital (AO) and C_{ij} is the coefficient for the j-th AO in the i-th molecular wave function. By minimizing the orbital energy with respect to the C_{ij}'s, secular equations of the form $\left|H_{ij} - ES_{ij}\right| = 0$ are resulted. So the main difficulty remained then is the evaluation of the overlap (S_{ij}) and Hamiltonian (H_{ij}) matrix elements. It is at this stage that different levels of approximation are taken. In the present work, the Wolfsberg-Helmholz (WH) method has been employed [27].

In the WH scheme, it is assumed that the exchange integrals, H_{ij}, are proportional to the overlap integrals as well as the stabilities of the concerned atomic orbitals:

$$\psi_M \phi_L \simeq \tfrac{1}{2} G_{ML} (\psi_M \psi_M + \phi_L \phi_L), \tag{3}$$

$$\therefore \quad H_{ij} = k[(H_{ii} + H_{jj})/2]\, G_{ij} \quad ; \tag{4}$$

$$\text{or} \quad H_{ij} = -k\,(H_{ii} H_{jj})^{\frac{1}{2}}\, G_{ij} \quad . \tag{5}$$

In equation (3)-(5), ψ_M and ϕ_L are the AO's on atoms M and L respectively; H_{ii} and H_{ij} are the valence state ionization potentials (VSIP) for the i-th and j-th AO's respectively; k is the WH constant which is usually taken to be 2 [32]; G_{ML} is the overlap between the AO's ψ_M and ϕ_L; and G_{ij} is the "group overlap" between the i-th and j-th AO's . The value of 2 for k is arbitrarily chosen in order to fit the electronic spectra of transition metal complexes [27] where this model was first applied. In this work, the geometrical mean approximation for H_{ij} i.e., equation (5), is adopted.

In the actual calculation, the AO's of the ligands are linearly combined to match in symmetry with the AO's of the central atom. (There will be one set of secular equations for each symmetry species.) Then, the overlap between every two entries of the secular determinant, i.e., the group overlap G_{ij}, is calculated. The overlap G_{ij} is usually a function of the σ- and/or π-type two-atom overlaps in terms of two-atom overlaps which is described in detail in the literature [32] and will not be further discussed here.

A more sophisticated WH treatment takes into account the ligand-ligand overlap in the linear combination of ligand AO's. For example, for the simple linear combination $(2)^{-\frac{1}{2}}(s_1-s_2)$, when ligand-ligand overlap is considered the normalized linear combination has the form $(2)^{-\frac{1}{2}}(s_1-s_2)/[1 - S(s_L,s_L,R')]^{\frac{1}{2}}$, where $S(s_L,s_L,R')$ is

the overlap between the ligand s orbitals whose centers are separated by the distance R'. For octahedral and tetrahedral systems, where more complicated linear combinations are encounted, reference [32] may be consulted. In this work, the correction factor due to ligand-ligand overlap is included for consideration.

The Coulomb integrals, H_{ii}, are just the VSIP for the concerned AO, which also should be corrected for ligand-ligand overlap, if there is any. The VSIP of a certain AO is a function of the charge and orbital configuration of the atom. The VSIP's for different atoms have been well tabulated in the literature, from where such parameters employed in the present work are taken.

When there is a net positive (negative) overlap in the ligand group orbital, a corresponding lowering (raising) in energy of that orbital as a whole is resulted. If X_i stands for the net overlap between the fundamental AO's in the linear combination, applying the WH approximation for differently centered AO's, the corrected H_{ii} will take the form [32]

$$H_{ii} = H'_{ii} (1 + 2 X_i)/(1 + X_i) , \qquad (6)$$

where H'_{ii} stands for the uncorrected Coulomb integral of the i-th orbital.

As a final remark for this Chapter, it should be pointed out that the method of calculation as well as the parameters employed in such a calculation have been applied, to a varying degree of success, to different chemical systems. Therefore, the degree of success of the present calculation may also be viewed as a test for the method and the empirical parameters.

Chapter IV

DETAILS OF CALCULATION

A. Symmetry Basis Functions

The accuracy of MO calculations may be obtained to any degree by appropriate adjustment of the number of basis functions employed in the LCAO expansion. For convenience and compatibility, the valence basis set is used in the present calculation without consideration for d orbitals in xenon and sulfur compounds because of the afore-mentioned reasons (chapter I). Except the orbitals of the central atom, almost all the others are not individually basis functions for an irreducible representation in the symmetry under consideration. It is, therefore, necessary to construct symmetry basis functions (group orbitals). According to Ballhausen and Gray [32], this can be attained with the help of the character tables for the required symmetry.

The group orbitals can first be normalized with the zero-overlap approximation. However, the ligand valence orbitals overlap is in reality different from zero, this should be considered when the group orbitals are normalized. Using similar techniques as did Ballhansen and Gray [32], the required renormalization process is performed for all the ligand group orbitals, for every structure assumed for each molecule a table of the groupings will be given forming the basis for the calculations. These are given in Tavles IV to IX with R being the averaged bond length used for calculation. (see part D in this chapter).

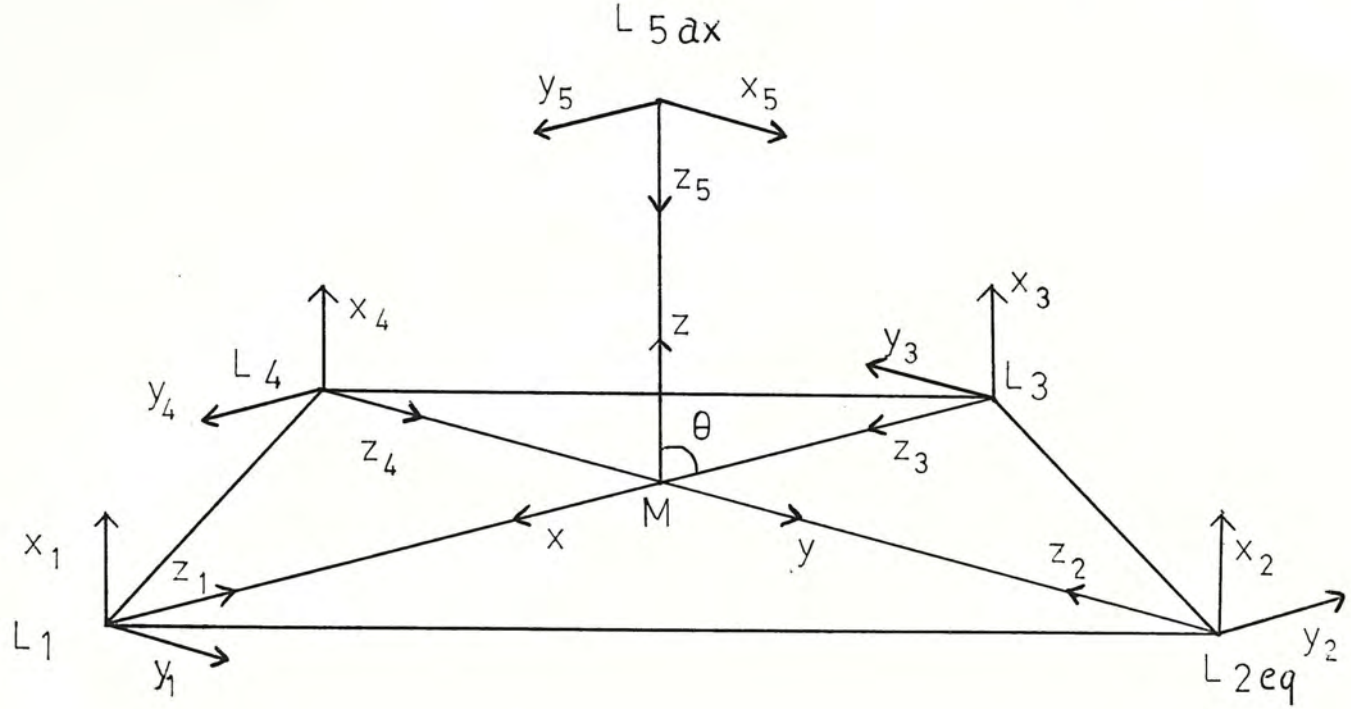

Fig. 4 Co-ordinate System for C_{4v} Symmetry $[XeOF_4, PH_5]$

Irreducible Representation	Central Atom M	Ligands (equatorial) L_1, L_2, L_3, L_4	Ligand (axial) L_5
a_1	s	$\dfrac{(s_1 + s_2 + s_3 + s_4)}{2[1+S(s_L,s_L,2R)+2S(s_L,s_L,1.414R)]^{\frac{1}{2}}}$	s_5
	p_z	$\dfrac{(z_1 + z_2 + z_3 + z_4)}{2[1+S(p_L,p_L,\sigma,2R)+S(p_L,p_L,\sigma,1.414R)+S(p_L,p_L,\pi,1.414R)]^{\frac{1}{2}}}$	z_5
	d_{z^2}	$\dfrac{(x_1 + x_2 + x_3 + x_4)}{2[1+S(p_L,p_L,\pi,2R)+2S(p_L,p_L,\pi,1.414R)]^{\frac{1}{2}}}$	
a_2		$\dfrac{(y_1 + y_2 + y_3 + y_4)}{2[1+S(p_L,p_L,\pi,2R)-S(p_L,p_L,\pi,1.414R)-S(p_L,p_L,\sigma,1.414R)]^{\frac{1}{2}}}$	
b_1	$d_{x^2-y^2}$	$\dfrac{(s_1 - s_2 + s_3 - s_4)}{2[1-2S(s_L,s_L,1.414R)+S(s_L,s_L,2R)]^{\frac{1}{2}}}$	

Table IV. (cont'd)

$$\frac{(z_1 - z_2 + z_3 - z_4)}{2[1-S(p_L,p_L,\sigma,1.414R)-S(p_L,p_L,\pi,1.414R)+S(p_L,p_L,\sigma,2R)]^{\frac{1}{2}}}$$

$$\frac{(x_1 - x_2 + x_3 - x_4)}{2[1-2S(p_L,p_L,\pi,1.414R)+S(p_L,p_L,\pi,2R)]^{\frac{1}{2}}}$$

b_2 $\quad$ d_{xy} $\quad$ $\dfrac{(y_1 - y_2 + y_3 - y_4)}{2[1-S(p_L,p_L,\pi,2R)+S(p_L,p_L,\pi,1.414R)+S(p_L,p_L,\sigma,1.414R)]^{\frac{1}{2}}}$

e $\quad$ p_x $\quad$ $\dfrac{(s_1 - s_3)}{2^{\frac{1}{2}}[1-S(s_L,s_L,2R)]^{\frac{1}{2}}}$, $\dfrac{(z_1 - z_3)}{2^{\frac{1}{2}}[1-S(p_L,p_L,\sigma,2R)]^{\frac{1}{2}}}$ $\quad$ y_5

d_{xz} $\quad$ $\dfrac{(x_1 - x_3)}{2^{\frac{1}{2}}[1-S(p_L,p_L,\pi,2R)]^{\frac{1}{2}}}$. , $\dfrac{(y_4 - y_2)}{2^{\frac{1}{2}}[1+S(p_L,p_L,\pi,2R)]^{\frac{1}{2}}}$

Table IV. (cont'd)

p_y	$\dfrac{(s_2 - s_4)}{2^{\frac{1}{2}}[1-S(s_L,s_L,2R)]^{\frac{1}{2}}}$,	$\dfrac{(z_2 - z_4)}{2^{\frac{1}{2}}[1-S(p_L,p_L\sigma,2R)]^{\frac{1}{2}}}$	x_5
d_{yz}	$\dfrac{(x_2 - x_4)}{2^{\frac{1}{2}}[1-S(p_L,p_L,\pi,2R)]^{\frac{1}{2}}}$,	$\dfrac{(y_1 - y_3)}{2^{\frac{1}{2}}[1+S(p_L,p_L,\pi,2R)]^{\frac{1}{2}}}$	

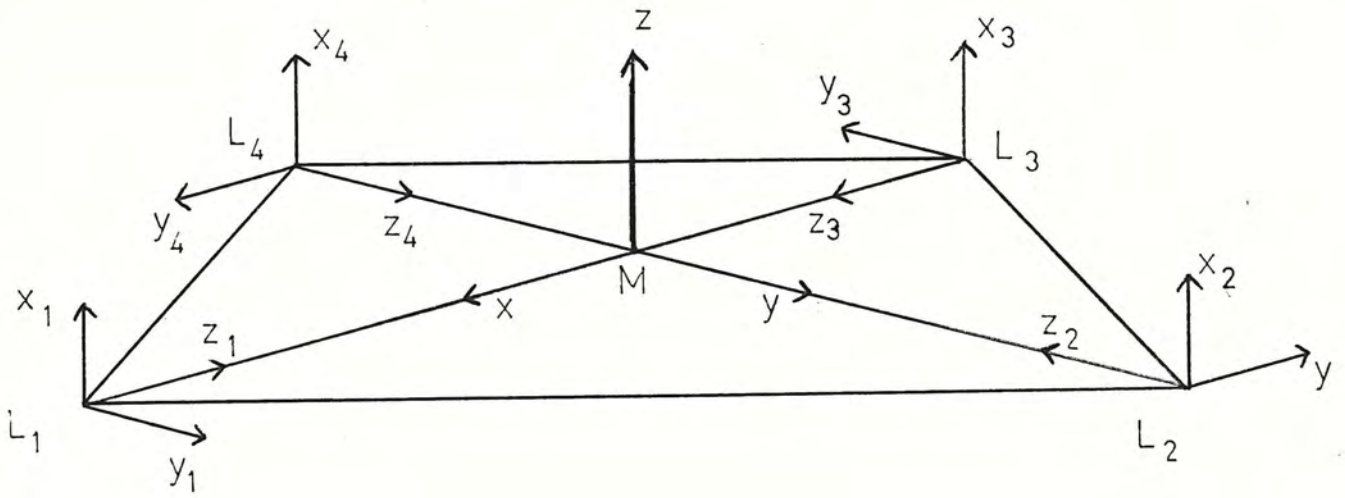

Fig. 5 Co-ordinate System for D_{4h} Symmetry $[SF_4]$

Table V. The Symmetry Basis Functions for D_{4h} Symmetry

Irreducible Representation	Central Atom M	Ligands L_1, L_2, L_3, L_4
a_{1g}	s	$\dfrac{(s_1 + s_2 + s_3 + s_4)}{2[1+S(s_L, s_L, 2R)+2S(s_L, s_L 1.414R)]^{\frac{1}{2}}}$
	d_{z^2}	$\dfrac{(z_1 + z_2 + z_3 + z_4)}{2[1+S(p_L, p_L, \sigma, 2R)+S(p_L, p_L, \sigma, 1.414R)+S(p_L, p_L \pi, 1.414R)]^{\frac{1}{2}}}$
a_{2u}	p_{z^2}	$\dfrac{(x_1 + x_2 + x_3 + x_4)}{2[1+S(p_L, p_L \pi, 2R)+2S(p_L, p_L, \pi, 1.414R)]^{\frac{1}{2}}}$
a_{2g}		$\dfrac{(y_1 + y_2 + y_3 + y_4)}{2[1+S(p_L, p_L, \pi, 2R)-S(p_L, p_L, \pi, 1.414R)-S(p_L, p_L \sigma, 1.414R)]^{\frac{1}{2}}}$
b_{1g}	$d_{x^2-y^2}$	$\dfrac{(s_1 - s_2 + s_3 - s_4)}{2[1-2S(s_L, s_L, 1.414R)+S(s_L, s_L 2R)]^{\frac{1}{2}}}$

Table V. (cont'd)

$$\frac{(z_1 - z_2 + z_3 - z_4)}{2[1-S(p_L,p_L,\sigma,1.414R)-S(p_L,p_L\pi,1.414R)+S(p_L,p_L\tfrac{1}{2},2R)]^{\frac{1}{2}}}$$

b_{2u}

$$\frac{(x_1 - x_2 + x_3 - x_4)}{2[1-2S(p_L,p_L,\pi,1.414R)+S(p_L,p_L,\pi,2R)]^{\frac{1}{2}}}$$

b_{2g} d_{xy}

$$\frac{(y_1 - y_2 + y_3 - y_4)}{2[1-S(p_L,p_L\pi,2R)+S(p_L,p_L,\pi,1.414R)+S(p_L,p_L,\sigma,1.414R)]^{\frac{1}{2}}}$$

e_u p_x

$$\frac{(s_1 - s_3)}{2^{\frac{1}{2}}[1-S(s_L,s_L2R)]^{\frac{1}{2}}} \quad , \quad \frac{(z_1 - z_3)}{2^{\frac{1}{2}}[1-S(p_L,p_L\sigma,2R)]^{\frac{1}{2}}}$$

$$\frac{(y_4 - y_2)}{2^{\frac{1}{2}}[1+S(p_L,p_L,\pi,2R)]^{\frac{1}{2}}}$$

Table V. (cont'd)

	p_y	$\dfrac{(s_2 - s_4)}{2^{\frac{1}{2}}[1-S(s_L,s_L 2R)]^{\frac{1}{2}}}$,	$\dfrac{(z_2 - z_4)}{2^{\frac{1}{2}}[1-S(p_L,p_L,\sigma,2R)]^{\frac{1}{2}}}$
		$\dfrac{(y_1 - y_3)}{2^{\frac{1}{2}}[1+S(p_L,p_L,\pi,2R)]^{\frac{1}{2}}}$	
e_g	d_{xz}	$\dfrac{(x_1 - x_3)}{2^{\frac{1}{2}}[1-S(p_L,p_L,\pi,2R)]^{\frac{1}{2}}}$	
	d_{yz}	$\dfrac{(x_2 - x_4)}{2^{\frac{1}{2}}[1-S(p_L,p_L,\pi,2R)]^{\frac{1}{2}}}$	

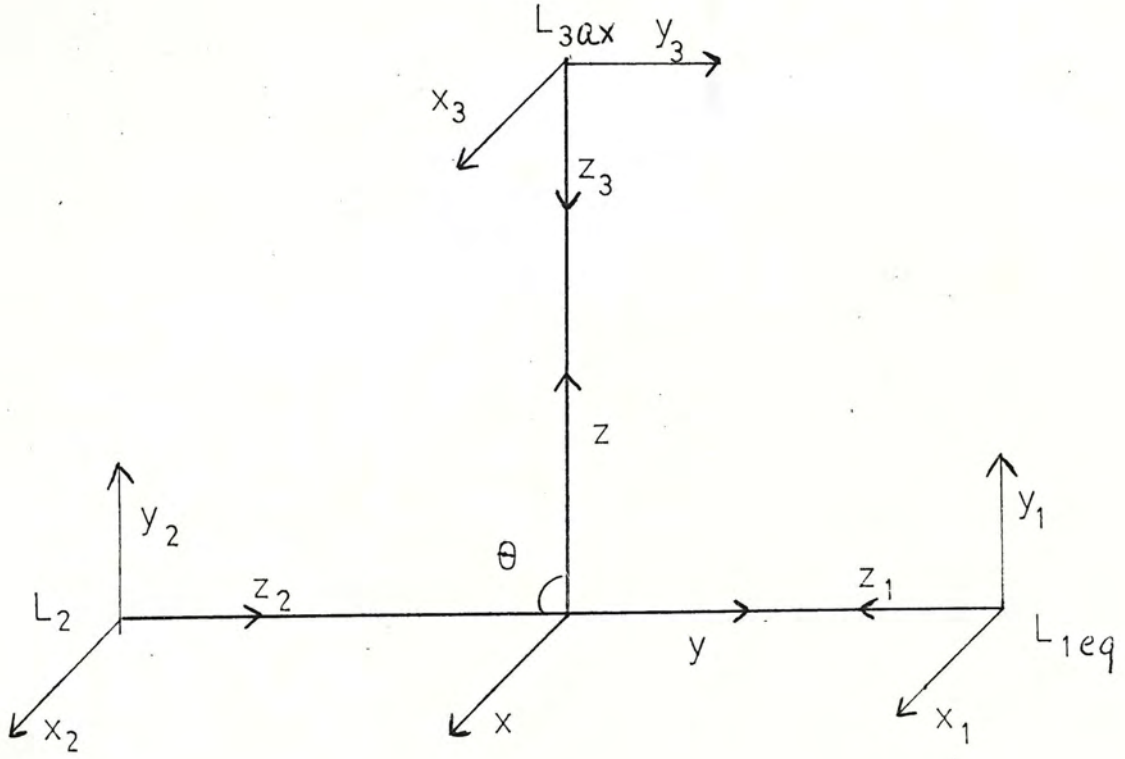

Fig. 6 Co-ordinate System for C_{2v} Symmetry [$XeOF_2$]

Table VIa. The Symmetry Basis Functions for C_{2v} Symmetry (T-shaped molecules)

Irreducible Representation	Central Atom M	Ligands (equatorial) L_1, L_2	Ligand (axial) L_3
a_1	s	$\dfrac{(s_1 + s_2)}{2^{\frac{1}{2}}[1+S(s_L, s_L, 2R)]^{\frac{1}{2}}}$	s_3
	p_z	$\dfrac{(z_1 + z_2)}{2^{\frac{1}{2}}[1+S(p_L, p_L, \sigma, 2R)]^{\frac{1}{2}}}$	z_3
	d_{z^2}	$\dfrac{(y_1 + y_2)}{2^{\frac{1}{2}}[1+S(p_L, p_L, \pi, 2R)]^{\frac{1}{2}}}$	
	$d_{x^2-y^2}$		
a_2	d_{xy}	$\dfrac{(x_1 - x_2)}{2^{\frac{1}{2}}[1-S(p_L, p_L, \pi, 2R)]^{\frac{1}{2}}}$	

Table VIa. (cont'd)

b_1	p_x, d_{xz}	$\dfrac{(x_1 + x_2)}{2^{\frac{1}{2}}[1+S(p_L,p_L,\pi,2R)]^{\frac{1}{2}}}$	x_3
b_2	p_y	$\dfrac{(s_1 - s_2)}{2^{\frac{1}{2}}[1-S(s_L,s_L,2R)]^{\frac{1}{2}}}$	y_3
	d_{yz}	$\dfrac{(z_1 - z_2)}{2^{\frac{1}{2}}[1-S(p_L,p_L,\sigma,2R)]^{\frac{1}{2}}}$	
		$\dfrac{(y_1 - y_2)}{2^{\frac{1}{2}}[1-S(p_L,p_L,\pi,2R)]^{\frac{1}{2}}}$	

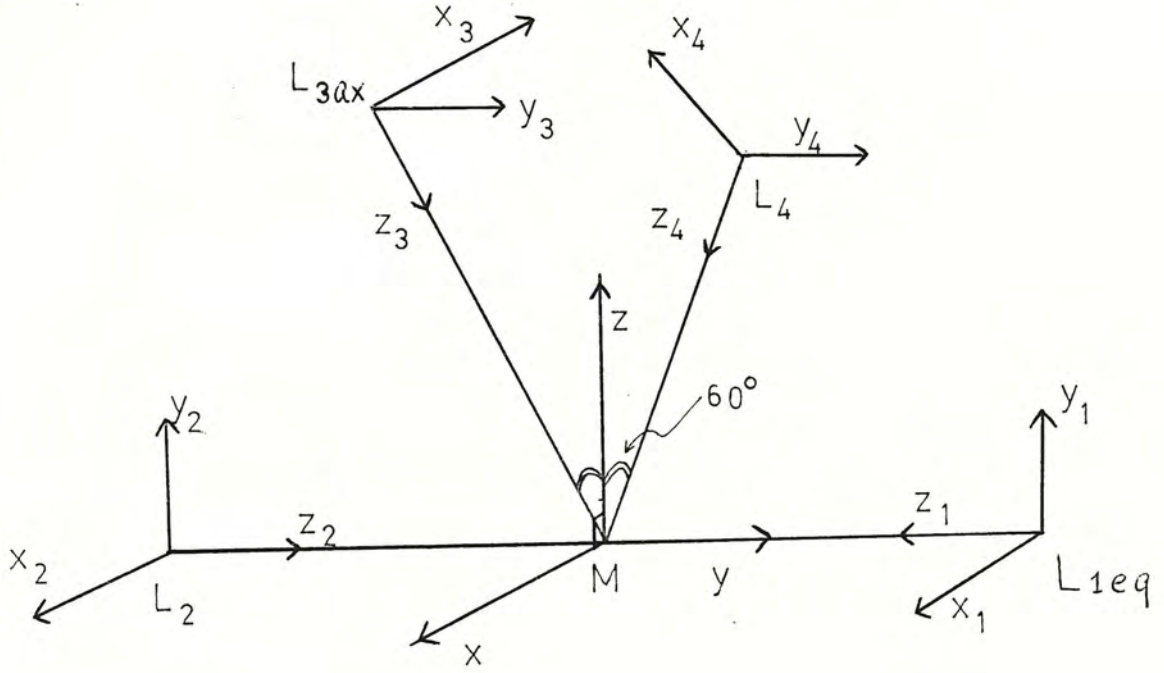

Fig. 7. Co-ordinate System for C_{2v} Symmetry $[XeO_2F_2, SF_4]$

Table VIb. The Symmetry Basis Functions for C_{2v} Symmetry (Distorted Tetrahedral Molecules)

Irreducible Representation	Central Atom M	Ligands (equatorial) L_1, L_2	Ligands (axial) L_3, L_4
a_1	s	$\dfrac{(s_1 + s_2)}{2^{\frac{1}{2}}[1+S(s_L, s_L, 2R)]^{\frac{1}{2}}}$	$\dfrac{(s_3 + s_4)}{2^{\frac{1}{2}}[1+S(s_L, s_L, 1.732R)]^{\frac{1}{2}}}$
	p_z	$\dfrac{(z_1 + z_2)}{2^{\frac{1}{2}}[1+S(p_L, p_L, \sigma, 2R)]^{\frac{1}{2}}}$	$\dfrac{(z_3 + z_4)}{2^{\frac{1}{2}}[1+.75S(p_L, p_L, \sigma, 1.732R)+.25S(p_L, p_L, \pi, 1.732R)]^{\frac{1}{2}}}$
	d_{z^2}		
	$d_{x^2-y^2}$	$\dfrac{(y_1 + y_2)}{2^{\frac{1}{2}}[1+S(p_L, p_L, \pi, 2R)]^{\frac{1}{2}}}$	$\dfrac{(x_3 + x_4)}{2^{\frac{1}{2}}[1+.25S(p_L, p_L, \sigma, 1.732R)+.75S(p_L, p_L, \pi, 1.732R)]^{\frac{1}{2}}}$
a_2	d_{xy}	$\dfrac{(x_1 - x_2)}{2^{\frac{1}{2}}[1-S(p_L, p_L, \pi, 2R)]^{\frac{1}{2}}}$	$\dfrac{(y_3 - y_4)}{2^{\frac{1}{2}}[1-S(p_L, p_L, \pi, 1.732R)]^{\frac{1}{2}}}$

Table VIb. (cont'd)

b_1	p_x	$\dfrac{(x_1 + x_2)}{2^{\frac{1}{2}}[1+S(p_L,p_L,\pi,2R)]^{\frac{1}{2}}}$	$\dfrac{(s_3 - s_4)}{2^{\frac{1}{2}}[1-S(s_L,s_L,1.732R)]^{\frac{1}{2}}}$
	d_{xz}		$\dfrac{(z_3 - z_4)}{2^{\frac{1}{2}}[1-.75S(p_L,p_L,\sigma,1.732R)-.25S(p_L,p_L,\pi,1.732R)]^{\frac{1}{2}}}$
b_2	p_y	$\dfrac{(s_1 - s_2)}{2^{\frac{1}{2}}[1-S(s_L,s_L,2R)]^{\frac{1}{2}}}$	$\dfrac{(y_3 + y_4)}{2^{\frac{1}{2}}[1+S(p_L,p_L,\pi,1.732R)]^{\frac{1}{2}}}$
		$\dfrac{(z_1 - z_2)}{2^{\frac{1}{2}}[1-S(p_L,p_L,\sigma,2R)]^{\frac{1}{2}}}$	
		$\dfrac{(y_1 - y_2)}{2^{\frac{1}{2}}[1-S(p_L,p_L,\pi,2R)]^{\frac{1}{2}}}$	

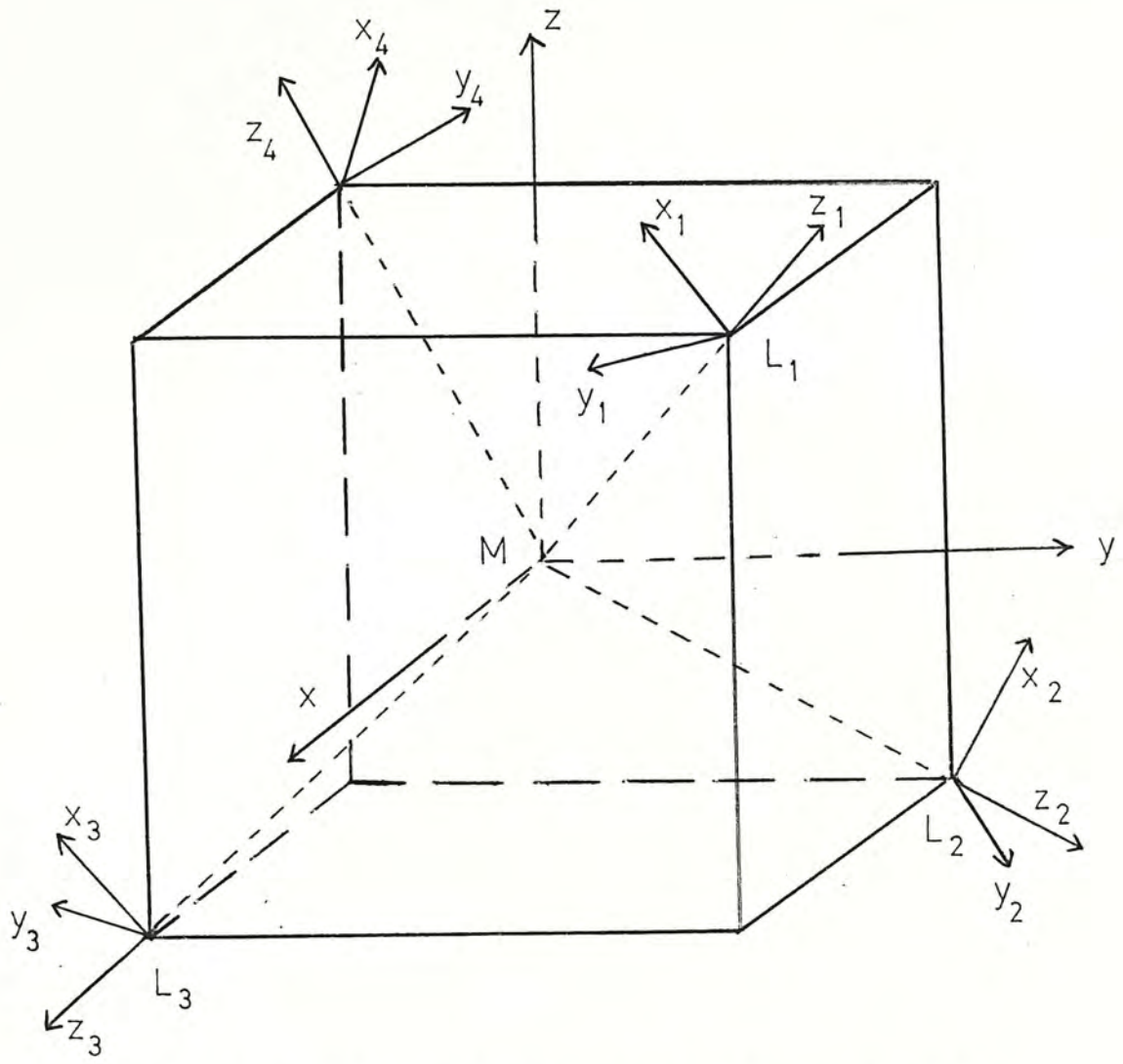

Fig. 8 Co-ordinate System for T_d Symmetry $[SF_4]$

Table VII. The Symmetry Basis Functions for T_d Symmetry

Irreducible Representation	Central Atom M	Ligands L_1, L_2, L_3, L_4
a_1	s	$\frac{(s_1 + s_2 + s_3 + s_4)}{2[1+3S(s_L, s_L, 3.266R)]^{\frac{1}{2}}}$
		$\frac{(z_1 + z_2 + z_3 + z_4)}{2[1+2S(p_L, p_L, \sigma, 3.266R)+S(p_L, p_L, \pi, 3.266R)]^{\frac{1}{2}}}$
e		$\frac{(x_1 - x_2 - x_3 + x_4)}{2[1+.5S(p_L, p_L, \sigma, 3.266R)-.5S(p_L, p_L, \pi, 3.266R)]^{\frac{1}{2}}}$
		$\frac{(y_1 - y_2 - y_3 + y_4)}{2[1+.5S(p_L, p_L, \sigma, 3.266R)-.5S(p_L, p_L, \pi, 3.266R)]^{\frac{1}{2}}}$
t_2	p_z	$\frac{(z_1 - z_2 - z_3 + z_4)}{2[1-.67S(p_L, p_L, \sigma, 3.266R)-.33S(p_L, p_L, \pi, 3.266R)]^{\frac{1}{2}}}$

Table VII. (cont'd)

$$\frac{(s_1 - s_2 - s_3 + s_4)}{2[1-S(s_L,s_L,3.266R)]^{\frac{1}{2}}}$$

$$\frac{-(x_1 + x_2 + x_3 + x_4)}{2[1+.33S(p_L,p_L,\sigma,3.266R)+1.83S(p_L,p_L,\pi,3.266R)]^{\frac{1}{2}}}$$

p_x

$$\frac{(z_1 - z_2 + z_3 - z_4)}{2[1-.67S(p_L,p_L,\sigma,3.266R)-.33S(p_L,p_L,\pi,3.266R)]^{\frac{1}{2}}}$$

$$\frac{(s_1 - s_2 + s_3 - s_4)}{2[1-S(s_L,s_L,3.266R)]^{\frac{1}{2}}}$$

$$\frac{[x_1+x_2-x_3-x_4+1.732(-y_1-y_2+y_3+y_4)]}{4[1+.33S(p_L,p_L,\sigma,3.266R)+1.83S(p_L,p_L,\pi,3.266R)]^{\frac{1}{2}}}$$

Table VII. (cont'd)

p_y

$$\frac{(z_1 + z_2 - z_3 - z_4)}{2[1-.67S(p_L,p_L,\sigma,3.266R)-.33S(p_L,p_L,\pi,3.266R)]^{\frac{1}{2}}}$$

$$\frac{(s_1 + s_2 - s_3 - s_4)}{2[1-S(s_L,s_L3.266R)]^{\frac{1}{2}}}$$

$$\frac{[x_1-x_2+x_3-x_4+1.732(y_1-y_2+y_3-y_4)}{4[1+.33S(p_L,p_L,\sigma,3.266R)+1.83S(p_L,p_L,\pi,3.266R)]^{\frac{1}{2}}}$$

t_1

$$\frac{(y_1 + y_2 + y_3 + y_4)}{2[1-.5S(p_L,p_L,\sigma,3.266R)-1.5S(p_L,p_L,\pi,3.266R)]^{\frac{1}{2}}}$$

$$\frac{[1.732(x_1+x_2-x_3-x_4)+y_1+y_2-y_3-y_4]}{4[1-.5S(p_L,p_L,\sigma,3.266R)-1.5S(p_L,p_L,\pi,3.266R)]^{\frac{1}{2}}}$$

$$\frac{[1.732(x_1-x_2+x_3-x_4)-y_1+y_2-y_3+y_4}{4[1-.5S(p_L,p_L,\sigma,3.266R)-1.5S(p_L,p_L,\pi,3.266R)]^{\frac{1}{2}}}$$

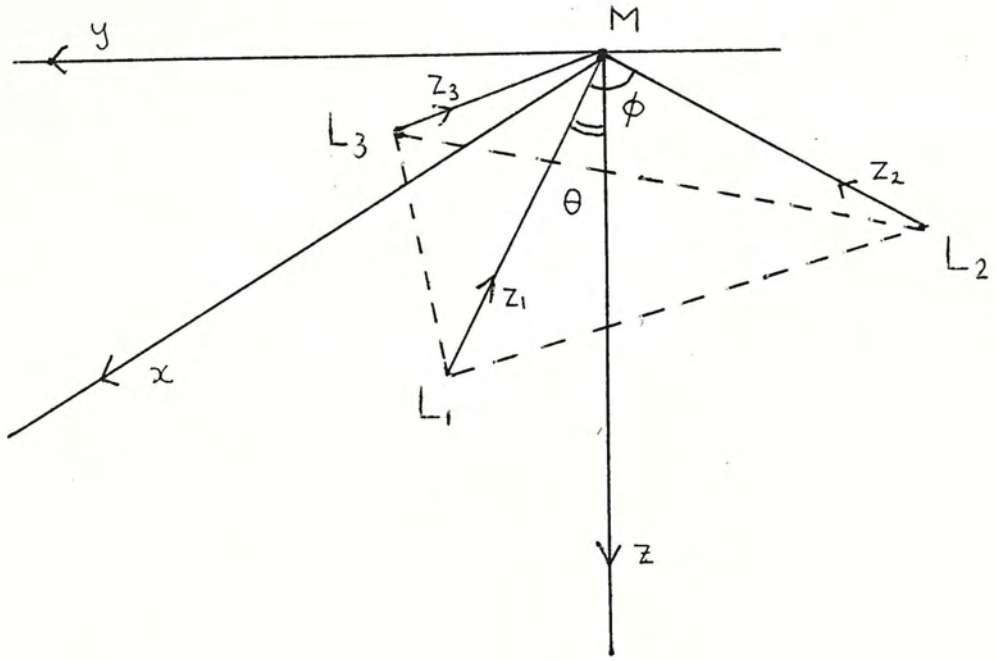

Fig. 9 Coordinate System for C_{3v} Symmetry $[PH_3]$.

Table VIII. The Symmetry Basis Functions for C_{3v} Symmetry

Irreducible Representation	Central Atom M	Ligands L_1, L_2, L_3
a_1	s , p_z	$\frac{(s_1 + s_2 + s_3)}{3^{\frac{1}{2}}[1+2S(s_L, s_L 1.46R)]^{\frac{1}{2}}}$
e	p_x	$\frac{(2s_1 - s_2 - s_3)}{3^{\frac{1}{2}}[2-3S(s_L, s_L 1.46R)]^{\frac{1}{2}}}$
	p_y	$\frac{(s_3 - s_2)}{2^{\frac{1}{2}}[1-S(s_L, s_L, 1.46R)]^{\frac{1}{2}}}$

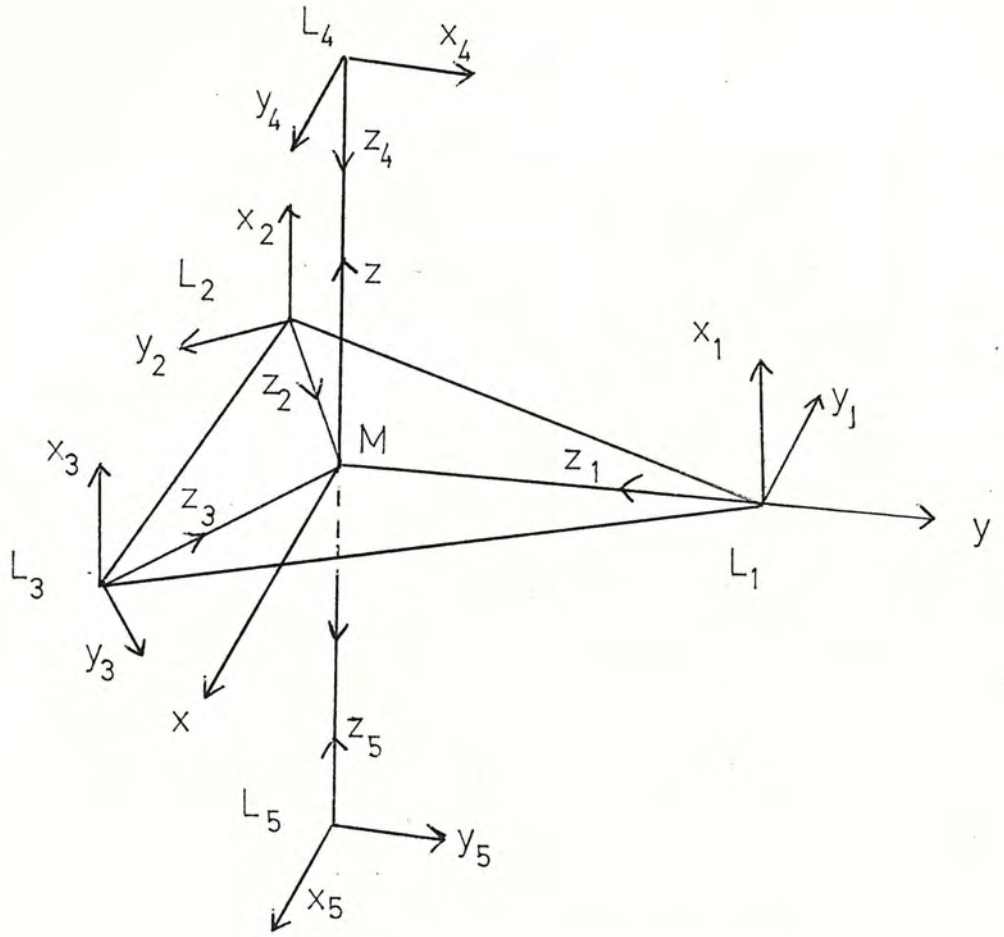

Fig. 10 Co-ordinate System for D_{3h} Symmetry $[PH_5]$

Table IX. The Symmetry Basis Functions for D_{3h} Symmetry

Irreducible Representation	Central Atom M	Ligands (equatorial) L_1, L_2, L_3	Ligands (axial) L_4, L_5
a_1'	s , d_{z^2}	$\dfrac{(s_1 + s_2 + s_3)}{3^{\frac{1}{2}}[1+2S(s_L, s_L, 1.46R)]^{\frac{1}{2}}}$	$\dfrac{(s_4 + s_5)}{2^{\frac{1}{2}}[1+S(s_L, s_L, 1.46R)]^{\frac{1}{2}}}$
a_2''	p_z		$\dfrac{(s_4 - s_5)}{2^{\frac{1}{2}}[1-S(s_L, s_L, 1.46R)]^{\frac{1}{2}}}$
e'	p_x , d_{xy}	$\dfrac{(s_2 - s_3)}{2^{\frac{1}{2}}[1-S(s_L, s_L, 1.46R)]^{\frac{1}{2}}}$	
	p_y , $d_{x^2-y^2}$	$\dfrac{(2s_1 - s_2 - s_3)}{3^{\frac{1}{2}}[2-3S(s_L, s_L, 1.46R)]^{\frac{1}{2}}}$	
e''	d_{xz}		
	d_{yz}		

B. The Expressions for Group Overlaps

As mentioned before (Chapter III), the group overlap between every two entries in the overlap matrix may be expressed in terms of two-atom overlap integrals. The techniques for obtaining these expression have been well described in, for example, Ballhausen and Gray [32]. A complete listing of these expression may be found in Table X to XVII.

Table X. The Group Overlap Integrals and the Normalization Constants for C_{4v} Symmetry

a. The Normalization Constants

$$N(A_1,s_{eq}) = \tfrac{1}{2}[1+S(s_L,s_L,2R)+2S(s_L,s_L,2^{\frac{1}{2}}R)]^{-\frac{1}{2}}$$

$$N(A_1,p\sigma_{eq}) = \tfrac{1}{2}[1+S(p_L,p_L,\sigma,2R)+S(p_L,p_L,\sigma,2^{\frac{1}{2}}R)+S(p_L,p_L,\pi,2^{\frac{1}{2}}R)]^{-\frac{1}{2}}$$

$$N(A_1,p\pi_{xeq}) = \tfrac{1}{2}[1+S(p_L,p_L,\pi,2R)+2S(p_L,p_L,\pi,2^{\frac{1}{2}}R)]^{-\frac{1}{2}}$$

$$N(A_2,p\pi_{yeq}) = \tfrac{1}{2}[1+S(p_L,p_L,\pi,2R)-S(p_L,p_L,\pi,2^{\frac{1}{2}}R)-S(p_L,p_L\sigma,2^{\frac{1}{2}}R)]^{-\frac{1}{2}}$$

$$N(B_1,s_{eq}) = \tfrac{1}{2}[1-2S(s_L,s_L2^{\frac{1}{2}}R)+S(s_L,s_L2R)]^{-\frac{1}{2}}$$

$$N(B_1,p\sigma_{eq}) = \tfrac{1}{2}[1-S(p_L,p_L,\sigma,2^{\frac{1}{2}}R)-S(p_L,p_L,\pi,2^{\frac{1}{2}}R)+S(p_L,p_L,\sigma,2R)]^{-\frac{1}{2}}$$

$$N(B_1,p\pi_{xeq}) = \tfrac{1}{2}[1-2S(p_L,p_L,\pi,2^{\frac{1}{2}}R)+S(p_L,p_L,\pi,2R)]^{-\frac{1}{2}}$$

$$N(B_2,p\pi_{yeq}) = \tfrac{1}{2}[1-S(p_L,p_L,\pi,2R)+S(p_L,p_L,\pi,2^{\frac{1}{2}}R)+S(p_L,p_L,\sigma,2^{\frac{1}{2}}R)]^{-\frac{1}{2}}$$

$$N(E,s_{eq}) = [2-2S(s_L,s_L,2R)]^{-\frac{1}{2}}$$

$$N(E,p\sigma_{eq}) = [2-2S(p_L,p_L,\sigma,2R)]^{-\frac{1}{2}}$$

$$N(E,p\pi_{yeq}) = [2+2S(p_L,p_L,\pi,2R)]^{-\frac{1}{2}}$$

$$N(E,p\pi_{xeq}) = [2-2S(p_L,p_L,\pi,2R)]^{-\frac{1}{2}}$$

b. The Group Overlap Integrals

A_1 Symmetry

$$G(s_M,s_{eq}) = 4N(A_1,s_{eq})S(s_M,s_L,R)$$

$$G(s_M,p\sigma_{eq}) = 4N(A_1,p\sigma_{eq})S(s_M,p_L,R)$$

Table X. (Cont'd)

$G(p_M, p\pi_{eq}) = 4N(A_1, p\pi_{eq})S(p_M, p_L, \pi, R)$

$G(s_{ax}, s_{eq}) = 4N(A_1, s_{eq})S(s_{ax}, s_L, 2^{\frac{1}{2}}R)$

$G(s_{ax}, p\sigma_{eq}) = 8^{\frac{1}{2}}N(A_1, p\sigma_{eq})S(s_{ax}, p_L, 2^{\frac{1}{2}}R)$

$G(s_{ax}, p\pi_{eq}) = 8^{\frac{1}{2}}N(A_1, p\pi_{eq})S(s_{ax}, p_L, 2^{\frac{1}{2}}R)$

$G(s_{eq}, p\sigma_{eq}) = 4N(A_1, s_{eq})[S(s_L, p_L, 2R)+2^{\frac{1}{2}}S(s_L, p_L, 2^{\frac{1}{2}}R)]$

B_1 Symmetry

$G(s_{eq}, p\sigma_{eq}) = 4N(B_1, s_{eq})N(B_1, p\sigma_{eq})[2^{\frac{1}{2}}S(s_L, p_L, 2^{\frac{1}{2}}R)+S(s_L, p_L, 2R)]$

E Symmetry

$G(p_M, s_{eq}) = 2N(E, s_{eq})S(p_M, s_L, R)$

$G(p_M, p\sigma_{eq}) = 2N(E, p\sigma_{eq})S(p_M, p_L, \sigma, R)$

$G(p_M, p\pi_{yeq}) = 2N(E, p\pi_{yeq})S(p_M, p_L, \pi, R)$

$G(p_M, p_{ax}) = S(p_M, p_{ax}, \pi, R)$

$G(s_{eq}, p\sigma_{eq}) = -2N(E, s_{eq})N(E, p\sigma_{eq})S(s_L, p_L, 2R)$

$G(s_{eq}, p\pi_{yeq}) = 8^{\frac{1}{2}}N(E, s_{eq})N(E, p\pi_{yeq})S(s_L, p_L, 2^{\frac{1}{2}}R)$

$G(s_{eq}, p_{ax}) = 2^{\frac{1}{2}}N(E, s_{eq})S(s_L, p_{ax}, 2^{\frac{1}{2}}R)$

$G(p\sigma_{eq}, p\pi_{yeq}) = 2N(E, p\sigma_{eq})N(E, p\pi_{yeq})[S(p_L, p_L, \sigma, 2^{\frac{1}{2}}R)-S(p_L, p_L, \pi, 2^{\frac{1}{2}}R)]$

$G(p\sigma_{eq}, p_{ax}) = N(E, p\sigma_{eq})[S(p_L, p_{ax}, \sigma, 2^{\frac{1}{2}}R)-S(p_L, p_{ax}, \pi, 2^{\frac{1}{2}}R)]$

$G(p\pi_{xeq}, p_{ax}) = N(E, p\pi_{xeq})[S(p_L, p_{ax}, \sigma, 2^{\frac{1}{2}}R)+S(p_L, p_{ax}, \pi, 2^{\frac{1}{2}}R)]$

$G(p\pi_{yeq}, p_{ax}) = 2N(E, p\pi_{yeq})S(p_L, p_{ax}, \pi, 2^{\frac{1}{2}}R)$

Table XI. The Group Overlap Integrals and the Normalization Constants for D_{4h} Symmetry

a. The Normalization Constants

$$N(A_{1g},s_{eq}) = \tfrac{1}{2}[1+S(s_L,s_L2R)+2S(s_L,s_L,2^{\frac{1}{2}}R)]^{-\frac{1}{2}}$$

$$N(A_{1g},p\sigma_{eq}) = \tfrac{1}{2}[1+S(p_L,p_L,\sigma,2R)+S(p_L,p_L,\sigma,2^{\frac{1}{2}}R)+S(p_L,p_L,\pi,2^{\frac{1}{2}}R)]^{-\frac{1}{2}}$$

$$N(A_{2u},p\pi_{xeq}) = \tfrac{1}{2}[1+S(p_L,p_L,\pi,2R)+2S(p_L,p_L,\pi,2^{\frac{1}{2}}R)]^{-\frac{1}{2}}$$

$$N(A_{2g},p\pi_{yeq}) = \tfrac{1}{2}[1+S(p_L,p_L,\pi,2R)-S(p_L,p_L,\pi,2^{\frac{1}{2}}R)-S(p_L,p_L,\sigma,2^{\frac{1}{2}}R)]^{-\frac{1}{2}}$$

$$N(B_{1g},s_{eq}) = \tfrac{1}{2}[1-2S(s_L,s_L,2^{\frac{1}{2}}R)+S(s_L,s_L,2R)]^{-\frac{1}{2}}$$

$$N(B_{1g},p\sigma_{eq}) = \tfrac{1}{2}[1-S(p_L,p_L,\sigma,2^{\frac{1}{2}}R)-S(p_L,p_L,\pi,2^{\frac{1}{2}}R)+S(p_L,p_L,\sigma,2R)]^{-\frac{1}{2}}$$

$$N(B_{2u},p\pi_{xeq}) = \tfrac{1}{2}[1-2S(p_L,p_L,\pi,2^{\frac{1}{2}}R)+S(p_L,p_L,\pi,2R)]^{-\frac{1}{2}}$$

$$N(B_{2g},p\pi_{yeq}) = \tfrac{1}{2}[1-S(p_L,p_L,\pi,2R)+S(p_L,p_L,\pi,2^{\frac{1}{2}}R)+S(p_L,p_L,\sigma,2^{\frac{1}{2}}R)]^{-\frac{1}{2}}$$

$$N(E_u,s_{eq}) = [2-2S(s_L,s_L,2R)]^{-\frac{1}{2}}$$

$$N(E_u,p\sigma_{eq}) = [2-2S(p_L,p_L,\sigma,2R)]^{-\frac{1}{2}}$$

$$N(E_u,p\pi_{yeq}) = [2+2S(p_L,p_L,\pi,2R)]^{-\frac{1}{2}}$$

b. The Group Overlap Integrals

A_{1g} Symmetry

$$G(s_M,s_{eq}) = 4N(A_{1g},s_{eq})S(s_M,s_L,R)$$

$$G(s_L,p\sigma_{eq}) = 4N(A_{1g},p\sigma_{eq})S(s_M,p_L,R)$$

$$G(s_{eq},p\sigma_{eq}) = 4N(A_{1g},s_{eq})N(A_{1g},p\sigma_{eq})[S(s_L,p_L,2R)+2^{\frac{1}{2}}S(s_L,p_L,2^{\frac{1}{2}}R)]$$

Table XI. (cont'd)

B_{lg} Symmetry

$$G(s_{eq},p\sigma_{eq}) = 4N(B_{lg},s_{eq})N(B_{lg},p\sigma_{eq})[S(s_L,p_L,2^{\frac{1}{2}}R)+S(s_L,p_L,2R)]$$

E_u Symmetry

$$G(p_M,s_{eq}) = 2N(E_u,s_{eq})S(p_M,s_L,R)$$

$$G(p_M,p\sigma_{eq}) = 2N(E_u,p\sigma_{eq})S(p_M,p_L,\sigma,R)$$

$$G(p_M,p\pi_{yeq}) = 2N(E_u,p\pi_{yeq})S(p_M,p_L,\pi,R)$$

$$G(s_{eq},p\sigma_{eq}) = -2N(E_u,s_{eq})N(E_u,p\sigma_{eq})S(s_L,p_L,2R)$$

$$G(s_{eq},p\pi_{yeq}) = 8^{\frac{1}{2}}N(E_u,s_{eq})N(E_u,p\pi_{yeq})S(s_L,p_L,2^{\frac{1}{2}}R)$$

$$G(p\sigma_{eq},p\pi_{yeq}) = 2N(E_u,p\sigma_{eq})N(E_u,p\pi_{yeq})[S(p_L,p_L,\sigma,2^{\frac{1}{2}}R)-S(p_L,p_L,\pi,2^{\frac{1}{2}}R)]$$

Table XII. The Group Overlap Integrals and Normalization Constants for C_{2v} Symmetry (T-shaped Molecules)

a. The Normalization Constants

$$N(A_1, s_{eq}) = [2+2S(s_L, s_L, 2R)]^{-\frac{1}{2}}$$

$$N(A_1, p\sigma_{eq}) = [2+2S(p_L, p_L, \sigma, 2R)]^{-\frac{1}{2}}$$

$$N(A_1, p\pi_{yeq}) = [2+2S(p_L, p_L, \pi, 2R)]^{-\frac{1}{2}}$$

$$N(A_2, p\pi_{xeq}) = [2-2S(p_L, p_L, \pi, 2R)]^{-\frac{1}{2}}$$

$$N(B_1, p\pi_{xeq}) = [2+2S(p_L, p_L, \pi, 2R)]^{-\frac{1}{2}}$$

$$N(B_2, s_{eq}) = [2-2S(s_L, s_L, 2R)]^{-\frac{1}{2}}$$

$$N(B_2, p\sigma_{eq}) = [2-2S(p_L, p_L, \sigma, 2R)]^{-\frac{1}{2}}$$

$$N(B_2, p\pi_{yeq}) = [2-2S(p_L, p_L, \pi, 2R)]^{-\frac{1}{2}}$$

b. The Group Overlap Integrals

A_1 Symmetry

$$G(s_M, s_{eq}) = 2N(A_1, s_{eq})S(s_M, s_L, R)$$

$$G(s_M, s_{ax}) = S(s_M, s_{ax}, R)$$

$$G(s_M, p\sigma_{eq}) = 2N(A_1, p\sigma_{eq})S(s_M, p_L, R)$$

$$G(s_M, p_{ax}) = S(s_M, p_{ax}, R)$$

$$G(p_M, s_{ax}) = S(p_M, s_{ax}, R)$$

$$G(p_M, p_{ax}) = S(p_M, p_{ax}, R)$$

Table XII. (cont'd)

$G(p_M,p\pi_{yeq}) = 2N(A_1,p\pi_{yeq})S(p_M,p_L,\pi,R)$

$G(s_{eq},s_{ax}) = 2N(A_1,s_{eq})S(s_L,s_{ax},2^{\frac{1}{2}}R)$

$G(s_{eq},p\sigma_{eq}) = 2N(A_1,s_{eq})N(A_1,p\sigma_{eq})S(s_L,p_L,2R)$

$G(s_{eq},p_{ax}) = 2^{\frac{1}{2}}N(A_1,s_{eq})S(s_L,p_{ax},2^{\frac{1}{2}}R)$

$G(s_{ax},p\sigma_{eq}) = 2^{\frac{1}{2}}N(A_1,p\sigma_{eq})S(s_{ax},p_L,2^{\frac{1}{2}}R)$

$G(s_{ax},p\pi_{yeq}) = 2^{\frac{1}{2}}N(A_1,p\pi_{yeq})S(s_{ax},p_L,2^{\frac{1}{2}}R)$

$G(p_{ax},p\sigma_{eq}) = N(A_1,p\sigma_{eq})[S(p_{ax},p_L,\sigma,2^{\frac{1}{2}}R)+S(p_{ax},p_L,\pi,2^{\frac{1}{2}}R)]$

$G(p_{ax},p\pi_{yeq}) = N(A_1,p\pi_{yeq})[S(p_{ax},p_L,\sigma,2^{\frac{1}{2}}R)-S(p_{ax},p_L,\pi,2^{\frac{1}{2}}R)]$

B_2 Symmetry

$G(p_M,s_{eq}) = 2N(B_2,s_{eq})S(p_M,s_L,R)$

$G(p_M,p\sigma_{eq}) = 2N(B_2,p\sigma_{eq})S(p_M,p_L,2R)$

$G(p_M,p_{ax}) = S(p_M,p_{ax},\pi,R)$

$G(s_{eq},p\sigma_{eq}) = -2N(B_2,s_{eq})N(B_2,p\sigma_{eq})S(s_L,p_L,2R)$

$G(s_{eq},p_{ax}) = 2^{\frac{1}{2}}N(B_2,s_{eq})S(p_{ax},s_L,2^{\frac{1}{2}}R)$

$G(p\sigma_{eq},p_{ax}) = N(B_2,p\sigma_{eq})[S(p_{ax},p_L,\sigma,2^{\frac{1}{2}}R)-S(p_{ax},p_L,\pi,2^{\frac{1}{2}}R)]$

$G(p_{ax},p\pi_{yeq}) = N(B_2,p\pi_{yeq})[S(p_{ax},p_L,\sigma,2^{\frac{1}{2}}R)+S(p_{ax},p_L,\pi,2^{\frac{1}{2}}R)]$

B_1 Symmetry

$G(p_M,p\pi_{eq}) = 2N(B_1,p\pi_{eq})S(p_M,p_L,\pi,R)$

$G(p_M,p\pi_{ax}) = S(p_M,p_{ax},\pi,R)$

$G(p\pi_{eq},p\pi_{ax}) = 2N(B_1,p\pi_{eq})S(p_L,p_{ax},\pi,2^{\frac{1}{2}}R)$

Table XIII. The Group Overlap Integrals and Normalization Constants for C_{2v} Symmetry (Distorted Tetrahedral Molecules)

a. The Normalization Constants

$$N(A_1, s_{eq}) = [2+2S(s_L, s_L, 2R)]^{-\frac{1}{2}}$$

$$N(A_1, p\sigma_{eq}) = [2+2S(p_L, p_L, \sigma, 2R)]^{-\frac{1}{2}}$$

$$N(A_1, p\pi_{yeq}) = [2+2S(p_L, p_L, \pi, 2R)]^{-\frac{1}{2}}$$

$$N(A_1, s_{ax}) = [2+2S(s_{ax}, s_{ax}, 3^{\frac{1}{2}}R)]^{-\frac{1}{2}}$$

$$N(A_1, p\sigma_{ax}) = [2+1.5S(p_{ax}, p_{ax}, \sigma, 3^{\frac{1}{2}}R)+.5S(p_{ax}, p_{ax}, \pi, 3^{\frac{1}{2}}R)]^{-\frac{1}{2}}$$

$$N(A_1, p\pi_{xax}) = [2+.5S(p_{ax}, p_{ax}, \sigma, 3^{\frac{1}{2}}R)+1.5S(p_{ax}, p_{ax}, \pi, 3^{\frac{1}{2}}R)]^{-\frac{1}{2}}$$

$$N(A_2, p\pi_{xeq}) = [2-2S(p_L, p_L, \pi, 2R)]^{-\frac{1}{2}}$$

$$N(A_2, p\pi_{yax}) = [2-2S(p_{ax}, p_{ax}, \sigma, 3^{\frac{1}{2}}R)]^{-\frac{1}{2}}$$

$$N(B_1, p\pi_{xeq}) = [2+2S(p_L, p_L, \pi, 2R)]^{-\frac{1}{2}}$$

$$N(B_1, s_{ax}) = [2-2S(s_{ax}, s_{ax}, 3^{\frac{1}{2}}R)]^{-\frac{1}{2}}$$

$$N(B_1, p\sigma_{ax}) = [2-1.5S(p_{ax}, p_{ax}, \sigma, 3^{\frac{1}{2}}R)-.5S(p_{ax}, p_{ax}, \pi, 3^{\frac{1}{2}}R)]^{-\frac{1}{2}}$$

$$N(B_2, s_{eq}) = [2-2S(s_L, s_L, 2R)]^{-\frac{1}{2}}$$

$$N(B_2, p\sigma_{eq}) = [2-2S(p_L, p_L, \sigma, 2R)]^{-\frac{1}{2}}$$

$$N(B_2, p\pi_{yeq}) = [2-2S(p_L, p_L, \pi, 2R)]^{-\frac{1}{2}}$$

$$N(B_2, p\pi_{yax}) = [2+2S(p_{ax}, p_{ax}, \pi, 3^{\frac{1}{2}}R)]^{-\frac{1}{2}}$$

Table XIII. (cont'd)

b. The Group Overlap Integrals

$G(s_M, s_{eq}) = 2N(A_1, s_{eq})S(s_M, s_L, R)$

$G(s_M, s_{ax}) = 2N(A_1, s_{ax})S(s_M, s_{ax}, R)$

$G(s_M, p\sigma_{eq}) = 2N(A_1, p\sigma_{eq})S(s_M, p_L, R)$

$G(s_M, p\sigma_{ax}) = 2N(A_1, p\sigma_{ax})S(s_M, p_{ax}, R)$

$G(p_M, s_{ax}) = N(A_1, s_{ax})S(p_M, s_{ax}, R)$

$G(p_M, p\sigma_{ax}) = N(A_1, p\sigma_{ax})S(p_M, p_{ax}, \sigma, R)$

$G(p_M, p\pi_{yeq}) = 2N(A_1, p\pi_{yeq})S(p_M, p_L, \pi, R)$

$G(p_M, p\pi_{xax}) = 3^{\frac{1}{2}}N(A_1, p\pi_{xax})S(p_M, p_{ax}, \pi, R)$

$G(s_{eq}, s_{ax}) = 4N(A_1, s_{eq})N(A_1, s_{ax})S(s_L, s_{ax}, 2^{\frac{1}{2}}R)$

$G(s_{eq}, p\sigma_{eq}) = 2N(A_1, s_{eq})N(A_1, p\sigma_{eq})S(s_L, s_L, 2R)$

$G(s_{eq}, p\sigma_{ax}) = 8^{\frac{1}{2}}N(A_1, s_{eq})N(A_1, p\sigma_{ax})S(s_L, p_{ax}, 2^{\frac{1}{2}}R)$

$G(s_{ax}, p\sigma_{eq}) = 8^{\frac{1}{2}}N(A_1, s_{ax})N(A_1, p\sigma_{eq})S(s_{ax}, p_L, 3^{\frac{1}{2}}R)$

$G(s_{ax}, p\pi_{yeq}) = 2^{\frac{1}{2}}N(A_1, s_{ax})N(A_1, p\pi_{yeq})S(p_L, s_{ax}, 2^{\frac{1}{2}}R)$

$G(s_{ax}, p\pi_{xax}) = N(A_1, s_{ax})N(A_1, p\pi_{xax})S(s_{ax}, p_{ax}, 3^{\frac{1}{2}}R)$

$G(p\sigma_{eq}, p\sigma_{ax}) = 2N(A_1, p\sigma_{eq})N(A_1, p\sigma_{ax})[S(p_L, p_{ax}, \sigma, 2^{\frac{1}{2}}R)+S(p_L, p_{ax}, \pi, 2^{\frac{1}{2}}R)]$

$G(p\sigma_{ax}, p\pi_{yeq}) = N(A_1 p\sigma_{ax})N(A_1, p\pi_{yeq})[S(p_L, p_{ax}, \sigma, 2^{\frac{1}{2}}R)-S(p_L, p_{ax}, \pi, 2^{\frac{1}{2}}R)]$

$G(p\sigma_{ax}, p\pi_{xax}) = \frac{3^{\frac{1}{2}}}{2} N(A_1, p\sigma_{ax})N(A_1, p\pi_{xax})[S(p_{ax}, p_{ax}, \sigma, 3^{\frac{1}{2}}R)+S(p_{ax}, p_{ax}, \pi, 3^{\frac{1}{2}}R)]$

$G(p\pi_{yeq}, p\pi_{xax}) = (12)^{\frac{1}{2}}N(A_1, p\pi_{yeq})N(A_1, p\pi_{xax})S(p_L, p_{ax}, \pi, 2^{\frac{1}{2}}R)$

Table XIII. (cont'd)

A_2 Symmetry

$$G(p\pi_{xeq},p\pi_{yax}) = 3^{\frac{1}{2}}N(A_2,p\pi_{xeq})N(p\pi_{yax})[S(p_L,p_{ax},\sigma,2^{\frac{1}{2}}R)+S(p_L,p_{ax},\pi,2^{\frac{1}{2}}R)]$$

B_1 Symmetry

$$G(p_M,p\pi_{xeq}) = 2N(B_1,p\pi_{xeq})S(p_M,p_L,\pi,R)$$

$$G(p_M,s_{ax}) = 3^{\frac{1}{2}}N(B_1,s_{ax})S(p_M,s_{ax},R)$$

$$G(p_M,p\sigma_{ax}) = 3^{\frac{1}{2}}N(B_1,p\sigma_{ax})S(p_M,p_{ax},\sigma,R)$$

$$G(p_M,p\pi_{xax}) = N(B_1,p\pi_{xax})S(p_M,p_{ax},\pi,R)$$

$$G(p\pi_{xeq},s_{ax}) = 6^{\frac{1}{2}}N(B_1,p\pi_{xeq})N(B_1,s_{ax})S(p_L,s_{ax},2^{\frac{1}{2}}R)$$

$$G(p\pi_{xeq},p\sigma_{ax}) = 3^{\frac{1}{2}}N(B_1,p\pi_{xeq})N(B_1,p\sigma_{ax})[S(p_L,p_{ax},\sigma,2^{\frac{1}{2}}R)-S(p_L,p_{ax},\pi,2^{\frac{1}{2}}R)]$$

$$G(p\pi_{xeq},p\pi_{xax}) = 2N(B_1,p\pi_{xeq})N(B_1,p\pi_{xax})S(p_L,p_{ax},\pi,2^{\frac{1}{2}}R)$$

$$G(s_{ax},p\sigma_{ax}) = -3^{\frac{1}{2}}N(B_1,s_{ax})N(B_1,p\sigma_{ax})S(s_{ax},p_{ax},3^{\frac{1}{2}}R)$$

$$G(s_{ax},p\pi_{xax}) = N(B_1,s_{ax})N(B_1,p\pi_{xax})S(s_{ax},p_{ax},3^{\frac{1}{2}}R)$$

$$G(p\sigma_{ax},p\pi_{xax}) = \frac{3^{\frac{1}{2}}}{2}N(B_1,p\sigma_{ax})N(B_1,p\pi_{xax})[S(p_{ax},p_{ax},\sigma,3^{\frac{1}{2}}R)-S(p_{ax},p_{ax},\pi,3^{\frac{1}{2}}R)]$$

B_2 Symmetry

$$G(p_M,s_{eq}) = 2N(B_2,s_{eq})S(p_M,s_L,R)$$

$$G(p_M,p\sigma_{eq}) = 2N(B_2,p\sigma_{eq})S(p_M,p_L,\sigma,R)$$

$$G(p_M,p\pi_{yax}) = 2N(B_2,p\pi_{yax})S(p_M,p_{ax},\pi,R)$$

$$G(s_{eq},p\sigma_{eq}) = -2N(B_2,s_{eq})N(B_2,p\sigma_{eq})S(s_L,p_L,2R)$$

$$G(s_{eq},p\pi_{yax}) = 8^{\frac{1}{2}}N(B_2,s_{eq})N(B_2,p\pi_{yax})S(s_L,p_{ax},2^{\frac{1}{2}}R)$$

Table XIII. (cont'd)

$$G(p\sigma_{eq},p\pi_{yax}) = 2N(B_2,p\sigma_{eq})N(B_2,p\pi_{yax})[S(p_L,p_{ax},\sigma,2^{\frac{1}{2}}R)-S(p_L,p_{ax},\pi,2^{\frac{1}{2}}R)]$$

$$G(p\pi_{yeq},p\pi_{yax}) = N(B_2,p\pi_{yeq})N(B_2,p\pi_{yax})[S(p_L,p_{ax},\sigma,2^{\frac{1}{2}}R)+S(p_L,p_{ax},\pi,2^{\frac{1}{2}}R)]$$

Table XIV. The Group Overlap Integrals with Normalization Constants for T_d Symmetry

a. The Normalization Constants

$$N(A_1,s_L) = \tfrac{1}{2}[1+3S(s_L,s_L,3.266R)]^{-\frac{1}{2}}$$

$$N(A_1,p\sigma) = \tfrac{1}{2}[1+2S(p_L,p_L,\sigma,3.266R)+S(p_L,p_L,\pi,3.266R)]^{-\frac{1}{2}}$$

$$N(E,p\pi) = \tfrac{1}{2}[1+.5S(p_L,p_L,\sigma,3.266R)-.5S(p_L,p_L,\pi,3.266R)]^{-\frac{1}{2}}$$

$$N(T_2,p\sigma) = \tfrac{1}{2}[1-.67S(p_L,p_L,\sigma,3.266R)-.33S(p_L,p_L,\pi,3.266R)]^{-\frac{1}{2}}$$

$$N(T_2,s_L) = \tfrac{1}{2}[1-S(s_L,s_L,3.266R)]^{-\frac{1}{2}}$$

$$N(T_2,p\pi) = \tfrac{1}{2}[1+.33S(p_L,p_L,\sigma,3.266R)-1.33S(p_L,p_L,\pi,3.266R)]^{-\frac{1}{2}}$$

$$N(T_1,p\pi) = \tfrac{1}{2}[1-.5S(p_L,p_L,\sigma,3.266R)-1.5(p_L,p_L,\pi,3.266R)]^{-\frac{1}{2}}$$

b. The Group Overlap Integrals

A_1 Symmetry

$$G(s_M,s_L) = 4N(A_1,s_L)S(s_M,s_L,R)$$

$$G(s_M,p\sigma) = -4N(A_1,p\sigma)S(s_M,p_L,R)$$

$$G(s_L,p\sigma) = -4(6)^{\frac{1}{2}}N(A_1,s_L)N(A_1,p\sigma)S(s_L,p_L,3.266R)$$

Table XIV. (cont'd)

T_2 Symmetry

$$G(p_M,p\sigma) = \frac{4(3)^{\frac{1}{2}}}{3} N(T_2,p\sigma)S(p_M,p_L,\sigma,R)$$

$$G(p_M,s_L) = \frac{4(3)^{\frac{1}{2}}}{3} N(T_2,s_L)S(p_M,s_L,R)$$

$$G(p_M,p\pi) = \frac{-4(6)^{\frac{1}{2}}}{3} N(T_2,p\pi)S(p_M,p_L,\pi,R)$$

$$G(p\sigma,s_L) = \frac{4(6)^{\frac{1}{2}}}{3} N(T_2,p\sigma)N(T_2,s_L)S(p_L,s_L,3.266R)$$

$$G(p\sigma,p\pi) = \frac{4}{3} N(T_2,p\sigma)N(T_2,p\pi)[2(2)^{\frac{1}{2}}S(p_L,p_L,\sigma,3.266R)-S(p_L,p_L,\pi,3.266R)]$$

$$G(s_L,p\pi) = \frac{-8(3)^{\frac{1}{2}}}{3} S(s_L,p_L,3.266R)]$$

Table XV. The Group Overlap Integrals and Normalization Constants for C_{3v} Symmetry

a. The Normalization Constants

$$N(A_1,s_L) = 3^{-\frac{1}{2}}[1+2S(s_L,s_L,1.46R)]^{-\frac{1}{2}}$$

$$N(E,s_L) = 3^{-\frac{1}{2}}[2-3S(s_L,s_L,1.46R)]^{-\frac{1}{2}}$$

b. The Group Overlap Integrals

A_1 Symmetry

$$G(s_M,s_L) = 3N(A_1,s_L)S(s_M,s_L,R)$$

$$G(p_M,s_L) = 3(.54)N(A_1,s_L)S(p_M,s_L,R)$$

E Symmetry

$$G(p_M,s_L) = 3^{\frac{1}{2}}(.84)S(p_M,s_L,R)$$

Table XVI. The Group Overlap Integrals and Normalization Constants for D_{3h} Symmetry

a. The Normalization Constants

$$N(A_1',s_{eq}) = [3+6S(s_L,s_L,1.46R)]^{-\frac{1}{2}}$$

$$N(A_1',s_{ax}) = [2+2S(s_L,s_L,1.46R)]^{-\frac{1}{2}}$$

$$N(A_2'',s_{ax}) = [2-2S(s_L,s_L,1.46R)]^{-\frac{1}{2}}$$

$$N(E',s_{eq}) = [2-2S(s_L,s_L,1.46R)]^{-\frac{1}{2}}$$

Table XVI. (cont'd)

b. The Group Overlap Integrals

A_1' Symmetry

$$G(s_M, s_{eq}) = 3N(A_1', s_{eq})S(s_M, s_L, R)$$

$$G(s_M, s_{ax}) = 2N(A_1', s_{ax})S(s_M, s_L, R)$$

$$G(s_{eq}, s_{ax}) = 6N(A_1', s_{eq})N(A_1', s_{ax})S(s_L, s_L, 2^{\frac{1}{2}}R)$$

$$G(d_M, s_{eq}) = -\frac{3}{2}N(A_1', s_{eq})S(d_M, s_L, R)$$

$$G(d_M, s_{ax}) = 2N(A_1', s_{ax})S(d_M, s_L, R)$$

A_2'' Symmetry

$$G(p_M, s_{ax}) = 2N(A_2'', s_{ax})S(p_M, s_L, R)$$

E' Symmetry

$$G(p_M, s_{eq}) = -3^{\frac{1}{2}}N(E', s_{eq})S(p_M, s_L, R)$$

$$G(d_M, s_{eq}) = \frac{3}{2}N(E', s_{eq})S(d_M, s_L, R)$$

C. Radial Function

For the evaluation of two-atom overlap integrals, the SCF radial functions employed are the best available in the literature. Most of these functions are taken from Clementi's table [33]. The valence orbital (3s, 3p, and 3d) functions for phosphorus are those reported in the paper by Berry et al. [29]. The xenon 5s and 5p functions have been kindly provided by Straub [34]. These functions are very similar to those calculated by Synek and Stungis [35] and those used by Yeranos [26] in his calculation for the XeF_4 system. The hydrogen 1s function has an exponent of 1.20 as given by Brintzinger et al. [36]. The SCF functions employed in this thesis are reproduced in Table XVII.

Table XVII. AO Functions: Principal Quantum Numbers, Coefficients, and Exponents

		n	Exponent	Coefficient	Ref.
Fluorine					
	2s	1	8.5126	-.22924	
		1	14.4130	-.00534	
		2	1.8599	.27178	
		2	2.7056	.65367	
		2	4.9019	.33031	
		2	6.4440	-.23130	
	2p	2	1.2655	.17003	
		2	2.0301	.55982	
		2	3.9106	.34875	
		2	8.6363	.01691	[33]
Hydrogen					
	1s	1	1.2000	1	[36]
Oxygen					
	2s	1	7.6160	-.21979	
		1	13.3243	.0057301	
		2	1.7582	.42123	
		2	2.5627	.54368	
		2	4.2832	.23061	
		2	5.9445	.17856	

Table XVII. (cont'd)

	2p	2	7,9070	.01495	
		2	3.4379	.33392	
		2	1.796	.57600	
		2	1.1536	.16371	[33]
Phosphorus					
	3s	1	17.4370	.060406	
		2	15.2390	.045089	
		2	8.7990	.000405	
		3	4.8330	-.396780	
		3	2.3330	.723752	
		3	1.4700	.397737	
	3p	2	12.5050	-.008374	
		2	7.1370	-.086949	
		2	4.3250	-.183247	
		3	2.0130	.645961	
		3	1.1900	.446393	
	3d	3	6.4000	.003312	
		3	2.2500	.052187	
		3	1.0303	.243268	
		3	.3928	.851656	[29]

Table XVII. (cont'd)

Sulfur				
	3s	1	16.0000	.07790
		3	18.1208	.00204
		3	12.8168	-.03170
		3	9.6270	-.09454
		3	6.4124	-.25461
		3	3.7743	-.07603
		3	2.7095	.65648
		3	1.6709	.51654
	3p	2	8.000	.15546
		4	14.1259	-.00995
		4	11.5718	.01287
		4	7.9171	-.09992
		4	5.6039	.05174
		4	2.8906	.55282
		4	1.6275	.50896
		4	.8665	.02556 [33]
Xenon				
	5s	1	52.9215	.028175
		2	19.9015	-.112792
		3	11.8588	.252174
		4	6.5432	-.429170
		5	2.8436	1.049517

Table XVII. (cont'd)

5p	2	24.9173	-.055953	
	3	11.8892	.157040	
	4	6.2393	.325591	
	5	2.4849	1.028584	[34]

D. Structural Parameter

The evaluation of overlap integrals requires the knowledge of the bond lengths and bond angles of the molecules concerned. For all the molecules under consideration, experimental data are employed wherever possible.

For the xenon oxyfluorides, only the structure of $XeOF_4$ has been determined. Using the technique of microwave spectroscopy, Martins and Wilson [37] have found that the Xe-O and Xe-F bonds are 1.703 $\pm$ .015 Å and 1.900 $\pm$ .005 Å respectively. The angle between the two bonds, angle F-Xe-O, is 91.8 $\pm$ .5°, which is slightly greater than a right angle. In order to make comparison easier, the arithmetic mean of the two bonds is taken for the evaluation of the two-atom overlap integrals. (1.900 + 1.703)/2, i.e. 1.800 Å. This is the bond length used for all the bonds in the xenon oxyfluorides.

In calculating the S matrix elements, certain geometric structure has to be assumed for the molecule under consideration. All three of the xenon oxyfluorides are assumed their idealized structures obtained with the VSEPR model. $XeOF_4$ has the square pyramidal structure with Xe-F and Xe-O bond lengths equal, and the angle between the two bonds taken to be right angle. For XeO_2F_2, the distorted tetrahedral falls into the C_{2v} point group. The two fluorines are supposed to take the linear sites, while the two Xe-O

bonds fall onto the plane perpendicular to that linear aggregate. The angle between the two Xe-O bonds is assumed to be 120° whereas that between the bonds Xe-F and Xe-O is 90° as for $XeOF_4$. Finally a T-shaped structure is predicted for $XeOF_2$. By analogy with the above assumptions, equal bond lengths are taken and the angle between the two, Xe-O, Xe-F bonds, is again 90°.

Besides the above set of calculation, similar calculations have also been performed with two-atom overlap integrals evaluated at experimental bond separations reported by Martins and Wilson [37].

Tolles and Gwinn [38] have determined the structure for SF_4, again utilizing microwave spectroscopy. There are two kinds of bonds, the nearly linear bonds (w.r.t. S) are at $1.646 \pm .003$ Å and the other two bonds at $1.545 \pm .003$ Å. The angle between the longer bonds is $186^{\circ}\ 56' \pm .30'$ where the angle between the shorter bonds is $101^{\circ}\ 33' \pm 30'$. As before, for convenience, the averaged bond length 1.595 Å is employed as R to obtain the two-atom overlaps. This molecule has been assumed to have three different structures, namely, square planar, tetrahedral and the distorted tetrahedral. In the structures all the S-F bonds are taken to have the averaged bond length as stated. The square planar structure has all the atoms on the same plane and right angles are assumed between every two adjacent bonds. The idealized tetrahedral structure is assumed in obtaining the S_{ij}'s for the T_d model. The remaining structure has the same assumptions for XeO_2F_2 in the previous part.

As mentioned in Dasent's "Nonexistent Compounds", [39] PH_5 does not exist. The necessary structural parameters are therefore obtained from other sources. For P-H bond length, the value found in PH_3 [40], is adopted. So the value of 1.42 Å is taken for all the five P-H bonds in the hypothetical molecule PH_5 in both the trigonal bipyramidal and the square pyramidal symmetries. In the former structure, the three equatorial hydrogens are orientated at the vertices of an equilateral triangle, taking phosphorus as the centroid. The other two fluorines will fall into a line perpendicular to the former plane. As for the square pyramid, the angle between the axial and equatorial P-H bonds is assumed to be a right angle with P-H bond length of 1.42 Å.

E. Coulomb Integrals (VSIP's)

The Coulomb integrals in the secular equation are approximated as valence-state ionization potential (VSIP) with necessary readjustments for ligand-ligand overlaps, if required. As a rule, all the VSIP values used here have been calculated using ab initio or semi-empirical techniques or they have been used in other MO calculations.

Since Boudreaux [41] has performed a semi-empirical MO calculation on XeF_6, his VSIP values for the xenon orbitals are therefore taken as one of the basis. The other set of VSIP data for xenon is obtained from the work of Jortner et al. [42]. For fluorine, corresponding values employed by Boudreaux [41] and Jortner et al. are taken for the

present calculations. Since their work does not involve oxygen, values for oxygen have beenpicked out from the table given in Ballhausen and Gray [32]. In order to avoid confusion due to many possible combinations, the two different sets of VSIP's employed in calculations are given in Table XVIII.

Table XVIII. VSIP Data for Xenon Oxyfluorides (in kK)

Atom	Valence orbital	Set I -VSIP	Set I Ref.	Set II -VSIP	Set II Ref.
Xe	5s	185.36	Jortner et al.	217.59	Boudreaux
	5p	97.52	[42]	96.71	[41]
O	2s	261.0	Ballhausen and Gray [32]	261.0	Ballhausen and Gray [32]
	2p	128.0		128.0	
F	2s	322.37	Jortner et al.	374.0	Boudreaux
	2p	140.23	[42]	151.0	[41]

For SF_4, two different sets of VSIP data are again employed. One set is taken from Clementi's table [33] and the other from Ballhausen and Gray [32]. These values are listed in Table XIX.

Table XIX. VSIP Data For Sulfur Tetrafluoride (in kK)

Atom	Valence orbital	I Clementi's data[33]	II Gray's data [32]
S	3s	139.06	167.0
	3p	96.0	94.0
F	2s	344.57	374.0
	2p	160.22	151.0

The VSIP data for the phosphorus 3s, 3p and 3d are indentical as that employed by Berry et al. [29] in their work on pentafluorides. These values are (in kK) -193.1, -113.5 and -14.4 respectively. For hydrogen 1s orbital, the value of -110.0 kK, which is reported in Gray [43], has been adopted.

F. Two-Atom Overlap Integrals

The two-atom overlap integrals have been calculated with the numerical method outlined by Yeranos [44]. These calculations were performed on an ICL 1904A computer at the Computing Centre of the Chinese University of Hong Kong.

Table XX. The Two-Atom Overlap Integrals for the Xenon Oxfluorides (Set I, R at averaged value i.e. 1.80 Å)

F - F Overlap Integrals at $2^{\frac{1}{2}}R$

$S(F_{2s} - F_{2s}, \sigma) = 0.0079617$

$S(F_{2s} - F_{2p}, \sigma) = 0.026050$

$S(F_{2p} - F_{2p}, \sigma) = 0.045686$

$S(F_{2p} - F_{2p}, \pi) = 0.010468$

F - F Overlap Integrals at 2R

$S(F_{2s} - F_{2s}, \sigma) = 0.000433$

$S(F_{2s} - F_{2p}, \sigma) = 0.002910$

$S(F_{2p} - F_{2p}, \sigma) = 0.007465$

$S(F_{2p} - F_{2p}, \pi) = 0.001151$

Xe - F Overlap Integrals at R

$S(Xe5s - F_{2s}, \sigma) = 0.154791$

$S(Xe5s - F_{2p}, \sigma) = 0.210085$

$S(Xe5p - F_{2s}, \sigma) = 0.290491$

$S(Xe5p - F_{2p}, \sigma) = 0.275987$

$S(Xe5p - F_{2p}, \pi) = 0.120624$

Table XX. (cont'd)

Xe - O Overlap Integrals at R

$S(Xe5s - O_{2s},\sigma) = 0.185728$

$S(Xe5s - O_{2p},\sigma) = 0.248627$

$S(Xe5p - O_{2s},\sigma) = 0.327257$

$S(Xe5p - O_{2p},\sigma) = 0.299105$

$S(Xe5p - O_{2p},\pi) = 0.145304$

F - O Overlap Integrals at $2^{\frac{1}{2}}R$

$S(F_{2s} - O_{2s},\sigma) = 0.012154$

$S(F_{2p} - O_{2s},\sigma) = 0.033990$

$S(F_{2s} - O_{2p},\sigma) = 0.035983$

$S(F_{2p} - O_{2p},\sigma) = 0.057564$

$S(F_{2p} - O_{2p},\pi) = 0.013920$

O - O Overlap Integrals at $3^{\frac{1}{2}}R$

$S(O_{2s} - O_{2s},\sigma) = 0.004436$

$S(O_{2s} - O_{2p},\sigma) = 0.015869$

$S(O_{2p} - O_{2p},\sigma) = 0.030485$

$S(O_{2p} - O_{2p},\pi) = 0.006058$

Table XXI. The Two-Atom Overlap Integrals for the Xenon Oxyfluorides (Set II, R_1=1.900 Å, R_2=1.703 Å)

F - F Overlap Integrals at $2^{\frac{1}{2}}R_1$

$S(F_{2s} - F_{2s},\sigma) = 0.005466$

$S(F_{2s} - F_{2p},\sigma) = 0.019555$

$S(F_{2p} - F_{2p},\sigma) = 0.036304$

$S(F_{2p} - F_{2p},\pi) = 0.007809$

F - F Overlap Integrals at $2R_1$

$S(F_{2s} - F_{2s},\sigma) = 0.000248$

$S(F_{2s} - F_{2p},\sigma) = 0.001921$

$S(F_{2p} - F_{2p},\sigma) = 0.005266$

$S(F_{2p} - F_{2p},\pi) = 0.000765$

Xe - F Overlap Integrals at R_1

$S(Xe5s - F_{2s},\sigma) = 0.127688$

$S(Xe5s - F_{2p},\sigma) = 0.187010$

$S(Xe5p - F_{2s},\sigma) = 0.249889$

$S(Xe5p - F_{2p},\sigma) = 0.255237$

$S(Xe5p - F_{2p},\pi) = 0.100748$

Table XXI. (cont'd)

Xe - O Overlap Integrals at R_2

$S(Xe5s - O_{2s},\sigma) = 0.218843$

$S(Xe5s - O_{2p},\sigma) = 0.271607$

$S(Xe5p - O_{2s},\sigma) = 0.370618$

$S(Xe5p - O_{2p},\sigma) = 0.30418$

$S(Xe5p - O_{2p},\pi) = 0.171180$

F - O Overlap Integrals at $(R_2^2 + R_2^2)^{\frac{1}{2}}$

$S(F_{2s} - O_{2s},\sigma) = 0.012039$

$S(F_{2p} - O_{2s},\sigma) = 0.033741$

$S(F_{2s} - O_{2p},\sigma) = 0.035703$

$S(F_{2p} - O_{2p},\sigma) = 0.057233$

$S(F_{2p} - O_{2p},\pi) = 0.013814$

O - O Overlap Integrals at $3^{\frac{1}{2}}R_2$

$S(O_{2s} - O_{2s},\sigma) = 0.006742$

$S(O_{2s} - O_{2p},\sigma) = 0.021885$

$S(O_{2p} - O_{2p},\sigma) = 0.039648$

$S(O_{2p} - O_{2p},\pi) = 0.008425$

Table XXII. The Two-Atom Overlap Integrals for Sulfur Tetrafluoride R = 1.595 Å

S - F Overlap Integrals at R

$S(S_{3s} - F_{2s}, \sigma) = 0.202471$

$S(S_{3p} - F_{2s}, \sigma) = 0.355534$

$S(S_{3s} - F_{2p}, \sigma) = 0.237511$

$S(S_{3p} - F_{2p}, \sigma) = 0.239720$

$S(S_{3p} - F_{2p}, \pi) = 0.163591$

F - F Overlap Integrals at $2^{\frac{1}{2}}R$

$S(F_{2s} - F_{2s}, \sigma) = 0.017318$

$S(F_{2s} - F_{2p}, \sigma) = 0.047050$

$S(F_{2p} - F_{2p}, \sigma) = 0.072778$

$S(F_{2p} - F_{2p}, \pi) = 0.019373$

F - F Overlap Integrals at $3^{\frac{1}{2}}R$

$S(F_{2s} - F_{2s}, \sigma) = 0.004451$

$S(F_{2s} - F_{2p}, \sigma) = 0.016739$

$S(F_{2p} - F_{2p}, \sigma) = 0.031994$

$S(F_{2p} - F_{2p}, \pi) = 0.006662$

Table XXII. (cont'd)

F - F Overlap Integrals at 2R

$S(F_{2s} - F_{2s}, \sigma) = 0.001375$

$S(F_{2s} - F_{2p}, \sigma) = 0.006891$

$S(F_{2p} - F_{2p}, \sigma) = 0.015412$

$S(F_{2p} - F_{2p}, \pi) = 0.002722$

F - F Overlap Integrals at $2(6)^{\frac{1}{2}}R/3$

$S(F_{2s} - F_{2s}, \sigma) = 0.006830$

$S(F_{2s} - F_{2p}, \sigma) = 0.023166$

$S(F_{2p} - F_{2p}, \sigma) = 0.041612$

$S(F_{2p} - F_{2p}, \pi) = 0.009287$

Table XXIII. The Two-Atom Overlap Integrals for PH_5 R= 1.42 Å

H - H Overlap Integrals

$S(H_{1s} - H_{1s}, 2^{\frac{1}{2}}R) = 0.131226$

$S(H_{1s} - H_{1s}, 3^{\frac{1}{2}}R) = 0.063978$

$S(H_{1s} - H_{1s}, 2R) = 0.033845$

P - H Overlap Integrals at R

$S(P_{3s} - H_{1s}, \sigma) = 0.389926$

$S(P_{3p} - H_{1s}, \sigma) = 0.508742$

$S(P_{3d}, H_{1s}, \sigma) = 0.241915$

Chapter V

RESULTS AND DISCUSSION

The approximate orbital energies and the MO functions are obtained with the ICL 1904A computer. The computer program for solving the secular equations was obtained from Quantum Chemistry Program Exchange at Indiana University. In this chapter, the results obtained are examined under three main categories. The groups are: A. the xenon oxyfluorides, B. the nonexistent PH_5, and C. SF_4.

A. The xenon oxyfluorides

There are three different xenon oxyfluorides under consideration, namely, $XeOF_2$, XeO_2F_2 and $XeOF_4$. Discussion will follow the trend of increasing complexity. Similar results have been obtained for the two different sets of VSIP data, therefore only one set (set I) will be discussed in detail.

(1) $XeOF_2$

The eigenvalues and eigenvectors for this molecule are given in Appendix 1. Applying aufbau and exclusion principles, the ground electronic configuration for this molecule is

$$\ldots [4b_2(-123.16)]^2[6a_1(-88.49)]^2[3b_1(-78.41)]^2[5b_2(11.56)]^0 \ldots$$

Because the VSEPR model for this molecule shows that there are two lone pairs, the two highest filled orbitals will be considered as the "lone-pair orbitals". So both $6a_1$ and $3b_1$ will be examined for any structural effect. These two MO's are given below (1 kK = 10^3 cm^{-1}) :

$6a_1$ (-77.16 kK)	5s (Xe)	5p (Xe)	2s eq (F)	2s ax (O)	2pσ eq (F)	2pσ ax (O)	2pπ eq (F)
AO coeff.	-.62	.62	.23	-.08	.71	.00	-.25
Population	.23	.34	.02	-.00	.37	.00	.04

$3b_1$ (-78.48 kK)	5p (Xe)	2pπ eq (F)	2pπ ax (O)
AO coeff.	.97	-.39	-.38
Population	.81	.09	.09

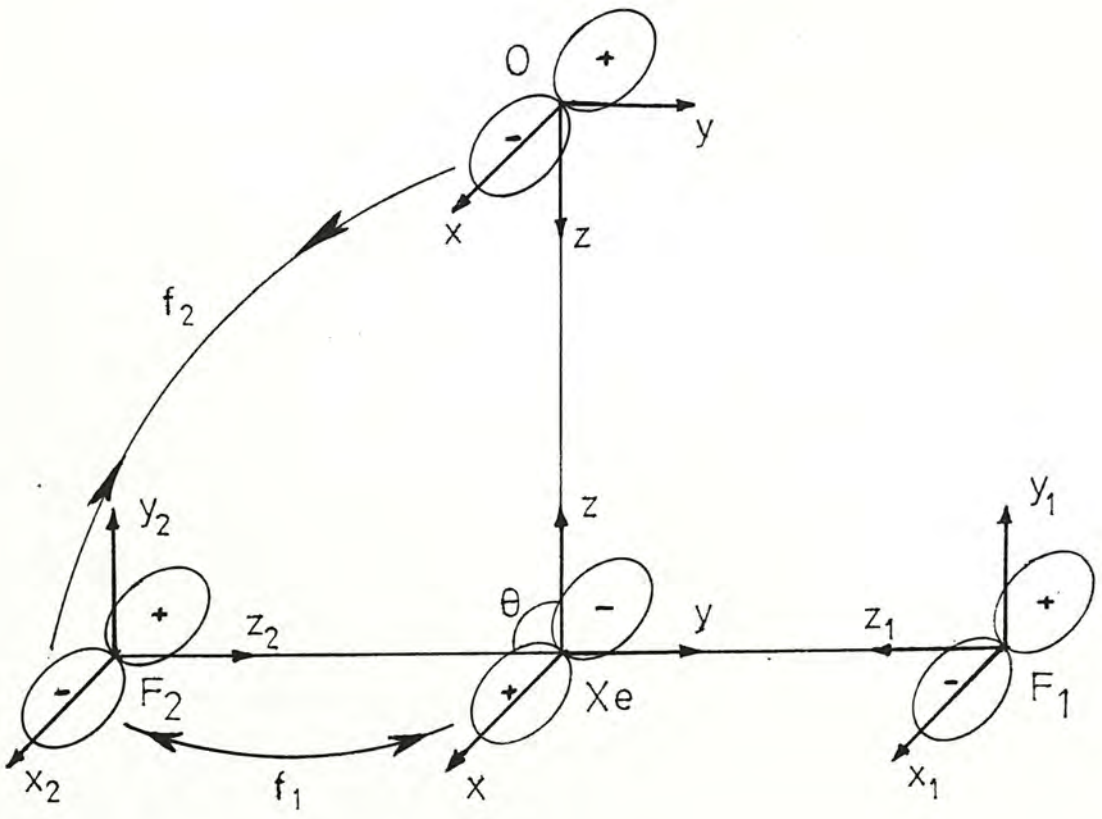

Fig. 11 The $3b_1$ MO for $XeOF_2$ (R=1.8 Å)

A diagramatic representation of the $3b_1$ orbital (Fig. 11) shows that f_1 is a repulsive force while f_2 is attractive. Therefore, it may be concluded that the equatorial ligands, i.e. the fluorine atoms, would be attracted towards the axial ligand, the oxygen atom. This would then lead to a decrease in magnitude for θ, i.e., θ should be less than the assumed right angle. This, of course, is in agreement with the VSEPR theory, which says lone pairs occupy more space in the coordination sphere. From the population viewpoint, the electron cloud is mainly localized on the central atom, xenon, and a very small portion resides around the ligands. This gives the idea that this orbital plays a small part in the overall molecular bonding. Besides this, the energy of this orbital lies mid-way between the low-lying bonding orbitals and the empty antibonding orbitals which also indicates its non-bonding nature. So considering this delocalized MO as a lone pair orbital is well justified. The $6a_1$ orbital gives a similar and even better picture. This MO has very similar energy as that of the $3b_1$. It may therefore be argued that this, too, is a non-bonding orbital. However, the populations show that this bonds stronger than $3b_1$. The AO's for all the atoms are "hybridized" to some extent. It is interesting to note that the populations in the axial orbitals (O orbitals) are so small as to have much effect on the final delocalization. The equatorial orbitals (F orbitals) are such that the resulting lobe may be orientated in a direction as to make an angle with the z-axis of the ligand coordinate. The magnitude

of this angle is supposed to be proportional to the ratio of the population in pπ and pσ orbitals. For the central atom, the mixing of the s and p_z orbital is to a greater extent as can be seen from the magnitudes of the populations. In order to have a clearer picture, this MO may be represented in the "hybridized" form given in Fig. 12. In this figure, the AO's are drawn qualitatively.

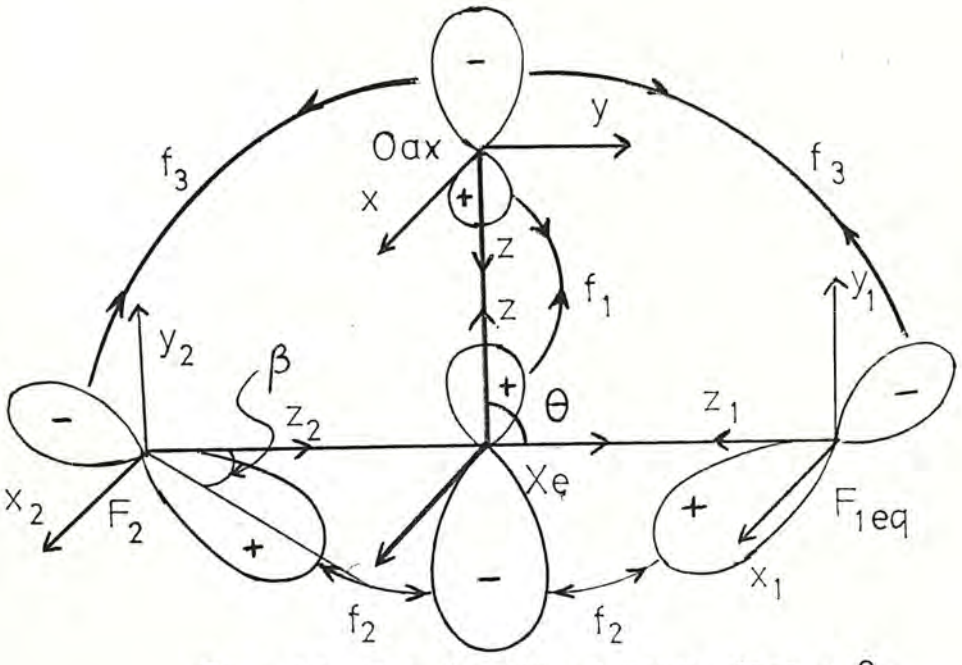

Fig. 12 The $6a_1$ MO of $XeOF_2$ (R=1.8 Å)

From the AO phases shown in Fig. 12, it can be readily seen that both f_1 and f_3 are attractive while f_2 is repulsive. Qualitatively, the composite result of these three forces would be (i) the Xe-F bonds should be longer than the Xe-O bond, even though they were assumed to be equal in this calculation; (ii) again, the angle θ should be less than the prescribed 90°. These two effects are also in accordance with the VSEPR theory.

When the experimental values of Xe-O and Xe-F distances are employed in the calculation, the qualitative features, such as the energy level ordering, the phase of each AO in the MO's, etc., of the results are quite similar. However, when the populations are examined more closely, the structural distortions due to the lone pairs are enhanced somewhat. In order to see this, the $6a_1$ and $3b_1$ MO's are given below for comparison.

$6a_1$ (-88.49 kK)	5s (Xe)	5p (Xe)	2s eq (F)	2s ax (O)	2pσ eq (F)	2pσ ax (O)	2pπ eq (F)
AO coeff.	-.60	.59	.18	-.06	.70	.11	-.24
Population	.22	.34	.01	-.00	.38	.02	.03

$3b_1$ (-78.41 kK)	5p (Xe)	2pπ eq (F)	2pπ ax (O)
AO coeff.	.96	-.32	-.46
Population	.83	.06	.13

Referring to Fig. 12, the decrease in magnitude of θ depends largely on the magnitude of β. When β is small, there will be an effective resulting torque in the anticlockwise direction which will enhance the overall delocalization and lead to a smaller θ value. The value of β, as mentioned before, should be governed by the population ratio

(2pπ eq)/(2pσ eq). This ratio is 0.04/0.37 ($\sim$ 1/10) when average bond length is used, and it decreases to 0.03/0.38 ($\sim$ 1/13) when experimental bond distances are employed. The decrease is rather small in this case. But it is a decrease nontheless. This in turn, shows the validity of the present argument. In addition, the population of the oxygen orbitals increases from 0.00 to 0.02, when only two significant figure are considered. So, again, the attractive forces f_1 and f_3 should become more significant when experimental bond distances are adopted in the calculation.

To conclude, the structure of $XeOF_2$ remains roughly T-shape. But, judging from the lone pair wave function, the Xe-O bond should be shorter than the Xe-F ones and the FXeO angles should be less than 90°. These effects are evident even when average bond lengths and 90° angles are assumed in the calculation; they become more enhanced when experimental distances are adopted.

(2) XeO_2F_2

The MO eigenvalues and eigenvectors are given in Appendix I, The ground state electronic configuration is

$$\ldots [2a_2(-122.56)]^2[7a_1(73.79)]^2[5b_1(42.23)]^0 \ldots \quad .$$

From VSEPR consideration, this molecule has one lone pair, and, from the electronic configuration, it is also observed that only one orbital, $7a_1$, lies inbetween the bonding and antibonding groups of orbitals. This readily leads to the picking out of the $7a_1$ as a representation for the "lone pair". The $7a_1$ MO wave function has the form:

$7a_1$ (-73.93kK)	5s (Xe)	5p (Xe)	2s ax (O)	2pσ ax (O)	2pπ ax (O)	2s eq (F)	2pσ eq (F)	2pπ eq (F)
AO coeff.	-.44	.82	-.06	.06	-.36	.16	.47	-.31
Populations	.11	.57	-.00	.01	.08	.01	.16	.05

There is certain extent of mixing among the AO's. After taking this hybridization into account, a picture similar to Fig. 12 can be drawn for this lone pair, as shown in Fig. 13.

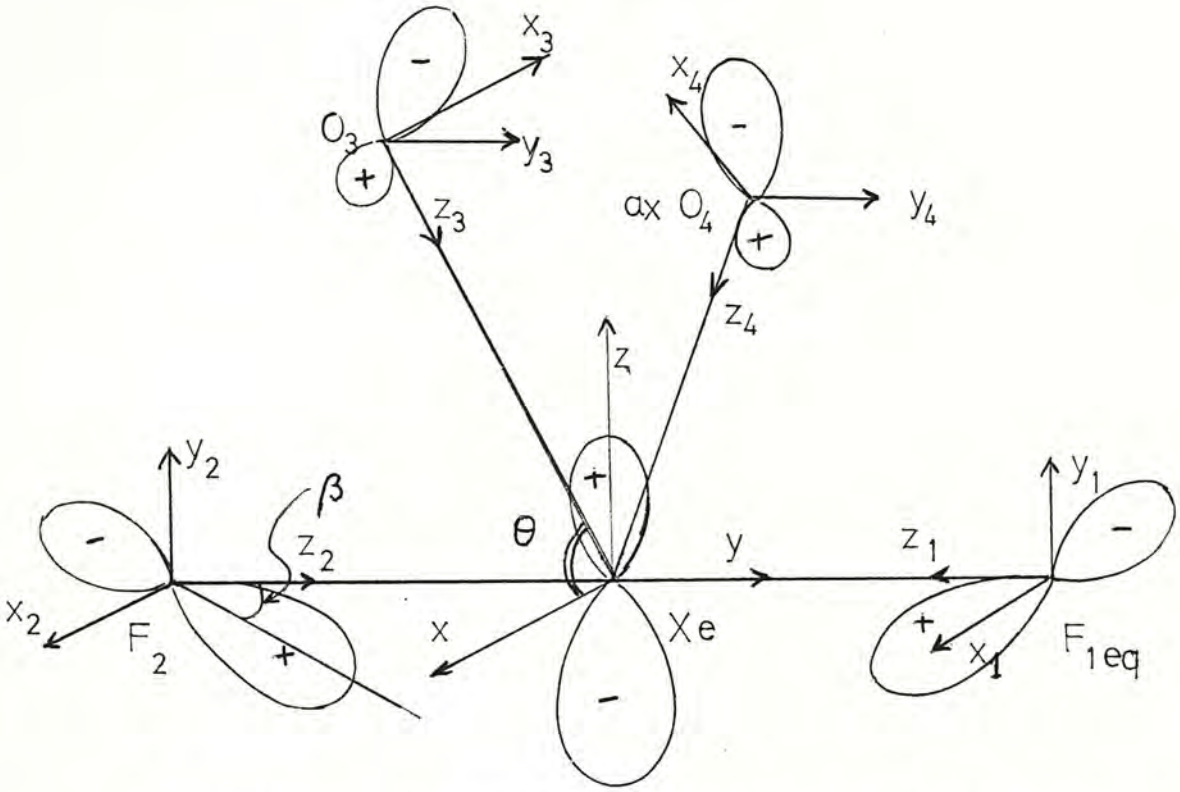

Fig. 13 The $7a_1$ MO for XeO_2F_2 after "Hybridization"

Fig. 13 is a three dimensional picture. In order to have a better view, this MO is separated into two parts each containing a plane perpendicular to the other. These two parts are shown in Figs. 14a and 14b.

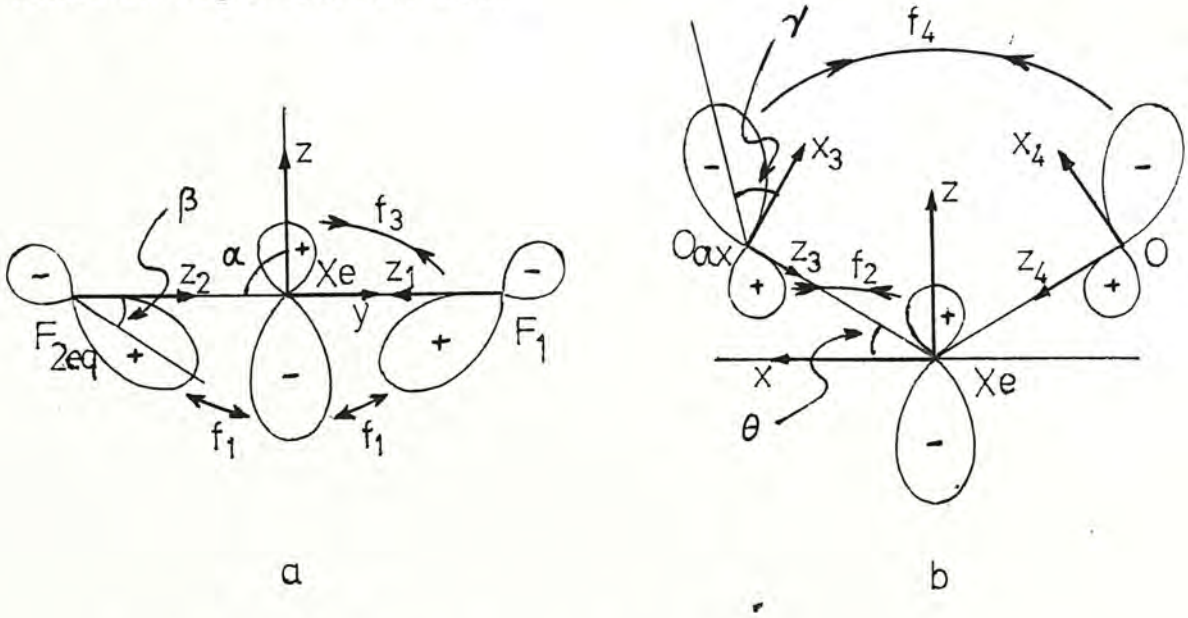

Fig. 14 a. The yz Plane of Xe b. The xz Plane of Xe

Looking at Fig. 14a, if similar argument concerning the phase of the participating AO's is adopted as for $XeOF_2$, f_1 is a repulsive force while f_3 is attractive. Both of these two forces would lead to a less-than-90° value for angle α. Furthermore, the molecule should be more stabilized if Xe-F distance is increased, since there is a node between the Xe and F atoms.

In Fig. 14b, both f_2 and f_4 are attractive. However, they lead to opposite structural effects; f_2 favors opening up of the OXeO angle while f_4 does not. Since the OXeO angle is assumed to be 120°, the xenon-oxygen distance is clearly much smaller than the O-O distance. Therefore, f_2 should be the prevailing force. The net effect then would cause a decrease in angle θ, which in turn leads to that the OXeO angles should be greater than the 120° assumed in the present calculation. In the language of VSEPR theory, this means the Xe-O double bonds occupy even more space than a lone pair in the coordination sphere. When bond length is considered, f_2 favors a shorter xenon-oxygen bond, since there is no node between the Xe and O atoms.

To summarize, it is expected that (i) Xe-F bond should be longer than the Xe-O double bond, even though they were assumed to be equal in the calculation; (ii) the FXeF angle (in the direction of the oxygen ligands) should be smaller than 180° i.e., the OXeF angle

should be less than 90°; and (iii) the OXeO angles should be greater than the prescribed 120°. It should be noted that points (i) and (ii) are in agreement with the VSEPR theory and such theory does not deal directly with point (iii). However, the present finding is not in accordance with the published X-ray results for $IO_2F_2^-$, an isoelectronic species for XeO_2F_2, by Claassen et al. [45]. According to these authors, the OIO angle is smaller than 120°. Nevertheless, they have not reported the experimental value for it.

When experimental distances for Xe-F and Xe-O bonds are used in the calculation, the lone pair $7a_1$ MO has the form:

$7a_1$ (-77.45kK)	5s (Xe)	5p (Xe)	2s ax (O)	2pσ ax (O)	2pπ ax (O)	2s eq (F)	2pσ eq (F)	2pπ eq (F)
AO coeff.	-.44	.79	-.03	.17	-.44	.12	.42	-.25
Population	.11	.55	-.00	.03	.13	.01	.13	.04

The values of β and γ in Figs. 14a and 14b are governed by the population ratios (pπ eq)/(pσ eq) and (pσ ax)/(pπ ax) respectively. From the result of this calculation, both β (from 1/3.6 to 1/3.3) and γ (from 1/8 to 1/4.3) have increased and such increases signify reinforcement for the structural distortion detailed before. In the case of β, it is obvious that f_1, which is dominant over f_3, is most effective when β is 45°. Since the β values for both sets of calculation are less than 45°, an increase in β in such a range means a higher effectiveness for f_1. In the case of γ, an increase of its

value would lead to an enhancement of the attractive force f_2 and lower the efficiency of f_4. This would mean calculation with experimental bond distances favors the opening up of OXeO angle even more. This may be viewed as a supporting argument for the previous assertion that the double bonds are bulkier than the lone pair in XeO_2F_2.

(3) $XeOF_4$

The ground state electronic configuration for this molecule is found to be:

$$\ldots[5e(-123.02)]^4[6a_1(-44.51)]^2[6e(54.49)]^0\ldots$$

The complete listing of the eigenvalues and eigenvectors for $XeOF_4$ can be found in Appendix 1. Again the outstanding eigenvalue for the $6a_1$ seems to imply its non-bonding and lone-pair nature. The AO coefficients and population for the $6a_1$ MO are given below.

$6a_1$(-61.77 kK)	5s (Xe)	5p (Xe)	2s eq (F)	2s ax (O)	2pσ eq (F)	2pσ ax (O)	2pπ eq (F)
AO coeff.	.56	-.81	-.26	.19	-.63	.22	.32
Populations	.17	.50	.02	.00	.24	.02	.05

Fig. 15 is a pictorial representation for the $6a_1$ lone pair.

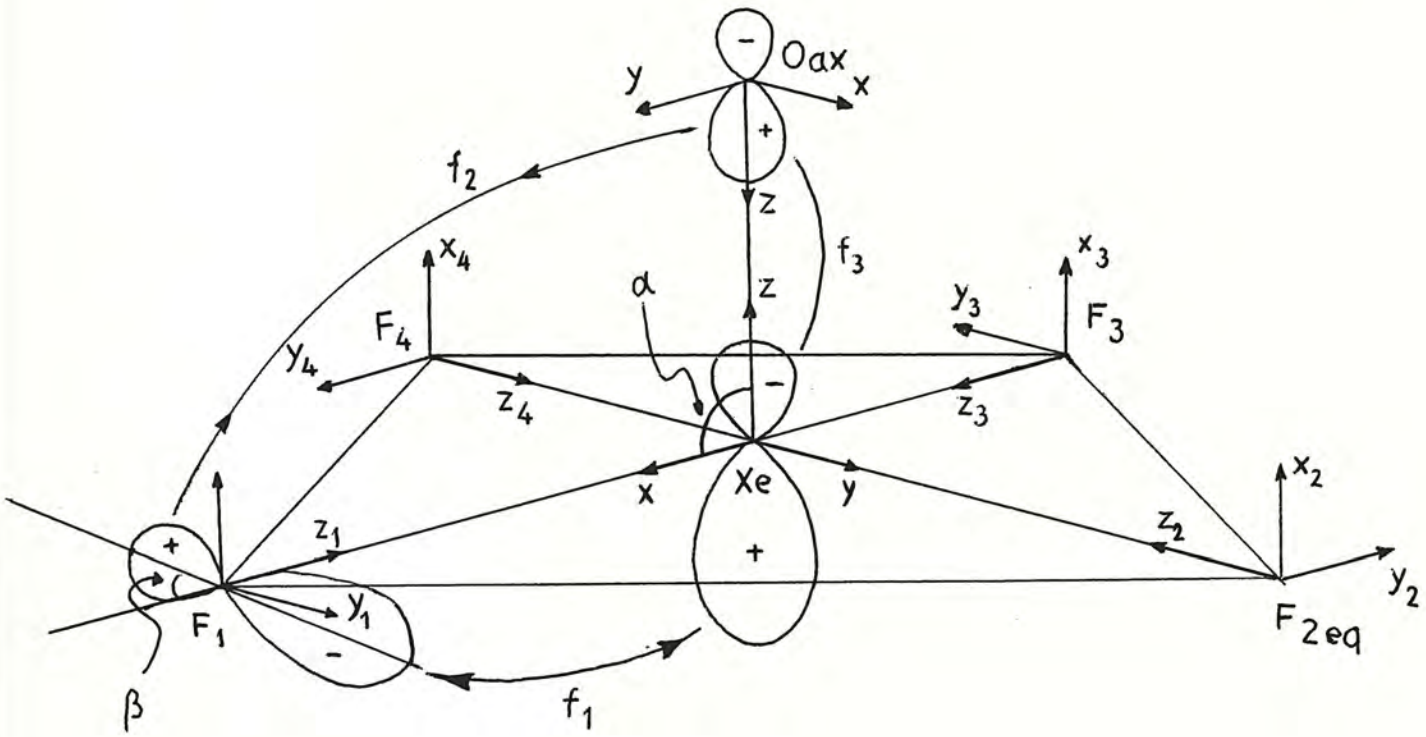

Fig. 15 The $6a_1$ MO of $XeOF_4$

Phases of the AO's are similar to the corresponding $6a_1$ MO for BrF_5 calculated by Berry et al. [29]. The $6a_1$ MO, which is the lone pair orbital, for BrF_5 (given in p. 15) is listed here again for direct comparison:

BrF_5

$6a_1$	4s (Br)	4p (Br)	4d (Br)	2s eq (F)	2s ax (F)	2pσ eq (F)	2pσ ax (F)	2pπ eq (F)
AO coeff.	.45	-.74	.07	-.21	.17	-.67	.26	.42
Population	.09	.40	.01	.02	.00	.33	.04	.11

The coefficients and relative populations for the AO's in these two MO's are rather similar. When the populations of the central atom orbitals are compared, lone pair nature in $XeOF_4$ is found to be even more pronounced.

Examining the MO shown in Fig. 15, the two forces f_1 and f_2 will be the determining factor for structural modification. The resultant of the two forces, as argued Berry et al.,will be a clockwise rotation which in effect will expose the outer fluorine positive lobe to the positive lobe in the axial ligand. This will tend to intensify the influence of f_2, causing a net rising up of the equatorial fluorine plane. However, it has been suggested in previous sections that the direction of rotation depends much on the magnitude of angle β which is defined by the population ratio of the (2pπ eq)/(2pσ eq). Comparison gives that for $XeOF_4$ the ratio is .05/.24, i.e. approximately

1/5 and for BrF_5 is .11/.33 i.e. 1/3. This means that for $XeOF_4$, an anticlockwise rotation will be more likely. Besides, the larger population in Xe p orbital also means a greater repulsive f_1 leading to an anticlockwise rotation. This, in effect will weaken f_2 and the positive lobe of the axial ligand will have effect pushing the fluorine atoms down. As result, an increase in α will be expected. The populations of the axial orbitals in BrF_5(.04) and $XeOF_4$(.02) also suggest why the effect found in BrF_5 is not likely to be observed in $XeOF_4$.

In order to test this argument, the same MO for $XeOF_4$ obtained with exact bond separations is given below for comparison.

$6a_1$(-61.77 kK)	5s (Xe)	5p (Xe)	2s eq (F)	2s ax (O)	2pσ eq (F)	2pσ ax (O)	2pπ eq (F)
AO coeff.	-.62	.70	.24	-.13	.69	-.08	-.27
Population	.22	.41	.02	.00	.32	-.00	.04

The participation of 5s orbital increases while that of the 5p decreases meaning a larger positive lobe below the plane of the fluorines and xenon. Also, the axial pσ orbital suffers quite a change with the coefficient reduced from .22 to .08. This leads to the idea that with $XeOF_4$, a picture similar to the one adopted for BrF_5 will be inadequate. Furthermore, the (2pπ eq)/(2pσ eq) population ratio shows a decrease from 1/5 to 1/8 meaning a significant decrease in the magnitude of β favoring the anticlockwise rotation which

finally leads to the increase of α. The population of the axial p orbital decreases to 0.00 for $XeOF_4$. This, again seems to follow the trend set by the present argument and drastically reduces the possibility of the fluorine atoms being raised out of the plane by the attraction f_2.

In brief, the final structure expected for $XeOF_4$ will be a square pyramid with the equatorial fluorine plane depressed below the central Xe atom. The extent of depression will be very much limited because the forces causing the distortion are very weak and short-ranged. This seems to lead to the conclusion that double bond is bulkier than lone pair for the $XeOF_4$ case. However, the difference in bulkiness may be quite marginal and dependent on other physical environment such as the nature of the central atom and that of the ligands.

When effect on bond lengths is considered, the $6a_1$ MO suggests that the molecule would be more stable if both Xe-F and Xe-O distances are increased. This is due to the repulsive nature of both f_1 and f_3 (Fig. 15). However, it can be observed that f_1 is active between two "major" lobes of the hybrid orbitals, while f_3 is between one "major" and one "minor" lobes of the hybrids. Therefore, it may be concluded that Xe-O should be shorter the Xe-F, even though both are assumed to be equal in the calculation. Again, this argument is reinforced in the calculation with experimental bond lengths. As

mentioned before, the lone pair nature below the equatorial plane in the new calculation is even more pronounced. Also, the population in oxygen AO's has decreased. These two modifications would lead to a more effective f_1 and a less effective f_3, which, in turn, favor a even longer Xe-F bonds comparing to the Xe-O one.

B. PH_5

Using the same method of calculation, the MO energies and wave functions have been obtained for the D_{3h} and C_{4v} structures of the hypothetical molecule PH_5. They are given in Appendix 2.

According to the simple sum of one-electron orbital energies, $\sum_i n_i \varepsilon_i$, the D_{3h} is the more stable structure, as expected from VSEPR considerations. Total energy for D_{3h} structure is -1529.2 kK while that for C_{4v} structure is -1523.2 kK. The difference of 6.0 kK is rather small when compared to the corresponding difference for these two structures in PF_5 (23.2 kK), AsF_5 (19.1 KK) and BrF_5(60.0 kK) as given by Berry et al. [29]. So the conclusion with PH_5 seems to be not as certain as in the pentafluoride. However, it should be noted that the ratios of (energy-difference)/(total-energy) for PH_5 and the pentafluorides are very similar. Also, the simple sum of one-electron orbital energy is actually something different from the exact total energy. This is because terms such as electron-electron repulsion have been ignored.

The stability of these structures may also be tested under the SOJT formalism which has been discussed in Chapter II. The ground electronic configurations for the two structures are given in Table XXIV.

Table XXIV. The Ground Electronic Configurations for PH_5 Energy in kK

D_{3h}	C_{4v}
$\ldots[1e'(-154.2)]^4[2a_1'(-74.7)]^2$	$\ldots[2a_1(-144.7)]^2[1b_1(-77.4)]^2$
$[2e'(-17.2)]^0\ldots$	$[3a_1(-26.4)]^0\ldots$
$\Delta E = E(2e') - E(2a_1') = 57.5$	$\Delta E = E(3a_1) - E(1b_1) = 51.0$
$(a_1')(e') = e'$	$(b_1)(a_1) = b_1$

The transition density for D_{3h} structure is e' and that for C_{4v} is b_1. The vibrational mode of e' symmetry will bring the D_{3h} symmetry into a C_{4v} one whereas the b_1 mode of vibration will bring the C_{4v} back into the D_{3h}. The energy gaps for the two cases are 57.5 kK(7.1ev) and 51.0 kK(6.3ev) which are both larger than the value of 4ev arbitrarily set by Pearson [31]. This makes the distortion rather marginal. However, it is observed that the gap for D_{3h} is larger than the C_{4v} one, this suggests that a larger activation energy is required to distort the D_{3h} structure implying higher stability. So both the sum of one-electron orbital energies and the SOJT effect favor the D_{3h} structure. One additional point which is worth mentioning is that the pseudorotation barrier for PH_5 should be

smaller than the ones found in the pentafluorides [29].

Considering only the one-electron orbital energy, there is a gain of 252.5 kK in the bonding energy for the process $P + 5H \rightarrow PH_5$. Therefore, the nonexistence of PH_5 cannot be explained by the formation of weak P-H bonds in this molecule. In order to have a better picture, similar calculation has been performed for PH_3. A gain of 218.9 kK is found for the process $P + 3H \rightarrow PH_3$. Similar treatment for H_2 gives a bonding energy of 88.6 kK. Adding up these results, there is a gain in energy for the process $PH_5 \rightarrow PH_3 + H_2$. This seems to be the cause of instability for the compound PH_5. In the MO calculations for H_2, PH_3 and PH_5, the same set of parameters such as experimental bond lengths, VSIP (in particular, the value of 1.20 is assigned to the H 1s orbital [36]), etc., is used throughout.

When the filled MO's for PH_5 are examined in detail, it is found that $1a_1'$ is a bonding MO between the P 3s and all the H 1s orbitals, with the equatorial hydrogen orbitals making a larger contribution. The MO $1a_2''$ is bonding between the P $3p_z$ and the axial hydrogen orbitals. The doubly degenerate MO's $1e'$ are bonding between the $3p_x$ and $3p_y$ orbitals of P and the equatorial hydrogens. The highest filled MO $2a_1'$ is essentially nonbonding and the electrons in this orbital are localized among all the hydrogens, with the axial ones claiming a larger share. Such MO description seems to confirm Pauling's theory that the resonance structures $PX_4^+ X^-$ should be

considered when the valence bond description for PX_5 is sought [46]. In fact, in view of the minor role the d orbitals play in this system, the five singly ionic resonance structures seem to have greater importance than the resonance structure with five covalent bonds.

In all these cases, all MO's with larger equatorial participation lie lower than the ones with larger axial contribution. These results, together with the total atomic population derived from Appendix 2, $3s^{1.28}3p^{3.20}3d^{0.04}H_{eq}^{3.00}H_{ax}^{2.48}$, are quite consistent with the consequence deduced by the VSEPR theory that the equatorial bonds are stronger and shorter than the axial ones. Similar results have been found by Issleib and Gründler in PH_5 [47] and Berry et al. in the pentafluorides [29]. To an even larger extent, the same situation is found in the C_{4v} results for PH_5. It can be derived from Appendix 2 that the atomic population now has the form $3s^{1.28}3p^{3.26}3d^{0.04}H_{eq}^{4.58}H_{ax}^{0.88}$, which again indicates that the axial bonds are longer and weaker. Another point that is worth mentioning is that the P 3d orbitals play a very minor role in the bonding MO's of PH_5.

C. SF_4

This molecule has the distorted tetrahedral structure, according to VSEPR theory, with one lone pair. It has been chosen both as a testing case for the nodal repulsion theory and as an independent

molecule with concern to stability of geometric structures. Detail MO descriptions for the three assumed symmetries, T_d, D_{4h}, and C_{2v} are given in Appendix 3. Closer examination of the C_{2v} MO gives the ground electronic configuration as:

$$\ldots [2a_2(-137.0)]^2[7a_1(-57.68)]^2[5b_1(38.98)]^0 \ldots \quad .$$

The outstanding $7a_1$ orbital, energywise, as before, gives the impression of its representation for the lone pair. The AO coefficients and population for this molecule are shown below:

$7a_1$ (-57.68 kK)	3s (S)	3p (S)	2s ax (F)	2pσ ax (F)	2pπ ax (F)	2s eq (F)	2pσ eq (F)	2pπ eq (F)
AO coeff.	-.43	.90	-.08	.00	-.31	.18	.41	-.36
Population	.11	.67	-.00	.00	.04	.01	.10	.06

Using the same argument as applied to XeO_2F_2, a picture can be drawn for this MO:

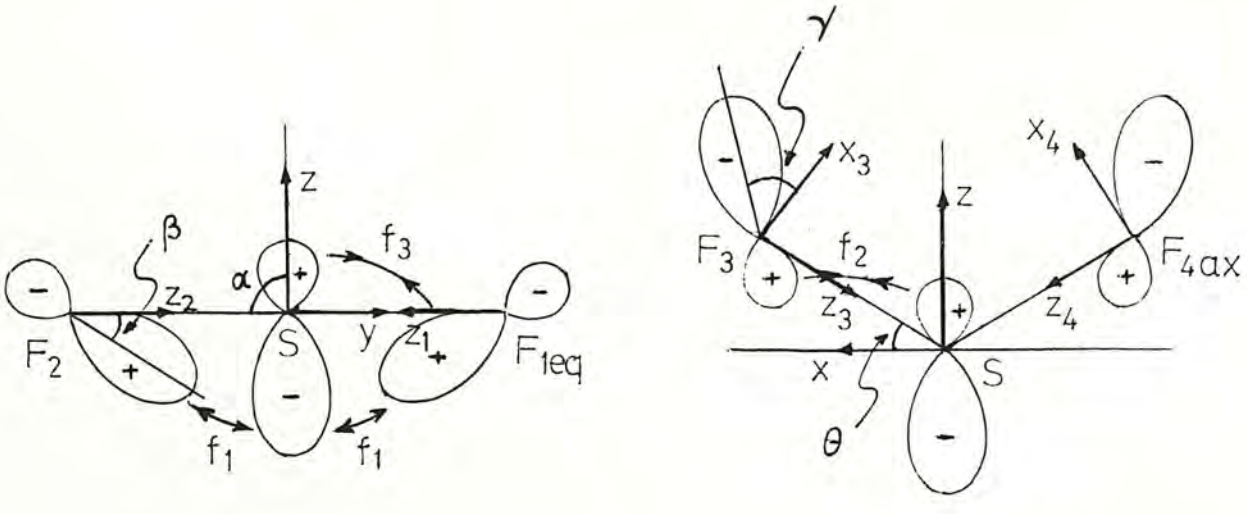

a. yz-plane b. xz-plane

Fig. 16 The $7a_1$ MO for SF_4 in C_{2v} Symmetry

According to Fig. 16, f_1 is repulsive and f_2 and f_3 are attractive. The effect of f_1 and f_3 will tend to rotate the fluorine "hybridized" orbital in the direction indicated. However, as stated earlier this depends very much on the magnitude of angle β which in this case has the ratio determining it as 6/10. This value is very large when compared with the corresponding values for the XeO_2F_2 (1/3.6). This indicates that the rotation effect may be of smaller significance. By consideration with the delocalization effect, the smear out of electron cloud in the region above the F_{eq}-S-F_{eq} plane tends to lead to a decrease in angle α. Besides, the small (2pσ ax)/(2pπ ax) ratio gives the idea that the axial fluorine atoms have the same signed lobe pointing towards each other instead of pointing away as in XeO_2F_2. These all show the closing up of angle α and the increase of angle θ. This picture agrees exceedingly well with the VSEPR model that it may be regarded as a successful test for the nodal repulsion theory.

The other two symmetries gives their corresponding ground state electronic wave functions as given below:

D_{4h} $\ldots[1a_{2g}(-143.43)]^2[2a_{2u}(-61.99)]^2[3a_{1g}(38.70)]^0\ldots$

T_d $\ldots[3t_2(-137.96)]^6[4t_2(-37.56)]^2[3a_1(50.95)]^0$.

The total orbital energies for the systems may be calculated using the same $\sum_i n_i \varepsilon_i$ expression. A summary for the necessary informations is given in Table XXV.

Table XXV. Total Energy (in kK). Transition Density and Energy Gap Between the HOMO and LUMO for SF_4

Symmetry	C_{2v}	D_{4h}
Total Energy	-6818.58	-6773.56
Transition Density Symmetry	$a_1 \times b_1 = b_1$	$a_{2u} \times a_{1g} = a_{2u}$
Energy Gap	100.11	100.69

From energy consideration, the C_{2v} structure is favored. The tetrahedral symmetry with its orbitally degenerate ground state is subjected to a first-order Jahn-Teller distortion, and cannot, therefore, be stable in the tetrahedral environment. The final structure of this distortion cannot be predicted except the conclusion of a lowering in symmetry can be made. The D_{4h} structure does not suffer the same fate. The transition density for this molecule has a_{2u} symmetry. The vibrational mode of A_{2u} symmetry for D_{4h} molecules leads the molecule to transfer into a C_{4v} structure instead of the expected C_{2v}. This does not resemble the picture obtained by Pearson [31] for this molecule under the same symmetry. His MO sequence runs

$$\ldots [3b_{1g}]^2[4a_1g]^2[2a_{2u}]^0 \ldots \quad .$$

The energy gap for the highest occupied MO(HOMO) and lowest unoccupied MO(LUMO) about 2.5ev for XeF_4 and the orbital energy for $3b_{1g}$ and $4a_{1g}$ are very close. His argument says that a combination of the transition density will result. The A_{2u} and B_{2u} vibrational modes

together will bring the square planar into a puckered C_{2v} structure. In the present work, however, the MO sequence gives only the A_{2u} transition density symmetry leading to a C_{4v} structure instead. The outstanding energy for the $2a_{2u}$ (-61.99 kK) when compared to the low lying bonding orbitals ($\leq$ -145 kK) does not give the Pearson picture. Even the energy gap between the two concerned MO's seems to be a bit large for SOJT effect to operate effectively. This cannot be concluded too definitely, other similar systems must be tested before any conclusion can be made.

Another point of interest is that for this molecule, two sets of VSIP data have been used. The above discussion is based on the values taken from Clementi's table [33]. When the other set, taken from Ballhausen and Gray [32], is considered, a rather unexpected situation is observed. The total energy terms for the different structures do not lie so much apart: T_d(-6842.34 kK), C_{2v}(-6802.34 kK) and D_{4h}(-6811.12 kK). The most stable structure total-orbital-energywise is the tetrahedral structure by about 30 to 40 kK. There seems to be some kind of contradiction because the ground electronic state for the T_d SF_4 is triply degenerate implying a first order Jahn-Teller distortion. Therefore, even the tetrahedral structure is unstable. So MO results obtained by the WH model seems to be highly dependent on the parameters used.

Chapter VI

CONCLUSION

The Wolfsberg-Helmholz calculation seems to give, to a varying degree, satisfactory MO functions for the molecules chosen in this thesis. The overall sequence of the bonding orbitals for each molecule display a qualitative picture of the gross geometry. With the xenon oxyfluorides, for example, the general trend gives first a set of low lying bonding orbitals mainly localized on the fluorine atoms. This actually corresponds to the mixing of the fluorine 2s orbitals only. The oxygen 2s and xenon 5s orbitals are the major contributors for the bonding MO's immediately above this set of low lying orbitals. Then, the other bonding MO's are found as a band lying within the limits of the p-orbitals of the xenon, oxygen and fluorine atoms. The outstanding lone pair orbital(s) fills the gap between the low lying p-like bonding orbitals and the antibonding orbitals. Fig. 17, which is the energy level diagram for $XeOF_4$, exemplifies this point.

In explaining the minor structural modifications in certain molecules, the proposed nodal repulsion effect seems to give a sensible picture. The nodal repulsion deals simply with electron delocalization and the property of avoidance of nodal surfaces. This comes from the quantum mechanical treatment on atomic and molecular

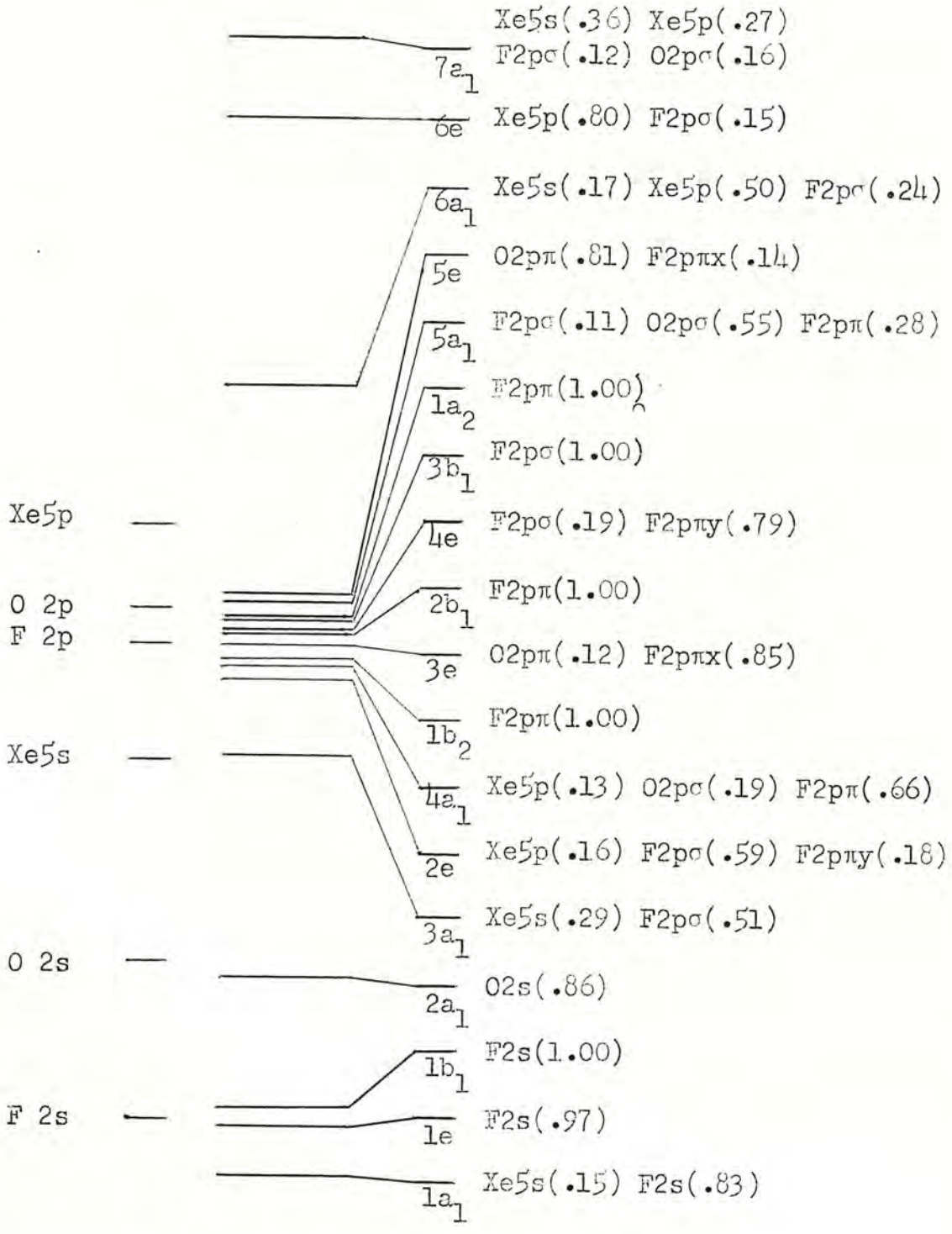

Fig. 17 The Energy Level Diagram for $XeOF_4$ at Averaged R

systems. The forces arising from this idea will be very sensitive to separation distance because the avoidance tends to lower the electron density around the nodal surfaces and this effect will be less important when the nodal surfaces are far away. The delocalization tendency has been viewed as an attractive force, again, when separation is too large, the extent of delocalization and the magnitude of the attractive force will be limited. With this argument, the nodal repulsion is a short-ranged force and deals mainly with electron cloud around the valence shell of the central atom. This theoretical approach, however, is very qualitative at this stage and quantitative prediction has bot been tried. So further work is still needed to be done in this area.

The above theory in explaining stereochemistry seems to be of very similar nature as the VSEPR theory. Both concern the valence sphere of one central atom, and short-ranged forces: Pauli force in VSEPR and nodal repulsion in the present model. With the VSEPR picture, the main concern is the number and arrangement of electron pairs, bonded and nonbonded, in the valence shell.

The electron pair repulsion governs the final structure of the molecule. This repulsion force is viewed as the short-ranged Pauli forces. So the Pauli force and nodal repulsion seem to come from entirely different theoretical origins. Yet they give very similar

qualitative results. This suggests intimate relationship between the two theories and thus provides a quantum mechanical background for the rather empirical VSEPR model. Finally, it should be pointed out that the quantum mechanical background for the localized bond model of VSEPR is furnished by the molecular orbital theory which, in principle, treats every bond as a delocalized one.

In $XeOF_4$, where there are one lone pair and one double bond, the FXeO angle of 91.8° obtained from microwave experiment and the present work agree that a double bond occupies more space than a lone pair in the same coordination sphere. However, the results for XeO_2F_2 do not indicate such a straight-forward conclusion. In $XeOF_2$, where there are two lone pairs and one double bond, the present result indicates that the FXeO angle should be less than 90°. This awaits experimental confirmation. In XeO_2F_2, where there are two double bond and one lone pair, the result predicts again that FXeO angle is less than 90°, but the OXeO angle is greater than 120°. (Once more, it is pointed out that the experiment result for this molecule is lacking and the structural data for the isoelectronic $IO_2F_2^-$ indicate that the OIO angle should be less than 120°.) When all the present results are grouped together, a definite conclusion concerning relative size for lone pair and double bond cannot be drawn. The only safe statement to make is that they are of comparable size.

In the calculation for the PH_5 system it is found that the

SOJT theory is a useful tool, in addition to the total orbital energy factor, in the determination of the most stable structure. As expected, the MO functions also rationalize structural modification, such as the axial bonds are longer than the equatorial bonds. The instability of this molecule is rationalized by the usual method of additivity of bond energies.

Regardless of the success in the nodal repulsion model with the mentioned molecules, the MO sequences obtained from the WH approximation method do not seem to be suitable for the SOJT consideration. The idea is that in this SOJT model, a more quantitative result is required. However, the work of Pearson [31] and Bartell [30] are quite successful in applying the SOJT formalism. One thing in common in their works is that both of them do not employ the MO directly obtained for the molecule under consideration.

In Bartell's treatment, he only considers σ bonds and lone pairs and he applies one qualitative MO energy sequence for all molecules with the same geometry. In Pearson's work, he gives a more quantitative treatment by imposing a 4eV limit. Nevertheless, he often uses one MO energy sequence for many molecules. For example, in treating SF_4 in D_{4h} symmetry, he uses the energy level ordering of XeF_4 and employs the energy values as well! So in retrospect, it may be said that it is very surprising they could obtain satisfactory results with such crude data.

Finally, one often mentioned statement concerning the WH model is required here: the quantitative result of a WH calculation is highly dependent on the parameters used. In the present SF_4 calculation, two different sets of VSIP data give rise to two vastly different results. Of course, this is a well known shortcoming of the WH method.

REFERENCES

1. L. Pauling, J. Am. Chem. Soc. 33, 1895 (1933)

2. G. C. Pimentel, J. Chem. Phys. 19, 446 (1951)

3. N. Bartlett, Proc. Chem. Soc. 218 (1962)

4. H. H. Claassen, H. Selig, and J. G. Malm, J. Am. Chem. Soc. 84, 3593 (1962)

5. See, for example, J. G. Malm, H. Selig, J. Jortner, and S. A. Rice, Chem. Rev. 65, 199 (1965)

6. L. C. Allen, Science 138, 892 (1962); Nature 197, 897 (1963); in "Noble-Gas Compounds" (H. H. Hyman, ed.), p.317, Univ. of Chicago Press, Chicago, Illinois (1963).

7. H. H. Michels, in "Noble-Gas Compounds" (H. H. Hyman, ed), p.329, Univ. of Chicago Press, Chicago, Illinois (1963)

8. C. A. Coulson, J. Chem. Soc. 1442 (1964)

9. R. E. Rundle, J. Am. Chem. Soc. 85, 112 (1963)

10. K. S. Pitzer, Science 139, 414 (1963)

11. L. L. Lohr, Jr., and W. N. Lipscomb, in "Noble-Gas Compounds" (H. H. Hyman, ed.), p.347, Univ. of Chicago Press, Chicago, Illinois (1963)

12. G. C. Pimentel, and R. D. Spratley, J. Am. Chem. Soc. 85, 826 (1963)

13. R. C. Catton, and K. A. R. Mitchell, Can. J. Chem. 48, 2695 (1970)

14. S. Reichman, and F. Schreiner, J. Chem. Phys. 51, 2355 (1969)

15. R. J. Gillespie, in "Noble-Gas Compounds" (H. H. Hyman, ed.), p.333, Univ. of Chicago Press, Chicago, Illinois (1963)

16. L. S. Bartell, and R. M. Gavin, Jr., J. Chem. Phys. 48, 2460, 2466 (1968)

17. R. Bersohn, J. Chem. Phys. 38, 2913 (1963)

18. W. E. Falconer, A. Buehler, J. C. Stauffer, and W. Klemperer, J. Chem. Phys. 48, 312 (1968).

19. E. H. Weibenga and D. Kracht, Inorg. Chem. 8, 738 (1969)

20. E. E. Havinga, and E. H. Weibenga, Recueil 78, 724 (1959)

21. G. H. Cheesman, A. J. T. Finney and I. K. Snook, Theor. Chim. Acta 16, 33 (1970)

22. K. Ramaswamy, J. Mol. Struct. 9, 193 (1971)

23. R. L. Oakland, and G. H. Duffey, J. Chem. Phys. 46, 19 (1967)

24. G. J. Moody, and J. D. R. Thomas, Rev. of Pure and Applied Chem. 16, 1 (1966)

25. J. Hinze, and K. S. Pitzer, in "Noble-Gas Compounds" (H. H. Hyman, ed.), p.340, Univ. of Chicago Press, Chicago, Illinois (1963)

26. W. A. Yeranos, Mol. Phys. 11, 85 (1966)

27. M. Wolfsberg, and L. Helmholz, J. Chem. Phys. 20, 837 (1952)

28. R. D. Willet, Theor. Chim. Acta 6, 186 (1966)

29. R. S. Berry, M. Tamres, C. J. Ballhausen, and H. Johanson, Acta Chem. Scand. 22, 231 (1968)

30. L. S. Bartell, J. Chem. Educ. 45, 754 (1968)

31. R. G. Pearson, J. Am. Chem. Soc. 91, 4947 (1969)

32. C. J. Ballhansen, and H. B. Gray, "Molecular Orbital Theory", Benjamin, New York.

33. E. Clementi, IBM Jl. Res. and Develop. 9, 2 (1965)

34. P. A. Straub, private communication.

35. M. Synek and G. E. Stungis, J. Chem. Phys. 42, 3068 (1965)

36. H. H. Brintzinger, and L. S. Bartell, J. Am. Chem. Soc. 92, 1105 (1970)

37. J. F. Martins, and E. B. Wilson, Jr., J. Mol. Spect. 26, 410 (1968)

38. W. M. Tolles and W. G. Gwinn, J. Chem. Phys. 36, 1119 (1962)

39. W. E. Dasent, "Nonexistent Compounds", Edward Arnold Publishers, London (1965)

40. A. F. Wells, "Structural Inorganic Chemistry", 3rd ed., p.642, Clarendon Press, Oxford (1962)

41. E. A. Boudreaux, in "Noble-Gas Compounds" (H. H. Hyman, ed.), p.354, Univ. of Chicago Press, Chicago, Illinois, (1963)

42. J. Jortner, E. G. Wilson, and S. A. Rice, in "Noble-Gas Compounds" (H. H. Hyman, ed.), p.358, Univ. of Chicago Press, Chicago, Illinois (1963)

43. H. B. Gray, "Electrons and Chemical Bonding", p.218, Benjamin, New York (1965)

44. W. A. Yeranos, Z. Naturforschg 21a, 1864 (1966)

45. H. H. Claassen, E. L. Gasner, H. Kim and J. L. Huston, J. Chem. Phys. 49, 253 (1968)

46. L. Pauling, "Nature of the Chemical Bond", 3rd ed., p.177, Cornell University Press, Ithaca (1960)

47. K. Issleib, and W. Griindler, Theor. Chim. Acta 8, 70 (1967)

APPENDIX 1 Orbitals and Energies of the Xenon Oxyfluorides.

The co-ordinate systems for $XeOF_2$ is given on p. 35, Fig. 6; for XeO_2F_2, p. 38, Fig. 7; for $XeOF_4$, p. 27, Fig. 4 of this thesis. The VSIP data are given in Table XVIII, p. 71. The eigenvalues, eigenvectors and populations for these three compounds are given below :

(1) Molecular Orbitals for $XeOF_2$:

A. VSIP data : Set I

Two-atom overlap data : At averaged R, i.e. 1.80 Å for both Xe-O and Xe-F distances.

Eigenvalues (kK)		Eigenvectors (populations)						
		5s (Xe)	5p (Xe)	2s eq (F)	2s ax (O)	2pσ eq (F)	2pσ ax (O)	2pπ eq (F)
$7a_1$	47.09	-.72	-.89	.18	.53	.31	.72	.15
		(.22)	(.43)	(.01)	(.07)	(.05)	(.22)	(.01)
$6a_1$	-77.17	-.62	.62	.23	-.08	.71	.00	-.25
		(.23)	(.34)	(.02)	(.00)	(.37)	(.00)	(.03)
$5a_1$	-129.19	-.02	-.21	.04	.04	.45	-.67	.56
		(.00)	(.06)	(.00)	(.00)	(.18)	(.47)	(.28)
$4a_1$	-145.51	-.03	.25	-.00	-.16	-.12	.40	.79
		(.00)	(.12)	(.00)	(.01)	(.01)	(.19)	(.67)

(Cont'd)

$3a_1$	-182.97	.56	-.12	-.27	-.29	.53	.29	-.05
		(.38)	(.02)	(.04)	(.06)	(.38)	(.12)	(.00)
$2a_1$	-268.39	.20	.09	-.26	.89	.05	-.00	.02
		(.06)	(.03)	(.05)	(.84)	(.01)	(.00)	(.00)
$1a_1$	-331.78	.23	-.00	.91	.12	-.00	.01	.00
		(.10)	(.00)	(.87)	(.02)	(.00)	(.00)	(.00)

		$2p\pi$ eq (F)
$1a_2$	-140.07	1.00 (1.00)

		5p (Xe)	$2p\pi$ eq (F)	$2p\pi$ ax (O)
$3b_1$	-78.49	.96	-.39	-.38
		(.81)	(.09)	(.09)
$2b_1$	-128.87	.14	-.43	.89
		(.01)	(.16)	(.81)
$1b_1$	-146.86	.32	.83	.29
		(.16)	(.74)	(.10)

		5p (Xe)	2s eq (F)	$2p\sigma$ eq (F)	$2p\pi$ ax (O)	$2p\pi$ eq (F)
$5b_2$	45.56	1.19	-.53	-.70	-.18	.02
		(.80)	(.02)	(.17)	(.01)	(.00)

(Cont'd)

$4b_2$	-123.08	-.01	-.04	-.22	.92	-.40
		(.00)	(.00)	(.04)	(.82)	(.14)
$3b_2$	-142.29	-.05	.01	-.18	.32	.91
		(.00)	(.00)	(.04)	(.10)	(.85)
$2b_2$	-151.83	.29	-.15	.81	.22	.11
		(.17)	(.00)	(.75)	(.06)	(.01)
$1b_2$	-323.03	.06	.97	-.01	.01	-.00
		(.02)	(.97)	(.00)	(.00)	(.00)

Ground State Electronic Configuration :

$[1a_1]^2[1b_2]^2[2a_1]^2[3a_1]^2[2b_2]^2[1b_1]^2[4a_1]^2[3b_2]^2[1a_2]^2[5a_1]^2$
$[2b_1]^2[4b_2]^2[6a_1]^2[3b_1]^2[5b_2]^0[7a_1]^0$

Total Orbital Energy = -4739.06 kK

B. VSIP data : Set I

Two-atom overlap data : at experimental separation, i.e.

Xe-F = 1.900 Å , Xe-O = 1.703 Å

Eigenvalues (kK)		Eigenvectors (populations)						
		5s (Xe)	5p (Xe)	2s eq (F)	2s ax (O)	2pσ eq (F)	2pσ ax (O)	2pπ eq (F)
$7a_1$	78.38	-.72	-.95	.13	.63	.24	.75	.11
		(.21)	(.45)	(.00)	(.09)	(.03)	(.22)	(.00)

(Cont'd)

$6a_1$	-88.49	-.60	.59	.18	-.06	.70	.11	-.24
		(.22)	(.34)	(.01)	(.00)	(.38)	(.02)	(.04)
$5a_1$	-130.05	.03	.21	-.04	-.06	-.52	.65	-.51
		(.00)	(.06)	(.00)	(.00)	(.25)	(.44)	(.24)
$4a_1$	-144.00	-.03	.22	-.00	-.15	-.12	.38	.83
		(.00)	(.09)	(.00)	(.01)	(.01)	(.18)	(.72)
$3a_1$	-182.15	.57	-.15	-.23	-.33	.49	.33	-.06
		(.39)	(.03)	(.03)	(.08)	(.32)	(.15)	(.00)
$2a_1$	-271.86	.24	.09	-.28	.85	.05	-.00	.02
		(.10)	(.03)	(.06)	(.80)	(.01)	(.00)	(.00)
$1a_1$	-329.49	.21	-.00	.92	.13	.00	.01	.00
		(.08)	(.00)	(.89)	(.02)	(.00)	(.00)	(.00)

		$2p\pi$ eq (F)
$1a_2$	-140.12	1.00 (1.00)

		5p (Xe)	$2p\pi$ eq (F)	$2p\pi$ ax (O)
$3b_1$	-78.41	.96 (.80)	-.31 (.06)	-.46 (.14)
$2b_1$	-130.03	.19 (.05)	-.49 (.22)	.84 (.73)
$1b_1$	-145.94	.30 (.15)	.82 (.72)	.33 (.13)

(Cont'd)

		5p (Xe)	2s eq (F)	2pσ eq (F)	2pπ ax (O)	2pπ eq (F)
$5b_2$	11.56	1.13	-.43	-.66	-.24	.02
		(.79)	(.02)	(.17)	(.02)	(.00)
$4b_2$	-123.16	.01	-.05	-.28	.91	-.39
		(.00)	(.00)	(.07)	(.80)	(.13)
$3b_2$	-142.21	-.05	.01	-.21	.30	.91
		(.00)	(.00)	(.05)	(.10)	(.85)
$2b_2$	-152.06	.30	-.14	.79	.25	.12
		(.18)	(.00)	(.72)	(.08)	(.02)
$1b_2$	-322.89	.05	.98	-.01	.01	-.00
		(.02)	(.98)	(.00)	(.00)	(.00)

Ground State Electronic Configuration :

$[1a_1]^2[1b_2]^2[2a_1]^2[3a_1]^2[2b_2]^2[1b_1]^2[4a_1]^2[3b_2]^2[1a_2]^2[5a_1]^2[2b_1]^2$
$[4b_2]^2[6a_1]^2[3b_1]^2[5b_2]^0[7a_1]^0$

Total Orbital Energy = -4761.70 kK

(2) Molecular Orbitals for XeO_2F_2 :

A. VSIP data : Set I

Two-atom overlap data : At averaged R, i.e. 1.80 Å for both Xe-O and Xe-F distances.

Eigenvalues (kK)		Eigenvectors (populations)							
		5s (Xe)	5p (Xe)	2s ax (O)	2pσ ax (O)	2pπ ax (O)	2s eq (F)	2pσ eq (F)	2pπ eq (F)
$8a_1$	59.04	-.95	-.64	.51	.74	.14	.23	.40	.10
		(.38)	(.21)	(.07)	(.24)	(.01)	(.02)	(.08)	(.00)
$7a_1$	-73.93	-.44	.82	-.06	.06	-.36	.16	.47	-.31
		(.11)	(.57)	(.00)	(.01)	(.08)	(.01)	(.16)	(.05)
$6a_1$	-125.76	-.07	-.06	.00	-.60	.53	.07	.63	.08
		(.00)	(.00)	(.00)	(.35)	(.27)	(.00)	(.36)	(.01)
$5a_1$	-131.03	.00	.15	-.02	.27	.69	-.02	-.25	-.61
		(.00)	(.04)	(.00)	(.08)	(.49)	(.00)	(.06)	(.34)
$4a_1$	-147.69	-.03	.30	-.12	.27	.35	.00	-.09	.74
		(.00)	(.15)	(.01)	(.09)	(.15)	(.00)	(.00)	(.59)
$3a_1$	-179.15	.48	-.12	-.39	.41	-.02	-.23	.50	-.06
		(.29)	(.02)	(.10)	(.23)	(.00)	(.03)	(.32)	(.00)
$2a_1$	-272.62	.24	.05	.85	.01	.00	-.36	.06	.01
		(.10)	(.01)	(.78)	(.00)	(.00)	(.10)	(.01)	(.00)
$1a_1$	-332.82	.24	-.00	.17	.01	.00	.89	-.00	.00
		(.11)	(.00)	(.04)	(.00)	(.00)	(.84)	(.00)	(.00)

(Cont'd)

		$2p\pi$ eq (F)	$2p\pi$ ax (O)
$2a_2$	-122.56	-.47	.91
		(.19)	(.81)
$1a_2$	-143.69	.88	.41
		(.81)	(.19)

		5p (Xe)	$2p\pi$ eq (F)	2s ax (O)	$2p\sigma$ ax (O)	$2p\pi$ ax (O)
$5b_1$	42.23	1.17	-.20	-.56	-.69	-.16
		(.75)	(.01)	(.05)	(.18)	(.01)
$4b_1$	-125.50	-.05	.06	.00	-.34	.94
		(.00)	(.00)	(.00)	(.12)	(.88)
$3b_1$	-131.05	-.20	.72	.05	-.60	-.28
		(.06)	(.47)	(.00)	(.39)	(.08)
$2b_1$	-146.66	.25	.69	-.20	.50	.17
		(.12)	(.51)	(.02)	(.32)	(.03)
$1b_1$	-263.12	.13	.03	.94	-.02	.00
		(.06)	(.00)	(.93)	(.00)	(.00)

		5p (Xe)	2s eq (F)	$2p\sigma$ eq (F)	$2p\pi$ eq (F)	$2p\pi$ ax (O)
$5b_2$	51.20	1.21	-.05	-.69	.02	-.26
		(.80)	(.02)	(.16)	(.00)	(.02)
$4b_2$	-123.61	-.02	-.06	-.32	-.29	.93
		(.00)	(.00)	(.09)	(.07)	(.83)
$3b_2$	-141.12	-.04	.00	-.16	.95	.22
		(.00)	(.00)	(.03)	(.92)	(.05)

(Cont'd)

$2b_2$	-152.69	.29	-.16	.79	.09	.27
		(.17)	(.00)	(.72)	(.01)	(.10)
$1b_2$	-323.05	.06	.97	-.01	-.00	.02
		(.03)	(.97)	(.00)	(.00)	(.00)

Ground State Electronic Configuration :

$$[1a_1]^2[1b_2]^2[2a_1]^2[1b_1]^2[3a_1]^2[2b_2]^2[4a_1]^2[2b_1]^2[1a_2]^2[3b_2]^2$$
$$[3b_1]^2[5a_1]^2[6a_1]^2[4b_1]^2[4b_2]^2[2a_2]^2[7a_1]^2[5b_1]^0[5b_2]^0[8a_1]^0$$

Total Orbital Energy = -5872.08 kK

B. VSIP data : Set II

Two-atom overlap data : At experimental bond separations, i.e. Xe-O at 1.703 Å and Xe-F at 1.900 Å .

Eigenvalues (kK)		Eigenvectors (populations)							
		5s (Xe)	5p (Xe)	2s ax (O)	2pσ ax (O)	2pπ ax (O)	2s eq (F)	2pσ eq (F)	2pπ eq (F)
$8a_1$	92.56	-.98	-.70	.61	.78	.16	.18	.31	.08
		(.37)	(.23)	(.10)	(.24)	(.01)	(.01)	(.04)	(.00)
$7a_1$	-77.45	-.44	.79	-.03	.17	-.45	.12	.42	-.26
		(.11)	(.55)	(.00)	(.03)	(.13)	(.00)	(.13)	(.04)
$6a_1$	-126.98	-.09	-.01	.01	-.53	.51	.07	.71	.00
		(.01)	(.00)	(.00)	(.27)	(.25)	(.00)	(.47)	(.00)
$5a_1$	-132.69	.00	.17	-.03	.26	.63	-.02	-.27	-.66
		(.00)	(.04)	(.00)	(.07)	(.41)	(.00)	(.09)	(.40)

(Cont'd)

$4a_1$	-146.90	-.03	.28	-.13	.28	.41	-.00	-.09	.71
		(.00)	(.14)	(.01)	(.10)	(.20)	(.00)	(.01)	(.55)
$3a_1$	-176.79	.46	-.15	-.42	.46	-.04	-.19	-.46	-.07
		(.27)	(.03)	(.12)	(.28)	(.00)	(.02)	(.27)	(.01)
$2a_1$	-278.07	.29	.05	.80	.01	.00	-.38	.05	.01
		(.14)	(.01)	(.72)	(.00)	(.00)	(.12)	(.01)	(.00)
$1a_1$	-330.72	.22	-.00	.19	.01	.00	.90	.00	.00
		(.10)	(.00)	(.05)	(.00)	(.00)	(.85)	(.00)	(.00)

		2pπ eq (F)	2pπ ax (O)
$2a_2$	-122.35	-.46	.92
		(.19)	(.81)
$1a_2$	-143.65	.89	.41
		(.81)	(.19)

		5p (Xe)	2pπ eq (F)	2s ax (O)	2pσ ax (O)	2pπ ax (O)
$5b_1$	76.84	1.23	-.14	-.66	-.71	-.19
		(.75)	(.00)	(.07)	(.17)	(.01)
$4b_1$	-124.49	-.06	.07	.00	-.38	.92
		(.01)	(.00)	(.00)	(.15)	(.84)
$3b_1$	-131.81	.21	-.70	-.07	.58	.32
		(.07)	(.45)	(.00)	(.37)	(.11)
$2b_1$	-145.20	.21	.71	-.20	.50	.18
		(.09)	(.54)	(.01)	(.31)	(.04)
$1b_1$	-263.39	.14	.03	.92	-.03	.00
		(.08)	(.00)	(.92)	(.00)	(.00)

(Cont'd)

		5p (Xe)	2s eq (F)	2pσ eq (F)	2pπ eq (F)	2pπ ax (O)
$5b_2$	19.68	1.15	-.43	-.64	.02	-.34
		(.80)	(.01)	(.15)	(.00)	(.04)
$4b_2$	-123.93	.01	-.07	-.39	-.28	.90
		(.00)	(.00)	(.14)	(.07)	(.79)
$3b_2$	-141.09	-.04	.00	-.18	.95	.21
		(.00)	(.00)	(.03)	(.92)	(.05)
$2b_2$	-153.21	.30	-.15	.76	.10	.31
		(.18)	(.00)	(.68)	(.01)	(.13)
$1b_2$	-322.91	.05	.98	-.01	-.00	.02
		(.02)	(.98)	(.00)	(.00)	(.00)

Ground State Electronic Configuration :

$$[1a_1]^2[1b_2]^2[2a_1]^2[1b_1]^2[3a_1]^2[2b_1]^2[4a_1]^2[2b_1]^2[1a_2]^2[3b_2]^2$$
$$[5a_1]^2[3b_1]^2[6a_1]^2[4b_1]^2[4b_2]^2[2a_2]^2[7a_1]^2[5b_2]^0[5b_1]^0[8a_1]^0$$

Total Orbital Energy = -5883.28 k K

(3) Molecular Orbitals for $XeOF_4$:

A. VSIP data : Set I

Two-atom overlap data : At averaged R, i.e. 1.80 Å for both Xe-O and Xe-F distances

Eigenvalue (k K)		Eigenvectors (populations)						
		5s (Xe)	5p (Xe)	2s eq (F)	2s ax (O)	2pσ eq (F)	2pσ ax (O)	2pπ eq (F)
$7a_1$	85.95	-.95	-.75	.32	.50	.53	.65	.16
		(.36)	(.27)	(.03)	(.06)	(.12)	(.16)	(.00)
$6a_1$	- 44.51	.56	-.81	-.26	.19	-.63	.22	.32
		(.17)	(.50)	(.02)	(.00)	(.24)	(.02)	(.05)
$5a_1$	-126.65	-.02	-.20	.04	.01	.36	-.74	.57
		(.00)	(.06)	(.00)	(.00)	(.11)	(.55)	(.28)
$4a_1$	-149.78	-.02	.26	-.00	-.19	-.06	.39	.78
		(.00)	(.13)	(.00)	(.01)	(.00)	(.19)	(.66)
$3a_1$	-183.36	.46	-.11	-.34	-.25	.63	.23	-.07
		(.29)	(.01)	(.06)	(.04)	(.51)	(.08)	(.01)
$2a_1$	-266.12	.14	.09	-.27	.90	.06	-.01	.03
		(.03)	(.04)	(.06)	(.86)	(.01)	(.00)	(.00)
$1a_1$	-342.07	.26	-.00	.87	.12	.00	.00	.00
		(.15)	(.00)	(.83)	(.02)	(.00)	(.00)	(.00)

		2pπ eq (F)
$1a_2$	-131.71	1.00
		(1.00)

(Cont'd)

		2s eq (F)	2pσ eq (F)	2pπ eq (F)
$3b_1$	-133.01	.01 (.00)	1.00 (1.00)	.00 (.00)
$2b_1$	-137.40	.00 (.00)	.00 (.00)	1.00 (1.00)
$1b_1$	-317.30	1.00 (1.00)	−.01 (.00)	.00 (.00)

		2pπ eq (F)
$1b_2$	-147.54	1.00 (1.00)

		5p (Xe)	2s eq (F)	2pσ eq (F)	2pπy eq (F)	2pπ ax (O)	2pπx eq (F)
6e	54.49	1.21 (.80)	-.53 (.02)	-.69 (.15)	-.21 (.01)	-.19 (.01)	.02 (.00)
5e	-123.02	-.00 (.00)	-.04 (.00)	-.23 (.05)	-.04 (.00)	.92 (.81)	-.39 (.14)
4e	-136.17	-.08 (.01)	-.01 (.00)	-.44 (.19)	.91 (.79)	-.04 (.00)	.06 (.00)
3e	-142.34	-.03 (.00)	.00 (.00)	-.12 (.02)	.11 (.01)	.33 (.12)	.91 (.85)
2e	-154.89	.28 (.16)	-.17 (.01)	.71 (.59)	.39 (.18)	.20 (.06)	.08 (.01)
1e	-323.08	.06 (.03)	.97 (.97)	-.01 (.00)	.02 (.00)	.01 (.00)	-.00 (.00)

Ground State Electronic Configuration :

$[1a_1]^2[1e]^4[1b_1]^2[2a_1]^2[3a_1]^2[2e]^4[4a_1]^2[1b_2]^2[3e]^4[2b_1]^2[4e]^4$
$[3b_1]^2[1a_2]^2[5a_1]^2[5e]^4[6a_1]^2[6e]^0[7a_1]^0$

Total Orbital Energy = -7476.92 kK

B. VSIP data : Set I

Two-atom overlap data : At experimental bond separations, i.e. Xe-O at 1.703 Å and Xe-F at 1.900 Å .

Eigenvalues (kK)	Eigenvectors (populations)						
	5s (Xe)	5p (Xe)	2s eq (F)	2s ax (O)	2pσ eq (F)	2pσ ax (O)	2pπ eq (F)
$7a_1$ 102.62	-.86	-.89	.22	.62	.39	.72	.14
	(.28)	(.36)	(.01)	(.08)	(.06)	(.19)	(.00)
$6a_1$ -61.77	-.62	.70	.24	-.13	.69	-.08	-.27
	(.22)	(.41)	(.02)	(.00)	(.32)	(.00)	(.04)
$5a_1$ -127.39	-0.03	-.21	.04	.04	.42	-.70	.55
	(.00)	(.06)	(.00)	(.00)	(.15)	(.51)	(.27)
$4a_1$ -147.41	-.02	.23	-.01	-.19	-.07	.40	.80
	(.00)	(.10)	(.00)	(.01)	(.00)	(.20)	(.68)
$3a_1$ -183.80	.49	-.14	-.30	-.29	.59	.26	-.08
	(.31)	(.03)	(.04)	(.06)	(.45)	(.10)	(.01)

(Cont'd)

$2a_1$ -269.22	.19	.09	-.31	.87	.06	-.01	.03
	(.06)	(.04)	(.07)	(.81)	(.01)	(.00)	(.00)
$1a_1$ -337.48	.24	-.01	.89	.14	.01	.01	.00
	(.12)	(.00)	(.85)	(.03)	(.00)	(.00)	(.00)

	2pπ eq (F)
$1a_2$ -133.64	1.00
	(1.00)

	2s eq (F)	2pσ eq (F)	2pπ eq (F)
$3b_1$ -134.54	.01	1.00	.00
	(.00)	(1.00)	(.00)
$2b_1$ -138.12	.00	.00	1.00
	(.00)	(.00)	(1.00)
$1b_1$ -318.89	1.00	-.00	.00
	(1.00)	(.00)	(.00)

	2pπ eq (F)
$1b_2$ -146.06	1.00
	(1.00)

(Cont'd)

		5p (Xe)	2s eq (F)	2pσ eq (F)	2pπyeq (F)	2pσ ax (O)	2pπxeq (F)
6e	17.74	1.15	-.43	-.64	-.18	-.25	.02
		(.80)	(.02)	(.15)	(.01)	(.02)	(.00)
5e	-123.13	.02	-.05	-.28	-.07	.90	-.39
		(.00)	(.00)	(.07)	(.00)	(.79)	(.13)
4e	-137.18	-.08	-.01	-.42	.91	-.03	.06
		(.01)	(.00)	(.17)	(.81)	(.00)	(.00)
3e	-142.25	-.03	.00	-.15	-.13	.31	.92
		(.00)	(.00)	(.02)	(.02)	(.11)	(.85)
2e	-154.69	.29	-.15	.70	.37	.24	.09
		(.17)	(.00)	(.58)	(.16)	(.08)	(.01)
1e	-322.92	.05	.98	-.01	.01	.01	.00
		(.02)	(.98)	(.00)	(.00)	(.00)	(.00)

Ground State Electronic Configuration :

$$[1a_1]^2\,[1e]^4[1b_1]^2[2a_1]^2[3a_1]^2[2e]^4[1b_2]^2[4a_1]^2[3e]^4[2b_1]^2[4e]^4$$
$$[3b_1]^2\,[1a_2]^2[5a_1]^2[5e]^4[6a_1]^2[6e]^0[7a_1]^0$$

Total Orbital Energy = -7517.32 k K

APPENDIX 2 Orbitals and Energies of PH_3 and PH_5

The co-ordinate systems used are given on p. 42, p. 46 and p. 48 for T_d, C_{3v} and D_{3h} symmetries. Due to the insignificant participation of P_{3d} orbitals in the MO's of PH_5, the basis set now includes only the 1s orbital of hydrogen and 3s and 3p orbitals of phosphorus. The P-H bond length is taken as 1.42 Å and the HPH bond angles are of the experimental value 93.5° for PH_3 [40]. For PH_5, the same P-H bond length is used with inclusion of d orbitals. The following will be a listing of the concerned MO wave functions.

(1) Molecular orbitals for PH_3 (C_{3v} symmetry) :

Eigenvalues (kK)		Eigenvectors (populations)		
		3s (P)	3p (P)	1s (H)
$3a_1$	200.3	-1.08 (0.23)	-0.82 (0.18)	1.42 (0.59)
$2a_1$	-125.6	-0.37 (0.08)	0.86 (0.82)	0.25 (0.10)
$1a_1$	-217.0	0.72 (0.69)	0.01 (0.00)	0.38 (0.31)

(Cont'd)

		3p (P)	1s (H)
2e	47.0	-1.03	1.09
		(0.43)	(0.57)
12	-147.6	0.63	0.50
		(0.57)	(0.43)

Ground State Electronic Configuration : $[1a_1]^2[1e]^4[2a_1]^2$

Total Orbital Energy = -1275.6 kK

(2) Molecular Orbitals for PH_5 (D_{3h} Symmetry)

	Eigenvalues (kK)	Eigenvectors (populations)			
		3s (P)	3d (P)	1s eq (H)	1s ax (H)
$4a_1'$	182.7	-1.32 (0.36)	-0.09 (0.00)	0.98 (0.39)	0.77 (0.25)
$3a_1'$	4.2	-0.03 (0.00)	1.12 (0.98)	0.44 (0.02)	-0.48 (0.01)
$2a_1'$	-74.7	-0.02 (0.00)	0.04 (0.02)	-0.75 (0.37)	0.90 (0.61)
$1a_1'$	-223.6	0.66 (0.64)	-0.01 (0.00)	0.28 (0.21)	0.23 (0.15)
		3p (P)	1a ax (H)		
$2a_2''$	200.6	-1.36 (0.48)	1.37 (0.52)		
$1a_2''$	-157.9	0.56 (0.52)	0.52 (0.48)		
		3p (P)	3d (P)	1s eq (H)	
$3e'$	132.8	1.19 (0.44)	-0.49 (0.07)	1.28 (0.49)	
$2e'$	-17.2	0.22 (0.03)	0.94 (0.93)	0.16 (0.04)	
$1e'$	-154.2	0.58 (0.54)	0.08 (0.00)	-0.53 (0.46)	

(Con'd)

		3d (P)
$1e''$	-14.4	1.00 (1.00)

Ground State Electronic Configuration :

$$[1a_1']^2[1a_2'']^2[1e']^4[2a_1']^2[2e']^0$$

Total Orbital Energy = -1529.2 kK

(3) Molecular Orbitals for PH_5 (C_{4v} Symmetry)

	Eigenvalues (kK)	Eigenvectors (populations)				
		3s (P)	3p (P)	3d (P)	ls eq (H)	ls ax (H)
$5a_1$	218.5	-1.28 (0.32)	-0.57 (0.08)	0.01 (0.00)	1.02 (0.35)	0.85 (0.25)
$4a_1$	45.0	0.33 (0.03)	-0.75 (0.23)	-0.81 (0.35)	-0.83 (0.20)	0.87 (0.20)
$3a_1$	-26.4	0.18 (0.01)	-0.41 (0.10)	0.74 (0.66)	-0.37 (0.12)	0.36 (0.11)
$2a_1$	-144.7	-0.10 (0.01)	0.65 (0.59)	-0.09 (0.01)	-0.24 (0.04)	0.51 (0.37)
$1a_1$	-223.7	0.66 (0.63)	0.00 (0.00)	0.03 (0.00)	0.35 (0.30)	0.14 (0.07)

		3d (P)	ls eq (H)
$2b_1$	5.4	1.14 (0.99)	-0.56 (0.01)
$1b_1$	-77.4	0.02 (0.01)	0.99 (0.99)

		3d (P)
$1b_2$	-14.4	1.00 (1.00)

(Cont'd)

		3d (P)	3p (P)	1s eq (H)
3e	200.6	0.00	-1.36	1.37
		(0.00)	(0.48)	(0.52)
2e	-14.4	1.00	0.00	0.00
		(1.00)	(0.00)	(0.00)
1e	-157.9	0.00	0.56	0.52
		(0.00)	(0.52)	(0.48)

Ground State Electronic Configuration :

$$[1a_1]^2[1e]^4[2a_1]^2[1b_1]^2[3a_1]^0$$

Total Orbital Energy = -1523.2

APPENDIX 3 Orbitals and Energies for SF_4 with varying Symmetries.

The following tables give the details of the Molecular Orbitals for SF_4 with C_{2v}, T_d and D_{4h} symmetries. Two sets of VSIP data have been employed in the calculation, so, for each symmetry there will be two sets of results. The energies are given in units of kK. The value of R is taken to be 1.595 Å throughout.

(1) Molecular Orbitals for SF_4 (C_{2v} Symmetry)

A.Gray's VSIP data

Eigenvalues (kK)		Eigenvectors (populations)							
		3s (S)	3p (S)	2s ax (F)	2pσ ax (F)	2pπ ax (F)	2s eq (F)	2pσ eq (F)	2pπ eq (F)
$8a_1$	81.13	-1.08	-.58	.47	.60	.13	.31	.45	.12
		(.55)	(.18)	(.03)	(.13)	(.00)	(.02)	(.08)	(.00)
$7a_1$	-57.68	-.43	.90	-.08	.00	-.31	.18	.41	-.36
		(.12)	(.67)	(.00)	(.00)	(.04)	(.01)	(.11)	(.06)
$6a_1$	-137.39	-.01	.09	.05	.69	-.12	-.06	-.68	-.36
		(.00)	(.01)	(.00)	(.44)	(.01)	(.00)	(.42)	(.12)

(Cont'd)

$5a_1$	-147.16	-.02	.03	-.02	.13	-.75	-.00	-.09	.67
		(.00)	(.00)	(.00)	(.02)	(.53)	(.00)	(.01)	(.44)
$4a_1$	-164.16	-.06	.26	-.07	.23	.60	.01	-.12	.57
		(.00)	(.14)	(.00)	(.06)	(.41)	(.00)	(.01)	(.38)
$3a_1$	-186.69	.39	-.06	-.21	.52	-.01	-.22	.54	-.03
		(.24)	(.00)	(.02)	(.35)	(.00)	(.02)	(.37)	(.00)
$2a_1$	-362.00	.00	-.01	-.71	.02	-.00	.73	-.02	-.01
		(.00)	(.00)	(.48)	(.00)	(.00)	(.51)	(.00)	(.00)
$1a_1$	-395.20	.17	-.01	.65	.00	.00	.63	-.00	.01
		(.09)	(.00)	(.47)	(.00)	(.00)	(.44)	(.00)	(.00)

		$2p\pi$ eq (F)	$2p\pi$ ax (F)
$2a_2$	-137.06	-.73	.75
		(.49)	(.51)
$1a_2$	-161.55	.69	.67
		(.51)	(.49)

		3p (S)	$2p\pi$ eq (F)	2s ax (F)	$2p\sigma$ ax (F)	$2p\pi$ ax (F)
$5b_1$	38.99	1.20	-.27	-.52	-.53	-.17
		(.88)	(.01)	(.00)	(.09)	(.01)
$4b_1$	-141.74	-.10	.80	-.04	-.64	-.02
		(.01)	(.59)	(.00)	(.40)	(.00)
$3b_1$	-147.76	-.01	-.20	.01	-.27	.95
		(.00)	(.04)	(.00)	(.07)	(.89)

(Cont'd)

$2b_1$	-162.36	.21	.56	-.13	.62	.30
		(.10)	(.36)	(.00)	(.44)	(.10)
$1b_1$	-372.50	.00	.03	1.00	-.01	.00
		(.00)	(.00)	(1.00)	(.00)	(.00)
		3p (S)	2s eq (F)	2pσ eq (F)	2pπ eq (F)	2pπ ax (F)
$5b_2$	86.56	1.28	-.63	-.59	.02	-.25
		(.90)	(.00)	(.10)	(.00)	(.01)
$4b_2$	-138.75	-.07	-.04	-.46	-.50	.78
		(.00)	(.00)	(.21)	(.23)	(.56)
$3b_2$	-152.32	-.12	.03	-.50	.82	.20
		(.03)	(.00)	(.26)	(.67)	(.04)
$2b_2$	-163.16	.17	-.14	.62	.30	.59
		(.07)	(.00)	(.44)	(.10)	(.39)
$1b_2$	-373.69	-.00	1.00	-.00	-.00	.03
		(.00)	(1.00)	(.00)	(.00)	(.00)

Ground State Electronic Configuration :

$$[1a_1]^2[1b_2]^2[1b_1]^2[2a_1]^2[3a_1]^2[4a_1]^2[2b_2]^2[2b_1]^2[1a_2]^2[3b_2]^2$$
$$[3b_1]^2[5a_1]^2[4b_1]^2[4b_2]^2[6a_1]^2[2a_2]^2[7a_1]^2[5b_1]^0[8a_1]^0[5b_2]^0$$

Total Orbital Energy = -6802.34 kK

B. Clementi's VSIP data

Eigenvalues (kK)		Eigenvectors (populations)							
		3s (S)	3p (S)	2s ax (F)	2pσ ax (F)	2pπ ax (F)	2s eq (F)	2pσ eq (F)	2pπ eq (F)
$8a_1$	88.62	-1.07	-.58	.50	.61	.12	.34	.46	.11
		(.51)	(.18)	(.05)	(.14)	(.00)	(.03)	(.09)	(.00)
$7a_1$	-60.14	-.42	.91	-.08	.01	-.30	.19	.41	-.36
		(.10)	(.68)	(.00)	(.00)	(.04)	(.01)	(.11)	(.06)
$6a_1$	-145.66	-.01	.09	.06	.70	-.12	-.07	-.68	-.36
		(.00)	(.01)	(.00)	(.44)	(.01)	(.00)	(.42)	(.11)
$5a_1$	-156.14	-.02	.03	-.02	.13	-.74	-.00	-.09	.68
		(.00)	(.00)	(.00)	(.02)	(.53)	(.00)	(.01)	(.45)
$4a_1$	-173.34	-.05	.24	-.07	.24	.61	.01	-.11	.58
		(.00)	(.12)	(.00)	(.06)	(.42)	(.00)	(.01)	(.38)
$3a_1$	-200.56	.39	-.07	-.26	.51	-.01	-.28	.53	-.04
		(.23)	(.00)	(.04)	(.33)	(.00)	(.04)	(.36)	(.00)
$2a_1$	-333.81	.01	-.02	-.71	.03	-.00	.72	-.03	-.02
		(.00)	(.00)	(.49)	(.00)	(.00)	(.50)	(.00)	(.00)
$1a_1$	-374.55	.27	-.01	.61	.01	.00	.59	.01	.01
		(.16)	(.00)	(.43)	(.00)	(.00)	(.41)	(.00)	(.00)

		2pπ eq (F)	2pπ ax (F)
$2a_2$	-145.43	-.73	.75
		(.49)	(.51)
$1a_2$	-177.42	.69	.67
		(.51)	(.49)

(Cont'd)

		3p (S)	2pσ eq (F)	2s ax (F)	2pσ ax (F)	2pπ ax (F)
$5b_1$	39.96	1.20	-.27	-.54	-.52	-.17
		(.88)	(.01)	(.01)	(.09)	(.01)
$4b_1$	-150.30	-.10	.79	-.04	-.64	-.02
		(.01)	(.63)	(.01)	(.45)	(.00)
$3b_1$	-156.78	-.01	-.20	.01	-.27	.95
		(.00)	(.04)	(.00)	(.07)	(.89)
$2b_1$	-171.54	.20	.57	-.14	.61	.30
		(.09)	(.36)	(.00)	(.43)	(.10)
$1b_1$	-343.62	.03	.04	.98	-.01	.00
		(.02)	(.00)	(.98)	(.00)	(.00)

		3p (S)	2s eq (F)	2pσ eq (F)	2pπ eq (F)	2pπ ax (F)
$5b_2$	88.68	1.28	-.66	-.59	.02	-.25
		(.88)	(.02)	(.09)	(.00)	(.01)
$4b_2$	-147.16	-.07	-.05	-.47	-.49	.78
		(.01)	(.00)	(.25)	(.23)	(.60)
$3b_2$	-161.46	-.12	.04	-.51	.81	.19
		(.03)	(.00)	(.28)	(.67)	(.03)
$2b_2$	-172.57	.15	-.15	.61	.32	.60
		(.09)	(.01)	(.44)	(.11)	(.40)
$1b_2$	-344.79	.04	.98	-.01	-.00	.04
		(.02)	(.96)	(.02)	(.00)	(.00)

(Cont'd)

Ground State Electronic Configuration :

$$[1a_1]^2[1b_2]^2[1b_1]^2[2a_1]^2[3a_1]^2[4a_1]^2[2b_2]^2[2b_1]^2[1a_2]^2[3b_2]^2$$
$$[3b_1]^2[5a_1]^2[4b_1]^2[4b_2]^2[6a_1]^2[2a_2]^2[7a_1]^2[5b_1]^0[8a_1]^0[5b_2]^0$$

Total Orbital Energy = -6818.58 kK

(2) Molecular Orbitals for SF_4 (T_d Symmetry)

A. Gray's VSIP data

Eigenvalues (kK)		Eigenvectors (populations)			
		2s (F)	2pσ (F)	3s (S)	
$3a_1$	57.44	-.54 (.06)	.83 (.27)	1.16 (.67)	
$2a_1$	-186.83	.31 (.04)	.78 (.73)	-.38 (.23)	
$1a_1$	-390.18	.91 (.90)	.01 (.00)	.18 (.10)	
		2pπ (F)			
1e	-153.40	1.00 (1.00)			
		2s (F)	2pσ (F)	2pπ (F)	3p (S)
$4t_2$	28.96	-.48 (.00)	-.44 (.05)	.44 (.05)	1.19 (.89)
$3t_2$	-163.45	-.07 (.00)	.93 (.89)	.30 (.08)	.10 (.02)
$2t_2$	-174.97	.08 (.00)	-.21 (.05)	.90 (.86)	-.18 (.08)

(Cont'd)

$1t_2$	-371.45	1.00	.01	.00	.00
		(1.00)	(.00)	(.00)	(.00)

$2p\pi$
(F)

$1t_1$	-145.57	1.00
		(1.00)

Ground State Electronic Configuration :

$$[1a_1]^2[1t_2]^6[2a_1]^2[2t_2]^6[3t_2]^6[1e]^4[1t_1]^6[4t_2]^2[3a_1]^0$$

Total Orbital Energy = -6842.34 kK

B. Clementi's VSIP data

	Eigenvalues (kK)	Eigenvectors (populations)			
		2s (F)	2pσ (F)	3s (S)	
$3a_1$	50.95	-.53 (.05)	.78 (.20)	1.19 (.75)	
$2a_1$	-187.72	.27 (.09)	.83 (.79)	-.31 (.18)	
$1a_1$	-356.41	.93 (.93)	-.01 (.00)	.14 (.07)	
		2pπ (F)			
1e	-162.77	1.00 (1.00)			
		2s (F)	2pσ (F)	2pπ (F)	3p (S)
$4t_2$	37.56	-.50 (.01)	-.52 (.00)	.46 (.07)	1.17 (.82)
$3t_2$	-137.96	-.07 (.01)	.81 (.67)	.57 (.31)	.10 (.02)
$2t_2$	-150.36	.14 (.00)	-.44 (.22)	.75 (.62)	-.28 (.15)
$1t_2$	-342.53	.98 (.98)	.01 (.00)	.01 (.00)	.03 (.01)

(Cont'd)

		$2p\pi$ (F)
$1t_1$	-154.45	1.00 (1.00)

Ground State Electronic Configuration :

$$[1a_1]^2[1t_2]^6[2a_1]^2[1e]^4[1t_1]^6[2t_2]^6[3t_2]^6[4t_2]^2[3a_1]^0$$

Total Orbital Energy = -6376.10 kK

(3) Molecular Orbitals for SF_4 (D_{4h} Symmetry) :

A. Gray's VSIP data

Eigenvalues (kK)		Eigenvectors (populations)		
		3s (S)	2s (F)	2p σ (F)
$3a_{1g}$	43.73	-1.16 (.68)	.51 (.06)	.81 (.27)
$2a_{1g}$	-186.41	.38 (.23)	-.31 (.03)	.79 (.73)
$1a_{1g}$	-394.69	.17 (.09)	.92 (.91)	-.00 (.00)
		3p (S)	2p π (F)	
$2a_{2u}$	-60.34	1.02 (.84)	-.60 (.16)	
$1a_{2u}$	-164.84	.29 (.16)	.87 (.84)	
		2p π (F)		
$1a_{2g}$	-135.17	1.00 (1.00)		

(Cont'd)

		2s (S)	2pσ (F)
$2b_{1g}$	-138.32	.02	1.00
		(.00)	(1.00)
$1b_{1g}$	-361.15	1.00	-.01
		(1.00)	(.00)

		2pπ (F)
$1b_{2u}$	-145.36	1.00
		(1.00)

		2pπ (F)
$1b_{2g}$	-163.40	1.00
		(1.00)

		3p (S)	2s (F)	2pσ (F)	2pπ (F)
$4e_u$	86.58	1.29	-.63	-.59	-.25
		(.90)	(.00)	(.10)	(.01)
$3e_u$	-141.80	-.10	-.04	-.58	.84
		(.01)	(.00)	(.33)	(.65)
$2e_u$	-161.86	.19	-.14	.71	.55
		(.09)	(.00)	(.57)	(.34)
$1e_u$	-373.69	-.00	1.00	-.00	.03
		(.00)	(1.00)	(.00)	(.00)

(Cont'd)

		$2p\pi$ (F)
$1e_g$	-150.59	1.00 (1.00)

Ground State Electronic Configuration :

$$[1a_{1g}]^2[1e_u]^4[1b_{1g}]^2[2a_{1g}]^2[1a_{2u}]^2[1b_{2g}]^2[2e_u]^4[1e_g]^4[1b_{2u}]^2$$
$$[3e_u]^4[2b_{1g}]^2[1a_{2g}]^2[2a_{2u}]^2[3a_{1g}]^0[4e_u]^0$$

Total Orbital Energy = -6911.12 kK

B. Clementi's VSIP data :

	Eigenvalues (kK)	Eigenvectors (populations)		
		3s (S)	2s (F)	2p σ (F)
$3a_{1g}$	38.70	1.19 (.76)	-.50 (.04)	-.76 (.20)
$2a_{1g}$	-187.54	.30 (.17)	-.27 (.03)	.84 (.80)
$1a_{1g}$	-360.84	.13 (.06)	.94 (.93)	.02 (.00)
		3p (S)	2p π (F)	
$2a_{2u}$	-61.99	1.02 (.85)	-.58 (.15)	
$1a_{2u}$	-173.86	.27 (.15)	.88 (.85)	
		2p π (F)		
$1a_{2g}$	-143.43	1.00 (1.00)		
		2s (F)	2p σ (F)	
$2b_{1g}$	-146.76	.03 (.00)	1.00 (1.00)	

(Cont'd)

$1b_{1g}$	-332.74	1.00 (1.00)	-.01 (.00)

		$2p\pi$ (F)
$1b_{2u}$	-154.23	1.00 (1.00)

		$2p\pi$ (F)
$1b_{2g}$	-173.37	1.00 (1.00)

		3p (S)	2s (F)	$2p\sigma$ (F)	$2p\pi$ (F)
$4e_u$	88.69	1.28 (.88)	-.66 (.02)	-.59 (.09)	-.25 (.01)
$3e_u$	-150.36	-.10 (.01)	-.04 (.00)	-.59 (.34)	.83 (.64)
$2e_u$	-171.08	.18 (.08)	-.16 (.01)	.71 (.57)	.55 (.34)
$1e_u$	-344.79	.04 (.02)	.98 (.98)	-.01 (.00)	.04 (.00)

		$2p\pi$ (F)
$1e_g$	-159.78	1.00 (1.00)

(Cont'd)

Ground State Electronic Configuration :

$$[1a_{1g}]^2[1e_u]^4[1b_{1g}]^2[2a_{1g}]^2[1a_{2u}]^2[1b_{2g}]^2[2e_u]^4[1e_g]^4[1b_{2u}]^2$$
$$[3e_u]^4[2b_{1g}]^2[1a_{2g}]^2[2a_{2u}]^2[3a_{1g}]^0[4e_u]^0$$

Total Orbital Energy = -6773.56 kK